Numerical Modeling of Electromagnetic Wave Scattering by Layered Random Surfaces

by

Kelsey Ulmer

A dissertation submitted to the Graduate Faculty of
Auburn University
in partial fulfillment of the
requirements for the Degree of
Doctor of Philosophy

Auburn, Alabama
December 12, 2020

Keywords: electromagnetic field scattering, random surfaces, Monte Carlo, Transformed Field Expansions

Approved by

Junshan Lin, Chair, Associate Professor of Mathematics and Statistics of Auburn University
David Nicholls, Professor of Mathematics, Statistics, and Computer Science of the University of Illinois at Chicago
Yanzhao Cao, Professor of Mathematics and Statistics of Auburn University
Dmitry Glotov, Associate Professor of Mathematics and Statistics of Auburn University
Hans-Werner Van Wyk, Assistant Professor of Mathematics and Statistics of Auburn University

Abstract

We present an efficient numerical method for modeling the scattering of electromagnetic fields by a multiply layered medium with random interfaces. We propose a combination of the Monte Carlo-Transformed Field Expansion (MCTFE) Method with the use of Impedance-Impedance Operators to formulate the boundary conditions between the inner layers. The utilization of Impedance-Impedance Operators avoids singularities that typically arise in the inner layers when implementing the more frequently used Dirichlet to Neumann Operators. The primary components of the MCTFE Method are a domain flattening change of variables, a high order perturbation of surfaces expansion of the solutions, and Monte Carlo sampling. By using this method, the discretized differential operator will be the same for every Monte Carlo sample and for each perturbation order. This allows for an LU decomposition of the differential operator, which can then be called upon to solve the boundary value problem in each layer via backward and forward substitution. This leads to greatly reduced computational costs. The Karhunen-Loève Expansion will be used to represent the random interfaces which separate each layer. After implementing the domain flattening change of variables and expanding the solutions as a Taylor series, the electromagnetic fields will be approximated using the Chebyshev polynomials, so that we can express the differential operator using Chebyshev differentiation matrices and solve the boundary value problems via collocation. Numerical results will be presented to demonstrate the accuracy of the method.

Acknowledgments

I am immensely grateful for everyone who has been a part of my educational experience throughout the years. I would especially like to thank my advisor Dr. Junshan Lin and Dr. David Nicholls for all of their guidance, encouragement, and support. You both have taught me so much and have been incredibly kind. I am beyond thankful for you both.

I also would like to give a huge thank you to my fiancé, Vincent Stewart, my family - especially my parents Benjamin and Laurie Ulmer; and my friends for their constant love, compassion, and encouragement. You all mean a great deal to me, and I am forever in awe of how blessed I am to have you all in my life.

Additionally, I would like to acknowledge the tremendous support from the National Science Foundation through grant number DMS-1719851.

Table of Contents

List of Figures

List of Tables

Chapter 1

Introduction

1.1 Introduction of the Model

We consider the scattering of electromagnetic waves by a structure consisting of multiple layers that are separated by random interfaces which are invariant in the y-direction. Note that x is the lateral direction, z is the vertical direction, and y is the invariant (lateral) direction. Refer to Figure 1.1 as an example of the setup we describe here. The material in each layer is characterized by its electromagnetic properties, the permeability and permittivity of the material. Suppose the incident radiation illuminates the structure from above and is aligned with the invariant direction (the y-direction) of the grooves of the interfaces. We are interested in efficiently finding the statistics (mean and variance) of the resulting scattered fields in each layer.

The model arises from applications in many research areas including remote sensing, oceanography, surface plasmon resonances, solar cells, etc. In this section, brief descriptions of examples of these applications are given to connect this model to problems of real-world interest.

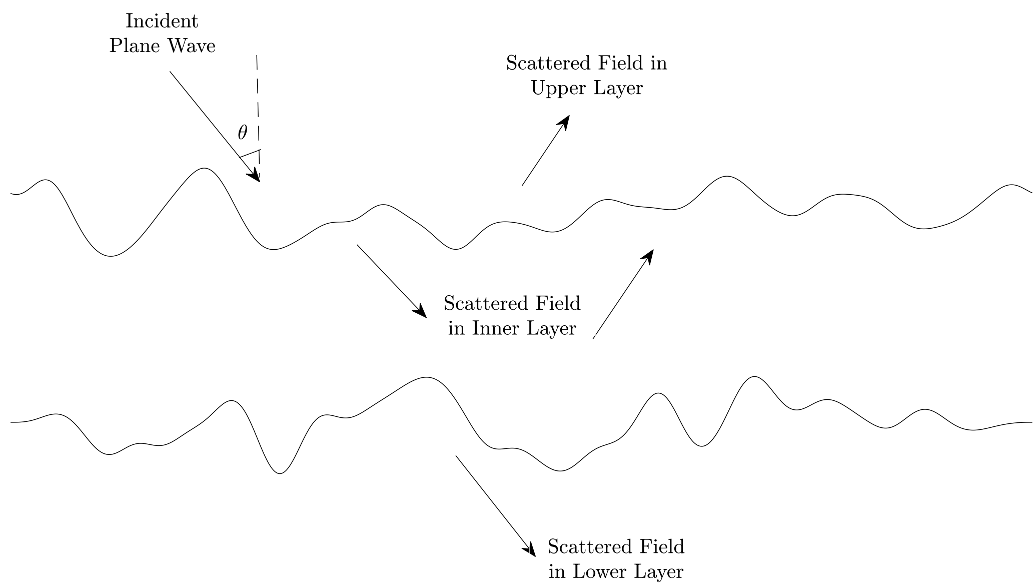

Figure 1.1: Sample of a structure with three layers separated by random interfaces and illuminated from above by an incident wave.

The primary concept of remote sensing is gathering information about something from a distance or without any physical contact. This can include the use of scattered electromagnetic fields to obtain information about the earth's surface, oceans, or atmosphere [14, 26, 52, 54]. Our model of interest could perhaps represent the earth's surface or the ocean's surface, which is constantly changing.

Surface plasmon resonances (SPRs) are strong highly localized electromagnetic fields which are present on the surface of certain metals. These SPRs are highly sensitive to the boundary shape, i.e. the surface on which they are appearing [55]. One could consider our setup to represent a surface designed for SPR excitation [34]. Examples of applications involving SPRs are found in biosensing [18, 48], extraordinary optical transmission (EOT)

[15, 49], and surface-enhanced Raman scattering (used in spectroscopy) [30]. SPR biosensors are used to detect chemical and biological analytes, which could be of importance in "medical diagnostics, environmental monitoring, food safety and security" [48]. EOT is the enhanced transmission of electromagnetic fields through very small apertures due to SPR excitation [49]. Applications of EOT includes improvements to spectroscopy [9].

Solar cells, which are also referred to as photovoltaic cells, are used to convert solar energy to electricity. These solar cells are strategically made up of layers of various materials such that the electrical properties of these materials working together allows for electrons to flow in one direction through the solar cell, creating an electric current. A current research topic surrounding solar cells is enhancing light trapping in solar cells by optimizing the statistical properties of the rough interfaces of the material in the solar cells [4, 24]. This enhancement of light trapping, or light absorption, leads to enhanced production of electricity.

1.2 Scattering of EM Waves by One Random Interface

The configuration studied here is an extension of the configuration posed by X. Feng, J. Lin, and D. Nicholls in their paper "An Efficient Monte Carlo-Transformed Field Expansion Method for Electromagnetic Wave Scattering by Random Rough Surfaces" [13]. In their paper, they consider the scattering of electromagnetic waves by one random surface. The Monte-Carlo Transformed Field Expansion Method (MCTFE) is used to efficiently find the statistics of the scattered fields in the layer above and the layer below the random interface. The MCTFE Method uses a change of variables to flatten the domain, a High-Order Perturbation of Surfaces (HOPS) expansion of the solution [17], the Legendre-Galerkin method [50] to discretize and solve the boundary value problem, and Monte Carlo sampling to find and calculate the statistics of the scattered fields. In implementing the MCTFE method, it can be seen that for each Monte Carlo sample and for each perturbation order, the boundary value problem has the same deterministic differential operator. Using this fact, an LU decomposition of the discretization of the differential operator can be used so that to solve each boundary value problem, simple forward and backward substitution can be used instead of using a full linear solver. Being able to use forward substitution and backward substitution leads to great computational savings.

1.3 Main Contribution of the Dissertation

The approach we present here is an efficient numerical method for modeling the scattering of electromagnetic fields by a multiply layered medium with random surfaces. We suggest a combination of the MCTFE Method [13] with the use of Impedance-Impedance Operators (IIOs) to formulate the boundary conditions separating the inner layers [39]. Of course, this is not the only method that can be applied to this type of problem. The method proposed here is significant in that it is highly accurate, greatly reduces computational costs, and provides a well-conditioned algorithm, particularly in the inner layers, which have shown to be problematic in other approaches.

The primary components of the MCTFE Method are Monte Carlo sampling, a domain flattening change of variables, and a high order perturbation of surface expansion of the solutions. The next question that must be addressed is why choose this method over others. D. Nicholls provides an excellent comparison of High-Order Perturbation of Surfaces methods to various other methods that could be applied to this problem [35, 39]. To summarize, the main advantages of the proposed method are the following. The method uses a reduced number of unknowns, particularly compared to traditional and volumetric numerical algorithms such as finite difference methods and finite element methods [25]. Similar to boundary methods such as integral equations, the method formulates the problem in terms of surface unknowns, and provides exact enforcement of the boundary conditions in the far-field. For our problem of interest, the boundaries separating each layer are parameterized by ε. A downfall of using integral equations is that the solution returned only holds for one particular value of ε, meaning that a new simulation must be run for each value of ε. An advantage of the Method of Transformed Field Equations is that, because it is structured around a Taylor series expansion in ε, the simulation only needs to be run once and then simply summed up at the end using whatever value of ε is of interest. Additionally, when using integral methods, the system of linear equations that must be inverted for each simulation are typically quite dense and not Symmetric Positive Definite (SPD), which is a challenge to iterative solvers [25], whereas the Method of Transformed Field Equations must invert a sparse (on the Fourier side) operator corresponding to the order $O(\varepsilon^0)$ solutions for each Taylor order $O(\varepsilon^n)$, $n \geq 1$. Furthermore, the Transformed Field Expansion method is a High-Order spectral method and demonstrates highly accurate results, as is characteristic of such methods [50, 53].

By using this method, we will see that the discretized differential operator that we must invert for the boundary value problems in each layer will be the same for every Monte Carlo sample and for each perturbation order. We may take advantage of this fact and find the LU decomposition of the discretized differential operators so that the LU decomposition may be called upon to solve the discretized boundary value problems using backward and forward substitution. Having the ability to use forward and backward substitution instead of a full linear solver leads to significantly reduced computational costs [13].

To formulate the boundary conditions separating the inner layers, we follow the lead of Nicholls in [39] and use Impedance-Impedance Operators (IIOs). In many previous approaches, Dirichlet to Neumann Operators were used to formulate the boundary conditions [16, 40]. A downfall of the Dirichlet to Neumann Operators is that "artificial" singularities ("artificial" in that in a fully coupled system, such singularities do not exist), often referred to as "Dirichlet eigenvalues", appear in the inner layers [39]. The IIOs have a major advantage in that they are not burdened by these Dirichlet eigenvalues, which are values of the wavenumber $k^{(m)}$ such that the Dirichlet boundary value problem in the inner layer does not have a unique solution. These operators in the inner layers exist for all values of $k^{(m)}$ and, in fact, are unitary, providing a well-conditioned algorithm [10, 16, 19, 39].

To represent the random interfaces that separate each layer, the Karhunen Loève Expansion will be used. After implementing the domain flattening change of variables and expanding the solutions as a Taylor series, the electromagnetic fields will be approximated using Fourier series and Chebyshev polynomials, so that we can express the differential operator using Chebyshev differentiation matrices and solve the discretized boundary value problems via collocation.

The details of the model will be thoroughly discussed and numerical results will be presented to demonstrate the accuracy and convergence of the algorithm.

1.4 Outline

An outline of the remainder of the dissertation is as follows. Chapter 2 will discuss the problem formulation for the mathematical model, including the governing equations, the outgoing wave condition, and the modeling of the random surfaces. Chapter 3 will explore the numerical algorithm. The topics covered in this chapter are the formulation of the boundary conditions; the method of Transformed Field Equations; the reduction of the partial differential equations to ordinary differential equations; discretization of the boundary value problems; Monte Carlo sampling; the numerical algorithm as a whole, including the computational costs; and finally a look at using a Padé summation versus a Taylor summation. Chapter 4 presents a discussion on how the accuracy of the algorithm is evaluated and some numerical results. Finally, Chapter 5 summarizes the results of using the numerical algorithm and presents some ideas for future work.

Chapter 2

The Mathematical Model

In this chapter, the formulation of the mathematical model is discussed. This includes looking at the differential equations and boundary conditions for each layer, the outgoing wave condition, and a description of how to model the random interfaces separating each layer.

2.1 Problem Formulation

Consider the scattering of electromagnetic waves by a structure consisting of multiple layers with M-many random two-dimensional interfaces separating the layers, where the random interfaces are invariant in the y-direction. Refer to Figure 2.1 as an example of the multiple layered structure. Let

$$\Gamma_m(\xi) = \{(x, z) : z = a_m + g_m(\xi; x), -\infty < x < \infty\},$$

for $m = 1, ..., M$, denote the m^{th} interface, and let

$$\Omega_0(\xi) = \{(x, z) : z > a_1 + g_1(\xi; x), -\infty < x < \infty\},$$

$$\Omega_m(\xi) = \{(x, z) : a_{m+1} + g_{m+1}(\xi; x) < z < a_m + g_m(\xi; x), -\infty < x < \infty\},$$

for $m = 1, ..., M - 1$, and

$$\Omega_M(\xi) = \{(x, z) : z < a_M + g_M(\xi; x), -\infty < x < \infty\}$$

denote the m^{th} layers. The interface shapes are stationary Gaussian processes. Let ξ denote the random sample.

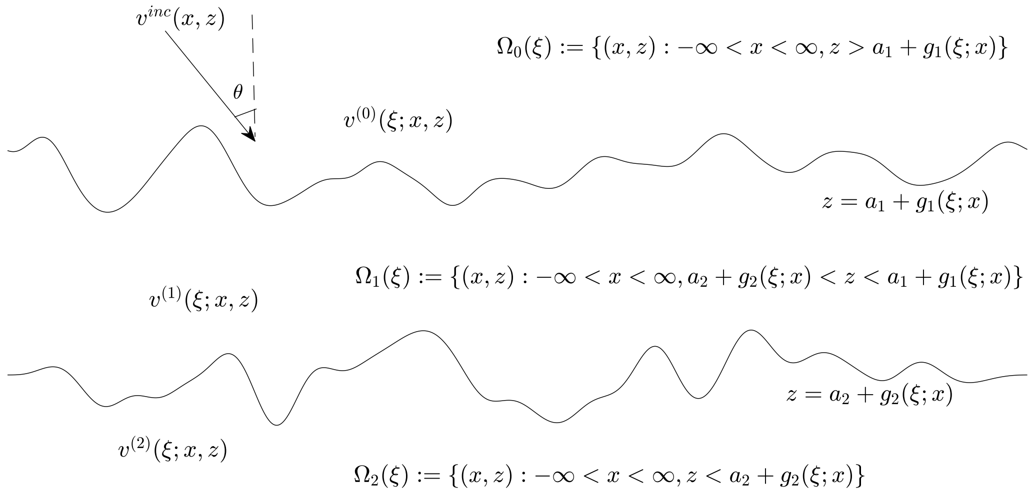

Figure 2.1: Sample of a structure with three layers separated by random interfaces.

Suppose an incident plane-wave illuminates the structure from above and is given by

$$\bar{v}^{inc}(x,z,t) = e^{i\omega t}e^{i(\alpha x - \gamma^{(0)}z)} = e^{i\omega t}v^{inc}(x,z)$$

where $\alpha = k^{(0}\sin(\theta)$, $\gamma^{(0)} = k^{(0)}\cos(\theta)$, and θ is the angle of incidence. In each layer, the wavenumber is given by $k^{(m)} = \dfrac{\omega}{c^{(m)}} = \omega^2\mu_0\epsilon_0\epsilon_{rel}^{(m)}$, where ω is the angular frequency of the incident wave, $c^{(m)}$ is the velocity of the wave corresponding to the m^{th} layer, μ_0 is the permeability in every layer, ϵ_0 is the permittivity in a vacuum, and $\epsilon_{rel}^{(m)}$ is the relative permittivity in the m^{th} layer. We will assume that the upper $(m = 0)$ and lower $(m = M)$

layers each consist of a dielectric medium dielectric and that the electromagnetic fields have a transverse electric (TE) polarization. The transverse magnetic (TM) polarization case works analogously with a small change in the boundary conditions, which is discussed below. We would like to efficiently find the statistics (mean and variance) of the scattered fields in each m^{th} layer, $v^{(m)}(\xi; x, z)$, for $m = 0, 1, ..., M$.

2.2 Time Harmonic Maxwell's Equations

The scattering of electromagnetic fields is governed by Maxwell's equations. Let $\bar{\mathbf{E}}(x, z, t)$ denote the total electric field and let $\bar{\mathbf{H}}(x, z, t)$ denote the total magnetic field. Let μ_0 denote the permeability in every layer, ϵ_0 denote the permittivity in a vacuum, $\epsilon_{rel}^{(m)}$ denote the relative permittivity in the m^{th} layer, and ω denote the angular frequency of the incident wave. $\bar{\mathbf{E}}(x, z, t)$ and $\bar{\mathbf{H}}(x, z, t)$ must satisfy Maxwell's Equations, which are given by [5]

$$\begin{cases} \nabla \times \bar{\mathbf{E}} = -\mu_0 \frac{\partial \bar{\mathbf{H}}}{\partial t} \\ \nabla \times \bar{\mathbf{H}} = \mathbf{J} + \epsilon_0 \epsilon_{rel}^{(m)} \frac{\partial \bar{\mathbf{E}}}{\partial t} \\ \nabla \cdot \bar{\mathbf{E}} = \frac{\rho}{\epsilon_0 \epsilon_{rel}^{(m)}} \\ \nabla \cdot \bar{\mathbf{H}} = 0. \end{cases} \tag{2.1}$$

In particular, we are assuming that our setup is source-free and that the incident field is a plane time-harmonic wave. This means that the electromagnetic fields of our model must satisfy the Time-Harmonic Maxwell's Equations [5, 43]. Here, ρ denotes the charge density and $\mathbf{J}$ denotes the current density. Since we are assuming that our model is source-free, $\rho = 0$ and $\mathbf{J} = 0$. Therefore, we have

$$\bar{\mathbf{E}}(x, z, t) = \mathbf{E}(x, z) e^{-i\omega t} \tag{2.2}$$

and

$$\bar{\mathbf{H}}(x,z,t) = \mathbf{H}(x,z)e^{-i\omega t}. \tag{2.3}$$

Inserting (2.2) and (2.3) into Maxwell's Equations (2.1) gives the Time-Harmonic Maxwell's Equations [43]

$$\begin{cases} \nabla \times \mathbf{E} = i\omega\mu_0 \mathbf{H} \\ \nabla \times \mathbf{H} = -i\omega\epsilon_0\epsilon_{rel}^{(m)}\mathbf{E} \\ \nabla \cdot \mathbf{E} = 0 \\ \nabla \cdot \mathbf{H} = 0. \end{cases} \tag{2.4}$$

At the interfaces, we will enforce tangential continuity

$$\mathbf{N} \times \mathbf{E} = \mathbf{0}$$

$$\mathbf{N} \times \mathbf{H} = \mathbf{0},$$

where $\mathbf{N^{(m)}} = \begin{bmatrix} -\partial_x g_m(\xi;x) \\ 0 \\ 1 \end{bmatrix}$ is the upward pointing normal vector at the m^{th} interface, for $m = 1, ..., M$.

Suppose we have a transverse electric (TE) polarization, i.e. $\mathbf{E} = \begin{bmatrix} 0 \\ v(\xi;x,z) \\ 0 \end{bmatrix}$, where $v(\xi;x,z)$ is the total field, and $\mathbf{H} = \begin{bmatrix} H_1(\xi;x,z) \\ 0 \\ H_2(\xi;x,z) \end{bmatrix}$. Recall that x is the lateral direction, z is the vertical direction, and y is the invariant (lateral) direction. Note that since $\nabla \times \mathbf{E} =$

$i\omega\mu_0\mathbf{H}$, we have

$$i\omega\mu_0 \begin{bmatrix} H_1(\xi;x,z) \\ 0 \\ H_2(\xi;x,z) \end{bmatrix} = \nabla \times \begin{bmatrix} 0 \\ v(\xi;x,z) \\ 0 \end{bmatrix} = \begin{bmatrix} \partial_z v(\xi;x,z) \\ 0 \\ -\partial_x v(\xi;x,z) \end{bmatrix}.$$

Therefore, $\mathbf{H} = \dfrac{1}{i\omega\mu_0} \begin{bmatrix} \partial_z v(\xi;x,z) \\ 0 \\ -\partial_x v(\xi;x,z) \end{bmatrix}$. Then taking the curl on both sides of $\nabla \times \mathbf{E} = i\omega\mu_0\mathbf{H}$ and using the identity $\nabla \times (\nabla \times A) = \nabla(\nabla \cdot A) - \nabla^2 A$, gives

$$\nabla^2\mathbf{E} + (k^{(m)})^2\mathbf{E} = \mathbf{0},$$

where $(k^{(m)})^2 = \omega^2\mu_0\epsilon_0\epsilon_{rel}^{(m)}$ is the wavenumber in the m^{th} layer. Also note that $k^{(m)} = \frac{\omega}{c^{(m)}}$, where $c^{(m)}$ is the velocity of the wave corresponding to the medium of the m^{th} layer. Finally, since we have a TE polarization, the time-harmonic Maxwell's equations reduce to the Helmholtz equation

$$\Delta v(\xi;x,z) + (k^{(m)})^2 v(\xi;x,z) = 0.$$

For the boundary conditions, we recall that tangential continuity across layers is enforced, giving $\mathbf{N}^{(m)} \times \mathbf{E} = \mathbf{0}$ and $\mathbf{N}^{(m)} \times \mathbf{H} = \mathbf{0}$, i.e.

$$\begin{aligned} \mathbf{0} &= \mathbf{N}^{(m)} \times \mathbf{E} \\ &= \begin{bmatrix} v(\xi;x,a_m + g_m(\xi,x)) \\ 0 \\ (\partial_x g_m(\xi;x))(v(\xi;x,a_m + g_m(\xi;x))) \end{bmatrix} \end{aligned}$$

and

$$
\begin{aligned}
\mathbf{0} &= \mathbf{N}^{(m)} \times \mathbf{H} \\
&= -\frac{1}{i\omega\mu_0} \begin{bmatrix} 0 \\ (-\partial_x g_m(\xi;x))(\partial_x v(\xi;x,a_m+g_m(\xi;x))) + \partial_z v(\xi;x,a_m+g_m(\xi;x)) \\ 0 \end{bmatrix},
\end{aligned}
$$

which enforces continuity of the total field across each interface,

$$v(\xi;x,z)=0,\ \ z=a_m+g_m(\xi;x) \text{ for } m=1,...,M$$

$$\frac{\partial v}{\partial \mathbf{n}^{(m)}}(\xi;x,z)=0,\ \ z=a_m+g_m(\xi;x) \text{ for } m=1,...,M.$$

Now, suppose we have a transverse magnetic (TM) polarization, i.e. $\mathbf{H} = \begin{bmatrix} 0 \\ v(\xi;x,z) \\ 0 \end{bmatrix}$ and $\mathbf{E} = \begin{bmatrix} E_1(\xi;x,z) \\ 0 \\ E_2(\xi;x,z) \end{bmatrix}$, where, again, $v(\xi;x,z)$ is the total field. Since $\nabla\times\mathbf{H} = -i\omega\epsilon_0\epsilon_{rel}^{(m)}\mathbf{E}$, we have

$$-i\omega\epsilon_0\epsilon_{rel}^{(m)} \begin{bmatrix} E_1(\xi;x,z) \\ 0 \\ E_2(\xi;,x,z) \end{bmatrix} = \nabla\times \begin{bmatrix} 0 \\ v(\xi;x,z) \\ 0 \end{bmatrix} = \begin{bmatrix} \partial_z v(\xi;x,z) \\ 0 \\ -\partial_x v(\xi;x,z) \end{bmatrix}.$$

Therefore, $\mathbf{E} = -\frac{1}{i\omega\epsilon_0\epsilon_{rel}^{(m)}} \begin{bmatrix} \partial_z v(\xi;x,z) \\ 0 \\ -\partial_x v(\xi;x,z) \end{bmatrix}$. Then taking the curl on both sides of $\nabla\times\mathbf{H} = -i\omega\epsilon_0\epsilon_{rel}^{(m)}\mathbf{E}$ gives

$$\nabla^2\mathbf{H} + (k^{(m)})^2\mathbf{H} = \mathbf{0}.$$

Since we have a TM polarization, the time-harmonic Maxwell's equations reduce to the Helmholtz equation

$$\Delta v(\xi; x, z) + (k^{(m)})^2 v(\xi; x, z) = 0.$$

Again, for the boundary conditions, we examine the tangential continuity across layers

$$\begin{aligned}\mathbf{0} &= \mathbf{N}^{(m)} \times \mathbf{H} \\ &= \begin{bmatrix} v(\xi; x, a_m + g_m(\xi; x)) \\ 0 \\ -(\partial_x g_m(\xi; x))(v(\xi; x, a_m + g_m(\xi; x))) \end{bmatrix}\end{aligned}$$

and

$$\begin{aligned}\mathbf{0} &= \mathbf{N}^{(m)} \times \mathbf{E} \\ &= \frac{1}{i\omega\epsilon_0\epsilon_{rel}^{(m)}} \begin{bmatrix} 0 \\ -(\partial_x g_m(\xi; x))(\partial_x v(\xi; x, a_m + g_m(\xi; x))) + \partial_z v(\xi; x, a_m + g_m(\xi; x)) \\ 0 \end{bmatrix},\end{aligned}$$

which gives the boundary conditions

$$v^{(0)}(\xi; x, z) - v^{(1)}(\xi; x, z) = -v^{inc}(x, z),\ z = a_1 + g_1(\xi; x)$$

$$\frac{\partial v^{(0)}}{\partial \mathbf{n}^{(1)}}(\xi; x, z) - (\tau_1)^2 \frac{\partial v^{(1)}}{\partial \mathbf{n}^{(1)}}(\xi; x, z) = -\frac{\partial v^{inc}}{\partial \mathbf{n}^{(1)}}(x, z),\ \ z = a_1 + g_1(\xi; x)$$

$$v^{(m-1)}(\xi; x, z) - v^{(m)}(\xi; x, z) = 0,\ z = a_m + g_m(\xi; x) \text{ for } m = 1, ..., M$$

$$\frac{\partial v^{(m-1)}}{\partial \mathbf{n}^{(m)}}(\xi; x, z) - (\tau_m)^2 \frac{\partial v^{(m)}}{\partial \mathbf{n}^{(m)}}(\xi; x, z) = 0,\ \ z = a_m + g_m(\xi; x) \text{ for } m = 1, ..., M,$$

where

$$\tau_m^2 = \frac{\epsilon_{rel}^{(m-1)}}{\epsilon_{rel}^{(m)}} = \frac{\omega^2 \mu_0 \epsilon_0 \epsilon_{rel}^{(m-1)}}{\omega^2 \mu_0 \epsilon_0 \epsilon_{rel}^{(m)}} = \frac{(k^{(m-1)})^2}{(k^{(m)})^2}.$$

Therefore, in general, the scattered electromagnetic fields satisfy

$$\begin{cases} \Delta v^{(m)} + (k^{(m)})^2 v^{(m)} = 0, \ (x,z) \in \Omega_m \text{ for } m = 0, 1, ..., M \\ v^{(0)} - v^{(1)} = -v^{inc}, \ z = a_1 + g_1(\xi; x) \\ \frac{\partial v^{(0)}}{\partial \mathbf{n}^{(1)}} - (\tau_1)^2 \frac{\partial v^{(1)}}{\partial \mathbf{n}^{(1)}} = -\frac{\partial v^{inc}}{\partial \mathbf{n}^{(1)}}, \ z = a_1 + g_1(\xi; x) \\ v^{(m-1)} - v^{(m)} = 0, \ z = a_m + g_m(\xi; x) \\ \frac{\partial v^{(m-1)}}{\partial \mathbf{n}^{(m)}} - (\tau_m)^2 \frac{\partial v^{(m)}}{\partial \mathbf{n}^{(m)}} = 0, \ z = a_m + g_m(\xi; x) \text{ for } m = 2, ..., M, \end{cases} \tag{2.5}$$

where $(\tau_m)^2 = \begin{cases} 1 \text{ for TE polarization} \\ \frac{(k^{(m-1)})^2}{(k^{(m)})^2} \text{ for TM polarization.} \end{cases}$

2.3 Mathematical Model for Scattering by Multiple Interfaces

Since the electromagnetic fields are governed by the time-harmonic Maxwell's equations (2.4), we have that in each layer, the electromagnetic fields satisfy the Helmholtz equation (2.5). We will assume that we have a TE polarization. So for each layer, $m = 0, 1, ..., M$, the scattered field $v^{(m)}$ satisfies

$$\Delta v^{(m)} + (k^{(m)})^2 v^{(m)} = 0, \ (x,z) \in \Omega_m(\xi).$$

Enforcing continuity between each layer gives the boundary conditions for each layer. Let $\mathbf{n}^{(m)} = \begin{bmatrix} -\partial_x g_m(\xi; x) \\ 1 \end{bmatrix}$, for $m = 1, ..., M$, be the upward pointing normal vectors. At the first interface, $m = 1$,

$$v^{(0)} - v^{(1)} = -v^{inc}, \ z = a_1 + g_1(\xi; x)$$

$$\frac{\partial v^{(0)}}{\partial \mathbf{n}^{(1)}} - \frac{\partial v^{(1)}}{\partial \mathbf{n}^{(1)}} = -\frac{\partial v^{inc}}{\partial \mathbf{n}^{(1)}},\ z = a_1 + g_1(\xi; x).$$

For the remaining interfaces, $m = 2, ..., M$,

$$v^{(m-1)} - v^{(m)} = 0,\ z = a_m + g_m(\xi; x)$$

$$\frac{\partial v^{(m-1)}}{\partial \mathbf{n}^{(m)}} - \frac{\partial v^{(m)}}{\partial \mathbf{n}^{(m)}} = 0,\ z = a_m + g_m(\xi; x).$$

Since the incident wave is quasiperiodic, i.e.

$$\begin{aligned} v^{inc}(x+d, z) &= e^{i\alpha(x+d) - i\gamma_0^{(0)} z} \\ &= e^{i\alpha d} e^{i\alpha x - \gamma_0^{(0)} z} \\ &= e^{i\alpha d} v^{inc}(x, z), \end{aligned}$$

and the interfaces are periodic, the fields in each layer must also be quasiperiodic [13, 43]

$$v^{(m)}(x+d, z) = e^{i\alpha d} v^{(m)}(x, z),\ m = 0, 1, ..., M.$$

Finally, we have discussed the model in each part of the domain, with the exception of the behavior of the electromagnetic fields as $z \to \infty$ and $z \to -\infty$, which we will refer to as the Outgoing Wave Condition. The governing equations are given by

$$
\begin{cases}
\Delta v^{(m)} + (k^{(m)})^2 v^{(m)} = 0, \ \ (x,z) \in \Omega_m(\xi), \ \ m = 0, 1, ..., M \\
v^{(0)} - v^{(1)} = -v^{inc}, \ \ z = a_1 + g_1(\xi; x) \\
\frac{\partial v^{(0)}}{\partial \mathbf{n}^{(1)}} - \frac{\partial v^{(1)}}{\partial \mathbf{n}^{(1)}} = -\frac{\partial v^{inc}}{\partial \mathbf{n}^{(1)}}, \ \ z = a_1 + g_1(\xi; x) \\
v^{(m-1)} - v^{(m)} = 0, \ \ z = a_m + g_m(\xi; x), \ \ m = 2, ..., M \\
\frac{\partial v^{(m-1)}}{\partial \mathbf{n}^{(m)}} - \frac{\partial v^{(m)}}{\partial \mathbf{n}^{(m)}} = 0, \ \ z = a_m + g_m(\xi; x), \ \ m = 2, ..., M \\
v^{(m)}(\xi; x + d, z) = e^{i\alpha d} v^{(m)}(\xi; x, z), \ \ m = 0, 1, ..., M \\
\text{Outgoing Wave Condition.}
\end{cases}
\tag{2.6}
$$

2.4 Outgoing Wave Condition and Dirichlet to Neumann Operators

To enforce the outgoing wave condition, we will begin by defining the artificial boundaries $\{z = a\}$ and $\{z = b\}$, where $a > a_1 + |g_1|_{L^\infty}$ and $b < a_M - |g_M|_{L^\infty}$, with generic Dirichlet data, $v^{(0)}(\xi; x, a) = \psi(x)$ and $v^{(M)}(\xi; x, b) = \mu(x)$ [13, 17, 39]. See Figure 2.2 below, which demonstrates the placement of the artificial boundaries.

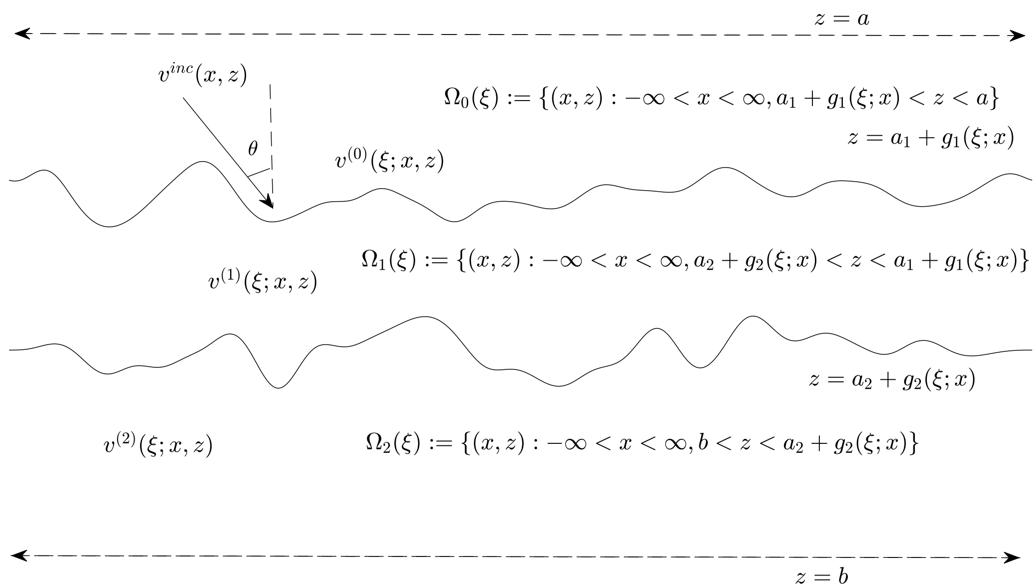

Figure 2.2: Sample of a structure with three layers separated by random interfaces with artificial boundaries.

On the domains $\{z > a\}$ and $\{z < b\}$, we can find the solutions of the fields using separation of variables. Temporarily, and for the sake of explanation, on the domain $\{z > a\}$ and $\{z < b\}$, let's name the fields $u^{(0)}(x,z)$ and $u^{(M)}(x,z)$, i.e. $u^{(0)}(x,z) := v^{(0)}(x,z)\Big|_{\{z>a\}}$ and $u^{(M)}(x,z) := v^{(M)}(x,z)\Big|_{\{z<b\}}$. Then separation of variables gives

$$u^{(0)}(x,z) = \sum_{p=-\infty}^{\infty} a_p^{(0)} e^{i\alpha_p x + i\gamma_p^{(0)} z} + \sum_{p=-\infty}^{\infty} b_p^{(0)} e^{i\alpha_p x - i\gamma_p^{(0)} z}$$

$$u^{(M)}(x,z) = \sum_{p=-\infty}^{\infty} a_p^{(M)} e^{i\alpha_p x + i\gamma_p^{(M)} z} + \sum_{p=-\infty}^{\infty} b_p^{(M)} e^{i\alpha_p x - i\gamma_p^{(M)} z},$$

where for $p \in \mathbb{Z}$,

$$\alpha_p := \alpha + \left(\frac{2\pi}{d}\right)p,$$

$$\gamma_p^{(0)} := \begin{cases} \sqrt{(k^{(0)})^2 - \alpha_p^2}, & p \in P^{(0)} \\ i\sqrt{\alpha_p^2 - (k^{(0)})^2}, & p \notin P^{(0)}, \end{cases}$$

$$\gamma_p^{(M)} := \begin{cases} \sqrt{(k^{(M)})^2 - \alpha_p^2}, & p \in P^{(M)} \\ i\sqrt{\alpha_p^2 - (k^{(M)})^2}, & p \notin P^{(M)} \end{cases}$$

$$k^{(0)} := \sqrt{\alpha_p^2 + (\gamma_p^{(0)})^2},$$

$$k^{(M)} := \sqrt{\alpha_p^2 + (\gamma_p^{(M)})^2},$$

$$P^{(0)} := \{p \in \mathbb{Z} : \alpha_p^2 \leq (k^{(0)})^2\},$$

and

$$P^{(M)} := \{p \in \mathbb{Z} : \alpha_p^2 \leq (k^{(M)})^2\}.$$

These are well known solutions, which are referred to as the Rayleigh expansions [43, 51]. Note that for $p \in P^{(0)}$, the first summation in the solution of $u^{(0)}$ is upward propagating and the second summation is downward propagating, which we do not desire. Whereas for $p \notin P^{(0)}$, the first summation is exponentially decreasing, or evanescent, and the second summation becomes unbounded, which is also undesired. Therefore, we must completely abandon the second summation in the solution to fulfill the restrictions given by the outward wave condition. Similarly, with regards to the solution of $u^{(M)}$, to satisfy the outgoing wave condition, we must abandon the first summation, which, if $p \in P^{(M)}$, gives upward propagating waves and, if $p \notin P^{(M)}$, becomes unbounded. Now, enforcing the Dirichlet boundary conditions at $z = a$ and $z = b$, respectively, we find that

$$u^{(0)}(\xi; x, z) = \sum_{p=-\infty}^{\infty} \hat{\psi}_p e^{i\alpha_p x + i\gamma_p^{(0)}(z-a)}$$

$$u^{(M)}(\xi; x, z) = \sum_{p=-\infty}^{\infty} \hat{\mu}_p e^{i\alpha_p x - i\gamma_p^{(M)}(z-b)},$$

where $\hat{\psi}_p$ and $\hat{\mu}_p$ are the Fourier coefficients of $\psi(x)$ and $\mu(x)$, respectively. At this point, let us redefine Ω_0 and Ω_M to be

$$\Omega_0(\xi) = \{(x, z) : -\infty < x < \infty, a_1 + g_1(\xi; x) < z < a\}$$

$$\Omega_M(\xi) = \{(x, z) : -\infty < x < \infty, b < z < a_M + g_M(\xi; x)\}.$$

Enforcing continuity across the artificial boundaries gives us the upper and lower transparent boundary conditions as well as defines the Dirichlet to Neumann Operators (DNOs) $T^{(0)}$ and $T^{(M)}$. We define the Dirichlet to Neumann Operators $T^{(0)}$ and $T^{(M)}$ as the operators which map the Dirichlet data to the Neumann data at the artificial boundaries $z = a$ and $z = b$.

$$T^{(0)} : v^{(0)}(\xi; x, a) \to \partial_z v^{(0)}(\xi; x, a)$$

$$T^{(M)} : v^{(M)}(\xi; x, b) \to \partial_z v^{(M)}(\xi; x, b).$$

Enforcing continuity across the artificial boundaries gives

$$u^{(0)}(x, a) = v^{(0)}(x, a)$$

$$u^{(M)}(x, b) = v^{(M)}(x, b)$$

$$\nabla u^{(0)}(x, a) \cdot \begin{bmatrix} 0 \\ 1 \end{bmatrix} = \nabla v^{(0)}(x, a) \cdot \begin{bmatrix} 0 \\ 1 \end{bmatrix}$$

$$\nabla u^{(M)}(x, b) \cdot \begin{bmatrix} 0 \\ -1 \end{bmatrix} = \nabla v^{(M)}(x, b) \cdot \begin{bmatrix} 0 \\ -1 \end{bmatrix}.$$

We can gather some understanding of these operators by observing the behavior of the solutions of the fields in the domains $\{z > a\}$ and $\{z < b\}$, respectively,

$$
\begin{aligned}
0 &= \nabla u^{(0)}(x,a) \cdot \begin{bmatrix} 0 \\ 1 \end{bmatrix} - \nabla v^{(0)}(x,a) \cdot \begin{bmatrix} 0 \\ 1 \end{bmatrix} \\
&= \partial_z u^{(0)}(x,a) - \partial_z v^{(0)}(x,a) \\
&= \partial_z u^{(0)}(x,a) - T^{(0)}[v^{(0)}(x,a)] \\
&= \partial_z u^{(0)}(x,a) - T^{(0)}[u^{(0)}(x,a)] \\
&= \sum_{p=-\infty}^{\infty} (i\gamma_p^{(0)})\hat{\psi}_p e^{i\alpha_p x} - T^{(0)}[u^{(0)}(x,a)]
\end{aligned}
$$

$$
\begin{aligned}
0 &= \nabla u^{(M)}(x,b) \cdot \begin{bmatrix} 0 \\ -1 \end{bmatrix} - \nabla v^{(M)}(x,b) \cdot \begin{bmatrix} 0 \\ -1 \end{bmatrix} \\
&= -\partial_z u^{(M)}(x,b) + \partial_z v^{(M)}(x,b) \\
&= -\partial_z u^{(M)}(x,b) + T^{(M)}[v^{(M)}(x,b)] \\
&= -\partial_z u^{(M)}(x,b) + T^{(M)}[u^{(M)}(x,b)] \\
&= -\sum_{p=-\infty}^{\infty} (-i\gamma_p^{(M)})\hat{\mu}_p e^{i\alpha_p x} + T^{(M)}[u^{(M)}(x,b)],
\end{aligned}
$$

to see that

$$
T^{(0)}[u^{(0)}(x,a)] = \sum_{p=-\infty}^{\infty} \hat{\psi}_p e^{i\alpha_p x} = \partial_z u^{(0)}(x,a)
$$

$$
T^{(M)}[u^{(M)}(x,b)] = \sum_{p=-\infty}^{\infty} (i\gamma_p^{(M)})\hat{\mu}_p e^{i\alpha_p x} = \partial_z u^{(M)}(x,b).
$$

Therefore, the Dirichlet to Neumann Operators $T^{(0)}$ and $T^{(M)}$ are the Fourier Multipliers

$$T^{(0)} = i\gamma_D^{(0)}$$

$$T^{(M)} = -i\gamma_D^{(M)},$$

where we note that the definition of a Fourier Multiplier, $m(D)$, is given by

$$m(D)[\nu(x)] := \sum_{p=-\infty}^{\infty} m(p)\hat{\nu}_p e^{i\alpha_p x}.$$

Now, we can state the outgoing wave condition as

$$\partial_z v^{(0)} - T^{(0)}[v^{(0)}] = 0,\ z = a$$

$$\partial_z v^{(M)} - T^{(M)}[v^{(M)}] = 0,\ z = b,$$

so that the governing equations are given by

$$\begin{cases} \Delta v^{(m)} + (k^{(m)})^2 v^{(m)} = 0, & (x,z) \in \Omega_m(\xi), \quad m = 0,1,...,M \\ v^{(0)} - v^{(1)} = -v^{inc}, & z = a_1 + g_1(\xi;x) \\ \frac{\partial v^{(0)}}{\partial \mathbf{n}^{(1)}} - \frac{\partial v^{(1)}}{\partial \mathbf{n}^{(1)}} = -\frac{\partial v^{inc}}{\partial \mathbf{n}^{(1)}}, & z = a_1 + g_1(\xi;x) \\ \partial_z v^{(0)} - T^{(0)}[v^{(0)}] = 0, & z = a \\ v^{(m-1)} - v^{(m)} = 0, & z = a_m + g_m(\xi;x), \quad m = 2,...,M \\ \frac{\partial v^{(m-1)}}{\partial \mathbf{n}^{(m)}} - \frac{\partial v^{(m)}}{\partial \mathbf{n}^{(m)}} = 0, & z = a_m + g_m(\xi;x), \quad m = 2,...,M \\ \partial_z v^{(M)} - T^{(M)}[v^{(M)}] = 0, & z = b \\ v^{(m)}(\xi; x+d, z) = e^{i\alpha d} v^{(m)}(\xi; x, z), & m = 0,1,...,M. \end{cases} \tag{2.7}$$

2.5 Random Surfaces: The Karhunen Loève Expansion

This section is dedicated to the modeling of the random surfaces that separate each layer. It is structured as follows. First, there will be a description of the Karhunen Loève expansion which explains the expansion and where it originates. This description follows the lead of [27]. From there, the Karhunen Loève expansion will be used to represent the random surfaces in our framework.

The Karhunen Loève expansion seeks to represent a random process as a linear combination of the eigenfunctions of the covariance operator associated with the process and independent and identically distributed (i.i.d.) random variables (coefficients) with zero mean and unit covariance. To understand the form of this expansion, let us first recall the spectral decomposition of a square, real-valued symmetric positive semi-definite matrix. If a matrix $A \in \mathbb{R}^{n\times n}$ is symmetric, then $A = UDU^T$, where λ_1, λ_2, ..., λ_n are the eigenvalues of A, $\mathbf{u}_1$, $\mathbf{u}_2$, ..., $\mathbf{u}_n$ are the corresponding eigenvectors of A, $U = \begin{bmatrix} \mathbf{u}_1 & \mathbf{u}_2 & \dots & \mathbf{u}_n \end{bmatrix}$ is orthogonal, and D is the diagonal matrix with diagonal entries λ_1, ..., λ_n [19]. Note that because A is symmetric, its eigenvalues $\lambda_j \in \mathbb{R}$ for $j = 1, ..., n$ [19, 27]. Furthermore, since A is positive semi-definite, its eigenvalues are all nonnegative [19]. This is called the spectral decomposition of A. By letting $V^T = UD^{1/2}$, where $D^{1/2}$ is the diagonal matrix with diagonal entries $\sqrt{\lambda_1}$, ..., $\sqrt{\lambda_n}$, we can write

$$V^TV = UD^{1/2}(UD^{1/2})^T = UD^{1/2}D^{1/2}U^T = UDU^T = A.$$

Because the covariance operator is symmetric and positive semi-definite, we will be able to use this spectral decomposition [27].

As discussed in Section 4.4 of [27], a sample $\mathbf{X}$ from a multivariate Gaussian distribution with mean μ and covariance matrix C can be given by

$$\mathbf{X} = \mu + V^T\zeta,$$

where $C = V^T V$, $\zeta = \begin{bmatrix} \zeta_1 & \zeta_2 & ... & \zeta_n \end{bmatrix}^T$, and ζ_1, ζ_2,..., ζ_n are i.i.d. Gaussian random variables with zero mean and unit covariance.

Now, let us use this representation to represent a sample of a real-valued Gaussian process $\{Y(x) : x \in R \subset \mathbb{R}\}$ with mean function $\mu(x)$ and covariance function $C(x, y)$. Then for $x_1, x_2, ..., x_n \in R$, let

$$\mathbf{Y} = \begin{bmatrix} Y(x_1) & Y(x_2) & ... & Y(x_n) \end{bmatrix}^T,$$

which is Gaussian with mean

$$\mu = \begin{bmatrix} \mu(x_1) & \mu(x_2) & ... & \mu(x_n) \end{bmatrix}^T$$

and covariance matrix $C_n \in \mathbb{R}^{n\times n}$ with entries $c_{ij} = C(x_i, y_j)$. Here, the subscript n is used to indicate the size of the covariance matrix and to differentiate it from the covariance function. Since the covariance matrix $C_n \in \mathbb{R}^{n\times n}$ is symmetric ($C(x, y) = C(y, x)$) and positive semi-definite, we can write $C_n = V_n^T V_n$, where $V_n^T = U_n D_n^{1/2}$, λ_1, λ_2,...,λ_n are the eigenvalues of C_n, $\mathbf{u}_1$, $\mathbf{u}_2$, ..., $\mathbf{u}_n$ are the corresponding eigenvectors, $D_n^{1/2}$ is the diagonal matrix with diagonal entries $\sqrt{\lambda_1}$, $\sqrt{\lambda_2}$, ..., $\sqrt{\lambda_n}$, and $U_n = \begin{bmatrix} \mathbf{u}_1 & \mathbf{u}_2 & ... & \mathbf{u}_n \end{bmatrix}$ is orthogonal. Now, using the above representation, we have

$$\begin{aligned} \mathbf{Y} &= \mu + V^T \zeta \\ &= \mu + \sum_{j=1}^{n} \sqrt{\lambda_j} \zeta_j \mathbf{u}_j. \end{aligned}$$

so that $Y(x_i) = \mu(x_i) + \sum_{j=1}^{n} \sqrt{\lambda_j} \zeta_j u_{i,j}$.

At this time, we have discussed this expansion representation in relation to the covariance matrix operator. The Karhunen Loève expansion is the generalization of this expansion to the covariance operator defined by

$$K\phi(x) := \int_R C(x,y)\phi(y)dy,\ \phi \in L^2(R),$$

where $C(x,y)$ is the covariance function of the stochastic process $Y(x)$ [27]. Then the Karhunen Loève expansion of the stochastic process $Y(x)$ is given by

$$Y(\xi;x) = \mu(x) + \sum_{j=1}^{\infty} \sqrt{\lambda_j}\zeta_j(\xi)\phi_j(x), \tag{2.8}$$

where λ_j are the eigenvalues of the covariance operator K, $\phi_j(x)$ are the corresponding eigenfunctions, and $\zeta_j(\xi)$ are i.i.d. Gaussian random variables with zero mean and unit covariance.

Now, returning to our problem of interest. We use the Karhunen Loève expansion to represent the stationary Gaussian processes $\tilde{g}_m(\xi;x)$, for $m = 1,...,M$, which describe the interfaces separating each layer. To start, we will assume the deviations of the surface from "flat" are small by letting $g_m(\xi;x) = \varepsilon\tilde{g}_m(\xi;x)$, for $m = 1,...,M$, where $\varepsilon \in (0,1)$, and $\tilde{g}_m(\xi;x)$ are of order 1 and are stationary Gaussian processes with continuous and bounded covariance functions. Furthermore, we assume the interfaces shapes are periodic with period d, i.e.

$$g_m(\xi;x+d) = \varepsilon\tilde{g}_m(\xi;x+d) = \varepsilon\tilde{g}_m(\xi;x) = g_m(\xi;x).$$

By the definition of a stationary Gaussian process, for each m^{th} interface, we have $\{\tilde{g}_m(\xi;x),\ \text{for all samples}\ \xi\}$ are jointly normal and have a continuous and bounded covariance function given by the Gaussian covariance function

$$C^{(m)}(x,y) = c^{(m)}(x-y) = (\sigma_0^{(m)})^2 e^{-|x-y|^2/(l_c)^2},$$

where $\sigma_0^{(m)}$ is the standard deviation of the surface and l_c is the correlation length [27]. The standard deviation of the surface, $\sigma_0^{(m)}$, and the correlation length, l_c, dictate the shape of the surface. As the value of $\sigma_0^{(m)}$ is increased, the size (in the z-direction) of the interface will also increase, and vice versa. Figure 2.3 demonstrates the effect of increasing the value of the standard deviation of the surface, $\sigma_0^{(m)}$.

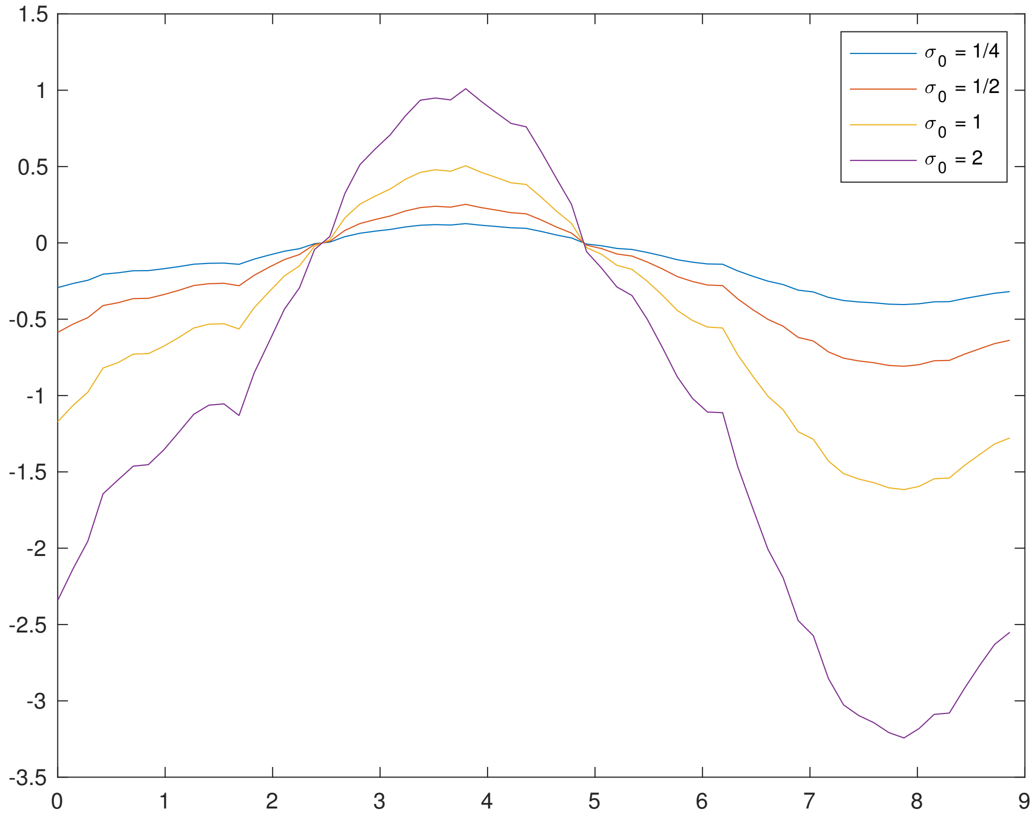

Figure 2.3: Sample Surface Represented by Karhunen Loève Expansion with Varying Standard Deviations of the Surface

As the value of the correlation length, l_c, is increased, the interface shapes will become "smoother" (less rough or "choppy"). Figure 2.4 demonstrates the effect of increasing the correlation length, l_c.

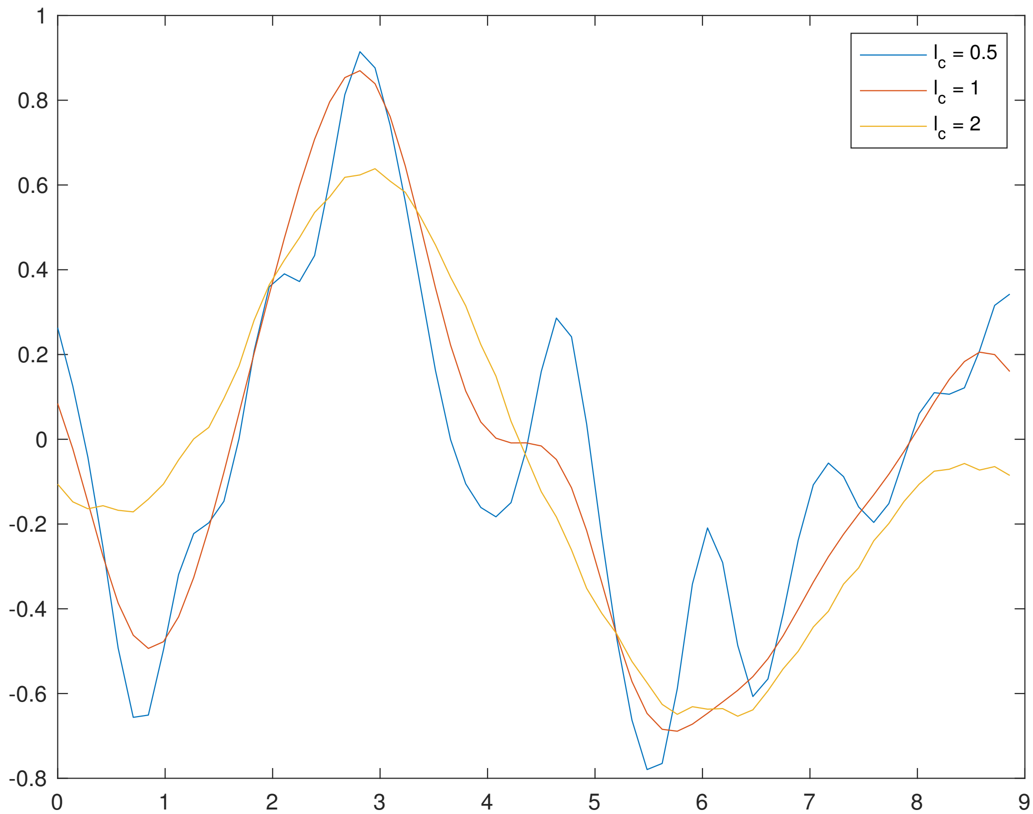

Figure 2.4: Sample Surface Represented by Karhunen Loève Expansion with Varying Correlation Lengths

Note that since

$$c^{(m)}(x-y) = C^{(m)}(x,y) = C^{(m)}(y,x) = c^{(m)}(y-x) = c^{(m)}(-(x-y)),$$

we have that $c^{(m)}(x)$ is an even function. Additionally, since $\tilde{g}_m(\xi;x)$ is periodic, we may expand the covariance function as a Fourier cosine series

$$c^{(m)}(x) = \frac{\hat{c}_0^{(m)}}{2} + \sum_{p=1}^{\infty} \hat{c}_p^{(m)} \cos\left(\frac{2\pi p x}{d}\right),$$

where $\hat{c}_p^{(m)}$ are the Fourier coefficients [13]. Let $K^{(m)}$ be the covariance operator for the m^{th} layer be defined by

$$K^{(m)}\phi(x) := \int_0^d c^m(x-y)\phi(y)dy$$
$$= \int_0^d \Big[\frac{\hat{c}_0^{(m)}}{2} + \sum_{p=1}^{\infty} \hat{c}_p^{(m)} \cos\Big(\frac{2\pi p(x-y)}{d}\Big)\Big]\phi(y)dy.$$

Through direct calculations, we have that the covariance operator $K^{(m)}$ has eigenvalues $\lambda_j^{(m)} = \dfrac{d\hat{c}_j^{(m)}}{2}$, for $j = 0, 1, ..$, with corresponding eigenfunctions

$$\phi_j^{(m)}(x) = \begin{cases} \sqrt{\frac{1}{d}}, \;\; j = 0 \\ \sqrt{\frac{2}{d}} \cos\left(\frac{2j\pi x}{d}\right), \;\; j \geq 2, \text{ when } j \text{ is even} \\ \sqrt{\frac{2}{d}} \sin\left(\frac{2j\pi x}{d}\right), \;\; j \geq 1, \text{ when } j \text{ is odd.} \end{cases}$$

The Karhunen Loève expansion of $\tilde{g}_m(\xi; x)$, for $m = 1, ..., M$, is now given by

$$\tilde{g}_m(\xi; x) = \bar{g}_m(x) + \sqrt{\lambda_0^{(m)}}\sqrt{\frac{1}{d}}\zeta_0^{(m)}(\xi) + \sum_{j=1}^{\infty} \sqrt{\lambda_j^{(m)}}\sqrt{\frac{2}{d}}\Bigg[\zeta_{2j}^{(m)}(\xi)\cos\Big(\frac{2(2j)\pi x}{d}\Big) +$$
$$\zeta_{2j-1}^{(m)}(\xi)\sin\Big(\frac{2(2j-1)\pi x}{d}\Big)\Bigg],$$

where $\bar{g}_m(x)$ is a deterministic function and $\zeta_j^{(m)}$, $j = 0, 1, ...$, are i.i.d. Gaussian random variables with zero mean and unit covariance [13].

Chapter 3

The Numerical Algorithm

The primary components of the numerical algorithm used to efficiently calculate the statistics of the scattered fields in each layer are the Transformed Field Expansions method, Impedance-Impedance Operators (IIOs), an LU decomposition of the discretization of the differential operator, and Monte Carlo sampling [13, 39].

The Transformed Field Expansions method uses a change of variables to flatten the domain and a High-Order Perturbation of Surfaces (HOPS) expansion of the solution [13, 39]. For the boundary formulation, IIOs will be used. In the paper "Stable, High-Order Computation of Impedance-Impedance Operators for Three Dimensional Layered Medium Simulations" by D. Nicholls [39], the approach of using the Transformed Field Expansions Method with IIOs to formulate the boundary conditions is proposed to model, with great success, the scattered fields of a multiple layered medium with deterministic interfaces.

After formulating the boundary conditions using the IIOs and implementing the method of Transformed Field Expansions, we will then be able to take advantage of the fact that each random sample will share the same deterministic differential operator. We can use an LU decomposition of this discretized differential operator to greatly reduce computational costs [13]. Monte-Carlo sampling will be used in solving the problem for many random samples and then finding the mean and variance over all samples.

3.1 Boundary Formulation and Impedance-Impedance Operators

The suggestion to formulate the boundary conditions using IIOs is credited to Kirsch and Monk in [23]; Gillman, Barnett, and Martinsson in [16]; and D. Nicholls in [39]. These IIOs are advantageous because they exist for all values of $k^{(m)}$, whereas the Dirichlet to

Neumann Operators used in previous approaches [28, 36, 40] do not exist for some values of $k^{(m)}$. An example of these "Dirichlet eigenvalues" (the values of $k^{(m)}$ for which the boundary value problems do not have a unique solution) will be shown using the "flat interface" case, i.e. $g_m \equiv 0$.

Let $\eta \in \mathbb{R}^+$, $\eta > 0$. Define the following (unknown) surface quantities as follows:

$$
\begin{aligned}
L^{(m)}(\xi;x) &:= -\frac{\partial v^{(m)}(\xi;x,z)}{\partial \mathbf{n}^{(m+1)}} - i\eta v^{(m)}(\xi;,x,z), \;\; z = a_{m+1} + g_{m+1}(\xi;x), \;\; m = 0,1,...,M-1 \\
U^{(m)}(\xi;x) &:= \frac{\partial v^{(m)}(\xi;x,z)}{\partial \mathbf{n}^{(m)}} - i\eta v^{(m)}(\xi;x,z), \;\; z = a_m + g_m(\xi;x), \;\; m = 1,2,..,M \\
\tilde{L}^{(m)}(\xi;x) &:= -\frac{\partial v^{(m)}(\xi;,x,z)}{\partial \mathbf{n}^{(m+1)}} + i\eta v^{(m)}(\xi;,x,z), \;\; z = a_{m+1} + g_{m+1}(\xi;x), \;\; m = 0,1,..,M-1 \\
\tilde{U}^{(m)}(\xi;x) &:= \frac{\partial v^{(m)}(\xi;x,z)}{\partial \mathbf{n}^{(m)}} + i\eta v^{(m)}(\xi;x,z), \;\; z = a_m + g_m(\xi;x), \;\; m = 1,2,..,M.
\end{aligned}
$$

We define the IIOs as follows [39]. The functions $g_m(\xi;x)$, $m = 1,...,M$, must be at least Lipschitz continuous to constitute "sufficiently smooth," as stated in the definitions below [10, 16, 39].

Definition 3.1. *For $g_1(\xi;x)$ sufficiently smooth, the unique quasiperiodic solution of*

$$
\begin{cases}
\Delta v^{(0)} + (k^{(0)})^2 v^{(0)} = 0, \;\; (x,z) \in \Omega_0(\xi) \\
\partial_z v^{(0)} - T^{(0)}[v^{(0)}] = 0, \;\; z = a \\
-\frac{\partial v^{(0)}}{\partial \boldsymbol{n}^{(1)}} - i\eta v^{(0)} = L^{(0)}, \;\; z = a_1 + g_1(\xi;x)
\end{cases}
$$

defines the IIO $Q[L^{(0)}] := \tilde{L}^{(0)}$.

Definition 3.2. *For $g_M(\xi;x)$ sufficiently smooth, the unique quasiperiodic solution of*

$$\begin{cases} \Delta v^{(M)} + (k^{(M)})^2 v^{(M)} = 0, & (x,z) \in \Omega_M(\xi) \\ \frac{\partial v^{(M)}}{\partial \boldsymbol{n}^{(M)}} - i\eta v^{(M)} = U^{(M)}, & z = a_M + g_M(\xi;x) \\ \partial_z v^{(M)} - T^{(M)}[v^{(M)}] = 0, & z = b \end{cases}$$

defines the IIO $S[U^{(M)}] := \tilde{U}^{(M)}$.

Definition 3.3. *: For $g_m(\xi;x)$ and $g_{m+1}(\xi;x)$, for $m = 1,..,M-1$, sufficiently smooth, the unique quasiperiodic solution of*

$$\begin{cases} \Delta v^{(m)} + (k^{(m)})^2 v^{(m)} = 0, & (x,z) \in \Omega_m(\xi) \\ \frac{\partial v^{(m)}}{\partial \boldsymbol{n}^{(m)}} - i\eta v^{(m)} = U^{(m)}, & z = a_m + g_m(\xi;x) \\ -\frac{\partial v^{(m)}}{\partial \boldsymbol{n}^{(m+1)}} - i\eta v^{(m)} = L^{(m)}, & z = a_{m+1} + g_{m+1}(\xi;x) \end{cases}$$

defines the IIO $R^{(m)} \left[\begin{pmatrix} U^{(m)} \\ L^{(m)} \end{pmatrix} \right] = \begin{bmatrix} R^{(m),uu} & R^{(m),ul} \\ R^{(m),lu} & R^{(m),ll} \end{bmatrix} \begin{bmatrix} U^{(m)} \\ L^{(m)} \end{bmatrix} := \begin{bmatrix} \tilde{U}^{(m)} \\ \tilde{L}^{(m)} \end{bmatrix}.$

It is important to note that it is a known result that unique solutions of the boundary value problems in the above definitions do exist as a result of the Fredholm Alternative [10, 11, 16, 29]. Therefore, the IIOs are guaranteed to exist, as well.

It is here that we can demonstrate how the IIOs outperform the Dirichlet to Neumann Operators (DNOs) in the interior layer. For the sake of explanation, let us temporarily define the DNOs for a fixed inner layer, say $m \in \{1, ..., M-1\}$ by starting with the following set of unknown surface quantities [36, 40]

$$
\begin{aligned}
V^{(m),l}(\xi;x) &:= v^{m}(\xi;x,a_{m+1}+g_{m+1}(\xi;x)) \\
V^{(m),u}(\xi;x) &:= v^{(m)}(\xi;x,a_{m}+g_{m}(\xi;x)) \\
\tilde{V}^{(m),l}(\xi;x) &:= -\frac{\partial v^{(m)}}{\partial \mathbf{n}^{(m+1)}}(\xi;x,a_{m+1}+g_{m+1}(\xi;x)) \\
\tilde{V}^{(m),u}(\xi;x) &:= \frac{\partial v^{(m)}}{\partial \mathbf{n}^{(m)}}(\xi;x,a_{m}+g_{m}(\xi;x)).
\end{aligned}
$$

For the m^{th} inner layer, if a unique solution exists to

$$
\begin{cases}
\Delta v^{(m)} + (k^{(m)})^2 v^{(m)} = 0,\ (x,z) \in \Omega_m \\
v^{(m)} = V^{(m),u},\ z = a_m + g_m(\xi;x) \\
v^{(m)} = V^{(m),l},\ z = a_{m+1} + g_{m+1}(\xi;x),
\end{cases}
$$

then it defines the Dirichlet to Neumann Operator by [36, 40]

$$
N^{(m)} \begin{bmatrix} V^{(m),u} \\ V^{(m),l} \end{bmatrix} := \begin{bmatrix} N^{(m),uu} & N^{(m),ul} \\ N^{(m),lu} & N^{(m),ll} \end{bmatrix} \begin{bmatrix} V^{(m),u} \\ V^{(m),l} \end{bmatrix} = \begin{bmatrix} \tilde{V}^{(m),u} \\ \tilde{V}^{(m),l} \end{bmatrix}.
$$

In particular, let us examine the "flat" interface case, $g_m \equiv 0$ and $g_{m+1} \equiv 0$. Then, for $\gamma_p^{(m)} \neq 0$, we have the solution

$$
v^{(m)}(x,z) = \sum_{p=-\infty}^{\infty} \Big(a_p^{(m)} \cos(\gamma_p^{(m)} z) + b_p^{(m)} \sin(\gamma_p^{(m)} z) \Big) e^{i\alpha_p x},
$$

where

$$
\gamma_p^{(m)} = \sqrt{(k^{(m)})^2 - \alpha_p^2}, \quad \mathrm{Im}(\gamma_p^{(m)}) \geq 0,
$$

for $m = 1, ..., M-1$. Now, at $z = a_m$,

$$\hat{V}_p^{(m,u)} = a_p^{(m)} \cos(\gamma_p^{(m)} a_m) + b_p^{(m)} \sin(\gamma_p^{(m)} a_m)$$

and at $z = a_{m+1}$,

$$\hat{V}_p^{(m,l)} = a_p^{(m)} \cos(\gamma_p^{(m)} a_{m+1}) + b_p^{(m)} \sin(\gamma_p^{(m)} a_{m+1}),$$

so that

$$\begin{bmatrix} \hat{V}_p^{(m),u} \\ \hat{V}_p^{(m),l} \end{bmatrix} = \begin{bmatrix} \cos(\gamma_p^{(m)} a_m) & \sin(\gamma_p^{(m)} a_m) \\ \cos(\gamma_p^{(m)} a_{m+1}) & \sin(\gamma_p^{(m)} a_{m+1}) \end{bmatrix} \begin{bmatrix} a_p^{(m)} \\ b_p^{(m)} \end{bmatrix}.$$

Note that

$$\begin{aligned} \det \begin{bmatrix} \cos(\gamma_p^{(m)} a_m) & \sin(\gamma_p^{(m)} a_m) \\ \cos(\gamma_p^{(m)} a_{m+1}) & \sin(\gamma_p^{(m)} a_{m+1}) \end{bmatrix} &= \cos(\gamma_p^{(m)} a_m) \sin(\gamma_p^{(m)} a_{m+1}) - \\ &\quad \cos(\gamma_p^{(m)} a_{m+1}) \sin(\gamma_p^{(m)} a_m) \\ &= -\sin(\gamma_p^{(m)} (a_m - a_{m+1})), \end{aligned}$$

which is 0 when $\gamma_p^{(m)}(a_m - a_{m+1})$ is a nonzero integer multiple of 2π. Then for $\gamma_p^{(m)}$ such that $\gamma_p^{(m)}(a_m - a_{m+1})$ is a nonzero integer multiple of 2π, the boundary value problems do not have a unique solution. Note that for $\gamma_p^{(m)} = 0$,

$$v^{(m)}(x,z) = \sum_{p=-\infty}^{\infty} \left(a_p^{(m)} z + b_p^{(m)} \right) e^{i\alpha_p x}.$$

Then at $z = a_m$,

$$\hat{V}_p^{(m),u} = a_p^{(m)} a_m + b_p^{(m)}$$

and at $z = a_{m+1}$,

$$\hat{V}_p^{(m),l} = a_p^{(m)} a_{m+1} + b_p^{(m)},$$

so that

$$\begin{bmatrix} \hat{V}_p^{(m),u} \\ \hat{V}_p^{(m),l} \end{bmatrix} = \begin{bmatrix} a_m & 1 \\ a_{m+1} & 1 \end{bmatrix} \begin{bmatrix} a_p^{(m)} \\ b_p^{(m)} \end{bmatrix}.$$

Since

$$\det \begin{bmatrix} a_m & 1 \\ a_{m+1} & 1 \end{bmatrix} = a_m - a_{m+1} \neq 0,$$

the boundary value problem will have a unique solution when $\gamma_p^{(m)} = 0$.

Now, returning to the use of IIOs, we note that a linear combination of the unknown surface (or impedance) quantities may be taken to describe the boundary conditions at $z = a_m + g_m(\xi; x)$ for $m = 1, ..., M$. For $m = 1$, at $z = a_1 + g_1(\xi; , x)$,

$$\begin{aligned}
(-2i\eta)(-v^{inc}) &= (-2i\eta)(v^{(0)} - v^{(1)}) \\
&= L^{(0)} - \tilde{L}^{(0)} - (U^{(1)} - \tilde{U}^{(1)}) \\
&= L^{(0)} - Q[L^{(0)}] - U^{(1)} + \big(R^{(1),uu} U^{(1)} + R^{(1),ul} L^{(1)}\big) \\
&= \big[I - Q\big] L^{(0)} + \big[-I + R^{(1),uu}\big] U^{(1)} + R^{(1),ul} L^{(1)}
\end{aligned}$$

and

$$\begin{aligned}
(-2)\Big(-\frac{\partial v^{inc}}{\partial \mathbf{n}^{(1)}}\Big) &= (-2)\Big(\frac{\partial v^{(0)}}{\partial \mathbf{n}^{(1)}} - \frac{\partial v^{(1)}}{\partial \mathbf{n}^{(1)}}\Big) \\
&= L^{(0)} + \tilde{L}^{(0)} + U^{(1)} + \tilde{U}^{(1)} \\
&= L^{(0)} + Q[L^{(0)}] + U^{(1)} + \big(R^{(1),uu} U^{(1)} + R^{(1),ul} L^{(1)}\big) \\
&= \big[I + Q\big] L^{(0)} + \big[I + R^{(1),uu}\big] U^{(1)} + R^{(1),ul} L^{(1)}.
\end{aligned}$$

For $m = 2, ..., M-1$, at $z = a_m + g_m(\xi; x)$,

$$
\begin{aligned}
0 &= (-2i\eta)(v^{(m-1)} - v^{(m)}) \\
&= L^{(m-1)} - \tilde{L}^{(m-1)} - (U^{(m)} - \tilde{U}^{(m)}) \\
&= L^{(m-1)} - \big(R^{(m-1),lu} U^{(m-1)} + R^{(m-1),ll} L^{(m-1)}\big) - U^{(m)} + \\
&\qquad \big(R^{(m),uu} U^{(m)} + R^{(m),ul} L^{(m)}\big) \\
&= -R^{(m-1),lu} U^{(m-1)} + \big[I - R^{(m-1),ll}\big] L^{(m-1)} + \big[-I + R^{(m),uu}\big] U^{(m)} \\
&\qquad + R^{(m),ul} L^{(m)}
\end{aligned}
$$

and

$$
\begin{aligned}
0 &= (-2)\Big(\frac{\partial v^{(m-1)}}{\partial \mathbf{n}^{(m)}} - \frac{\partial v^{(m)}}{\partial \mathbf{n}^{(m)}}\Big) \\
&= L^{(m-1)} + \tilde{L}^{(m-1)} + U^{(m)} + \tilde{U}^{(m)} \\
&= L^{(m-1)} + \big(R^{(m-1),lu} U^{(m-1)} + R^{(m-1),ll} L^{(m-1)}\big) + U^{(m)} + \\
&\qquad \big(R^{(m),uu} U^{(m)} + R^{(m),ul} L^{(m)}\big) \\
&= R^{(m-1),lu} U^{(m-1)} + \big[I + R^{(m-1),ll}\big] L^{(m-1)} + \big[I + R^{(m),uu}\big] U^{(m)} \\
&\qquad + R^{(m),ul} L^{(m)}.
\end{aligned}
$$

For $m = M$, at $z = a_M + g_M(\xi; x)$,

$$
\begin{aligned}
0 &= (-2i\eta)(v^{(M-1)} - v^{(M)}) \\
&= L^{(M-1)} - \tilde{L}^{(M-1)} - (U^{(M)} - \tilde{U}^{(M)}) \\
&= L^{(M-1)} - \big(R^{(M-1),lu}U^{(M-1)} + R^{(M-1),ll}L^{(M-1)}\big) - U^{(M)} + S[U^{(M)}]\big) \\
&= -R^{(M-1),lu}U^{(M-1)} + \big[I - R^{(M-1),ll}\big]L^{(M-1)} + \big[-I + S\big]U^{(M)}
\end{aligned}
$$

and

$$
\begin{aligned}
0 &= (-2)\Big(\frac{\partial v^{(M-1)}}{\partial \mathbf{n}^{(M)}} - \frac{\partial v^{(M)}}{\partial \mathbf{n}^{(M)}}\Big) \\
&= L^{(M-1)} + \tilde{L}^{(M-1)} + U^{(M)} + \tilde{U}^{(M)} \\
&= L^{(M-1)} + \big(R^{(M-1),ul}U^{(M-1)} + R^{(M-1),ll}L^{(M-1)}\big) + U^{(M)} + S[U^{(M)}] \\
&= R^{(M-1),ul}U^{(M-1)} + \big[I + R^{(M-1),ll}\big]L^{(M-1)} + \big[I + S\big]U^{(M)}.
\end{aligned}
$$

Now, in terms of the IIOs, the boundary conditions can be written as the linear system $A\bar{\mathbf{x}} = \mathbf{b}$, where

$$
A = \begin{bmatrix}
D_1 & U_1 & 0 & 0 & 0 & 0 & ... & 0 \\
L_2 & D_2 & U_2 & 0 & 0 & 0 & ... & 0 \\
0 & L_3 & D_3 & U_3 & 0 & 0 & ... & 0 \\
0 & 0 & \ddots & \ddots & \ddots & 0 & & \vdots \\
\vdots & \vdots & 0 & \ddots & \ddots & \ddots & \ddots & 0 \\
0 & 0 & & \ddots & \ddots & \ddots & \ddots & 0 \\
0 & 0 & ... & 0 & 0 & L_{M-1} & D_{M-1} & U_{M-1} \\
0 & 0 & ... & 0 & 0 & 0 & L_M & D_M
\end{bmatrix}
$$

$$\bar{\mathbf{x}} = \begin{bmatrix} L^{(0)} \\ U^{(1)} \\ \vdots \\ U^{(M-1)} \\ L^{(M-1)} \\ U^{(M)} \end{bmatrix}$$

$$\mathbf{b} = \begin{bmatrix} (-2i\eta)(-v^i(x, a_1 + g_1(\xi; x))) \\ (-2)\Big(- \frac{\partial v^i}{\partial \mathbf{n}^{(1)}}(x, a_1 + g_1(\xi; x))\Big) \\ 0 \\ \vdots \\ 0 \end{bmatrix}$$

$$D_1 = \begin{bmatrix} I - Q & -I + R^{(1),uu} \\ I + Q & I + R^{(1),uu} \end{bmatrix}$$

$$D_M = \begin{bmatrix} I - R^{(M-1),ll} & -I + S \\ I + R^{(M-1),ll} & I + S \end{bmatrix},$$

$$D_m = \begin{bmatrix} I - R^{(m-1),ll} & -I + R^{(m),uu} \\ I + R^{(m-1),ll} & I + R^{(m),uu} \end{bmatrix}, \text{ for } m = 2, ..., M-1$$

$$U_m = \begin{bmatrix} R^{(m),ul} & 0 \\ R^{(m),ul} & 0 \end{bmatrix}, \text{ for } m = 1, ..., M-1$$

$$L_m = \begin{bmatrix} 0 & -R^{(m-1),lu} \\ 0 & R^{(m-1),lu} \end{bmatrix}, \text{ for } m = 2, ..., M.$$

The mathematical model can now be stated as

$$\begin{cases} \Delta v^{(m)} + (k^{(m)})^2 v^{(m)} = 0, \ \ (x,z) \in \Omega_m(\xi), \ \text{ for } m = 0, ..., M \\ \partial_z v^{(0)} - T^{(0)}[v^{(0)}] = 0, \ \ z = a \\ A\bar{\mathbf{x}} = \mathbf{b}, \ \ z = a_m + g_m(\xi, x), \ \ m = 1, ..., M, \\ \partial_z v^{(M)} - T^{(M)}[v^{(M)}] = 0, \ \ z = b. \end{cases} \tag{3.1}$$

We can now break down the original problem into sub-problems. First, the linear system $A\bar{\mathbf{x}} = \mathbf{b}$ must be solved to find the surface quantities $L^{(m)}$ for $m = 0, 1..., M-1$ and $U^{(m)}$ for $m = 1, 2, ..., M$. Then the solutions $L^{(m)}$, $U^{(m)}$ may be input for the impedance data into the boundary value problem for each layer. The boundary value problems for the upper layer ($m = 0$), middle layers ($m = 1, ..., M-1$), and lower layer ($m = M$) are stated, respectively, below:

$$\begin{cases} \Delta v^{(0)} + (k^{(0)})^2 v^{(0)} = 0, \ \ (x,z) \in \Omega_0(\xi) \\ \partial_z v^{(0)} - T^{(0)}[v^{(0)}] = 0, \ \ z = a \\ -\frac{\partial v^{(0)}}{\partial \mathbf{n}^{(1)}} - i\eta v^{(0)} = L^{(0)}, \ \ z = a_1 + g_1(\xi; x) \end{cases} \tag{3.2}$$

$$\begin{cases} \Delta v^{(m)} + (k^{(m)})^2 v^{(m)} = 0, \ \ (x,z) \in \Omega_m(\xi) \\ \frac{\partial v^{(m)}}{\partial \mathbf{n}^{(m)}} - i\eta v^{(m)} = U^{(m)}, \ \ z = a_m + g_m(\xi; x) \\ -\frac{\partial v^{(m)}}{\partial \mathbf{n}^{(m+1)}} - i\eta v^{(m)} = L^{(m)}, \ \ z = a_{m+1} + g_{m+1}(\xi; x) \end{cases} \tag{3.3}$$

$$\begin{cases} \Delta v^{(M)} + (k^{(M)})^2 v^{(M)} = 0, \ \ (x,z) \in \Omega_M(\xi) \\ \frac{\partial v^{(M)}}{\partial \mathbf{n}^{(M)}} - i\eta v^{(M)} = U^{(M)}, \ \ z = a_M + g_M(\xi; x) \\ \partial_z v^{(M)} - T^{(M)}[v^{(M)}] = 0, \ \ z = b. \end{cases} \tag{3.4}$$

Finally, the boundary value problem in each layer may be solved independently of the other layers [46]. Since the boundary value problems above have a unique solution, the problem has been reduced to solving for the surface quantities $U^{(m)}$ for $m = 1, ..., M$ and $L^{(m)}$ for $m = 0, ..., M - 1$.

3.2 Method of Transformed Field Expansions

The method of Transformed Field Expansions was first proposed by Nicholls and Reitich in [37, 38]. The method of Transformed Field Expansions uses a change of variables to flatten the domain before utilizing the high order perturbation of surfaces expansions. This change of variables, which was introduced by Phillips in [44] and Chandezon in [8], provides stability to the numerical algorithms using high order perturbation of surfaces expansions and allows provable convergence of the solutions as is thoroughly shown by Nicholls and Reitich in [37, 38]. This section will discuss in detail the two primary components of the method of Transformed Field Expansions: the domain flattening change of variables and the high order perturbation of surfaces expansions.

3.2.1 Domain Flattening Change of Variables

At this point, the original problem has been broken down into sub-problems consisting of solving the linear system to find the impedance data and then using said impedance data to solve the boundary value problem in each layer (independently of the other layers). Our next step is to flatten the rough surfaces separating each layer. This is the start of implementing the method of Transformed Field Expansions. To do so we will perform the following domain-flattening change of variables for each random sample ξ [13, 31, 33, 36, 37, 38, 39]:

$$x' = x$$

and for each $m \in \{0, 1, ..., M\}$,

$$z' = a_{m+1}\Big(\frac{(a_m + g_m(\xi; x)) - z}{(h^{(m)} + g_m(\xi; x) - g_{m+1}(\xi; x)}\Big) + a_m\Big(\frac{z - (a_{m+1} + g_{m+1}(\xi; x))}{h^{(m)} + g_m(\xi; x) - g_{m+1}(\xi; x)}\Big)$$

for $a_{m+1} + g_{m+1}(\xi; x) < z < a_m + g_m(\xi; x)$, where $h^{(m)} = a_m - a_{m+1}$. Let $a_0 = a$, $a_{M+1} = b$, $g_0(\xi; x) = 0$, and $g_{M+1}(\xi; x) = 0$. Define the transformed fields to be

$$w^{(m)}(\xi; x', z') := v^{(m)}(\xi; x(x', z'), z(x', z'))$$

for $m = 0, 1, ..., M$.

Now we need the derivative formulas in terms of the new variables. These derivative formulas can be found via the chain rule. First, let

$$C^{(m)}(\xi; x) = C^{(m)}(\xi; x') = 1 + \frac{g_m(\xi; x') - g_{m+1}(\xi; x')}{h^{(m)}}$$

and

$$E^{(m)}(x', z') = \frac{(\partial_{x'} g_m - \partial_{x'} g_{m+1})z' + (a_m \partial_{x'} g_{m+1} - a_{m+1} \partial_{x'} g_m)}{h^{(m)}}.$$

Now, the derivative formulas are found as follows [36]:

$$
\begin{aligned}
C^{(m)}\partial_x &= C^{(m)}\Big(\frac{\partial}{\partial x'}\frac{\partial x'}{\partial x} + \frac{\partial}{\partial z'}\frac{\partial z'}{\partial x}\Big) \\
&= C^{(m)}\Big(\partial_{x'} + \\
&\quad (\partial_{z'})\Big(a_{m+1}\Big(\frac{(h^{(m)} + g_m - g_{m+1})(\partial_{x'}g_m) - (a_m + g_m - z)(\partial_{x'}g_m - \partial_{x'}g_{m+1})}{(h^{(m)} + g_m - g_{m+1})^2}\Big) + \\
&\quad a_m\Big(\frac{(h^{(m)} + g_m - g_{m+1})(-\partial_{x'}g_{m+1}) - (z - (a_{m+1} + g_{m+1}))(\partial_{x'}g_m - \partial_{x'}g_{m+1})}{(h^{(m)} + g_m - g_{m+1})^2}\Big)\Big) \\
&= C^{(m)}(\partial_{x'}) + (\partial_{z'})\Big(\frac{h^{(m)} + g_m - g_{m+1}}{h^{(m)}}\Big)\Big(\frac{a_{m+1}\partial_{x'}g_m}{h^{(m)} + g_m - g_{m+1}} - \\
&\quad (\partial_{x'}g_m - \partial_{x'}g_{m+1})\Big(a_{m+1}\Big(\frac{(a_m + g_m) - z}{(h^{(m)} + g_m - g_{m+1})^2}\Big) + a_m\Big(\frac{z - (a_{m+1} + g_{m+1})}{(h^{(m)} + g_m - g_{m+1}))^2}\Big)\Big) \\
&= C^{(m)}(\partial_{x'}) + (\partial_{z'})\Big(\frac{(a_{m+1}\partial_{x'}g_m - a_m\partial_{x'}g_{m+1}) - (\partial_{x'}g_m - \partial_{x'}g_{m+1})z'}{h^{(m)}}\Big) \\
&= C^{(m)}\partial_{x'} - E^{(m)}\partial_{z'} \\
C^{(m)}\partial_z &= C^{(m)}\Big(\frac{\partial}{\partial x'}\frac{\partial x'}{\partial z} + \frac{\partial}{\partial z'}\frac{\partial z'}{\partial z}\Big) \\
&= C^{(m)}\Big(0 + (\partial_{z'})\Big(\frac{-a_{m+1}}{h^{(m)} + g_m - g_{m+1}} + \frac{a_m}{h^{(m)} + g_m - g_{m+1}}\Big) \\
&= (\partial_{z'})\Big(\frac{h^{(m)} + g_m - g_{m+1}}{h^{(m)}}\Big)\Big(\frac{h^{(m)}}{h^{(m)} + g_m - g_{m+1}}\Big) \\
&= \partial_{z'}.
\end{aligned}
$$

With the derivative formulas in terms of the new variables, we can rewrite the differential equations and boundary conditions in terms of the change of variables. For each $m \in \{0, 1, ..., M\}$, multiplying $(C^{(m)})^2$ on both sides of the Helmholtz equation gives the following [36]:

$$
\begin{aligned}
0 &= (C^{(m)})^2\Big(\Delta v^{(m)} + (k^{(m)})^2 v^{(m)}\Big)\\
&= (C^{(m)})^2\frac{\partial}{\partial x}\Big(\frac{\partial w^{(m)}}{\partial x}\Big) + (C^{(m)})^2\frac{\partial}{\partial z}\Big(\frac{\partial w^{(m)}}{\partial z}\Big) + (C^{(m)})^2(k^{(m)})^2 w^{(m)}\\
&= C^{(m)}\frac{\partial}{\partial x}\Big(C^{(m)}\frac{\partial w^{(m)}}{\partial x}\Big) - C^{(m)}(\partial_x C^{(m)})\frac{\partial w^{(m)}}{\partial x} + C^{(m)}\frac{\partial}{\partial z}\Big(C^{(m)}\frac{\partial w^{(m)}}{\partial z}\Big) -\\
&\qquad C^{(m)}(\partial_z C^{(m)})\frac{\partial w^{(m)}}{\partial z} + (C^{(m)})^2(k^{(m)})^2 w^{(m)}\\
&= C^{(m)}\frac{\partial}{\partial x}\Big(C^{(m)}\partial_{x'}w^{(m)} - E^{(m)}\partial_{z'}w^{(m)}\Big) - (\partial_{x'}C^{(m)})\Big(C^{(m)}\partial_{x'}w^{(m)} - E^{(m)}\partial_{z'}w^{(m)}\Big) +\\
&\qquad C^{(m)}\frac{\partial}{\partial y}\Big(\partial_{z'}w^{(m)}\Big) + (C^{(m)})^2(k^{(m)})^2 w^{(m)}\\
&= C^{(m)}C^{(m)}\frac{\partial}{\partial x}\Big(\partial_{x'}w^{(m)}\Big) + C^{(m)}(\partial_{x'}C^{(m)})(\partial_{x'}w^{(m)}) - E^{(m)}C^{(m)}\frac{\partial}{\partial x}\Big(\partial_{z'}w^{(m)}\Big)\\
&\qquad - C^{(m)}\frac{\partial}{\partial x}\Big(E^{(m)}\Big)(\partial_{z'}w^{(m)}) - (\partial_{x'}C^{(m)})C^{(m)}(\partial_{x'}w^{(m)}) + (\partial_{x'}C^{(m)})E^{(m)}(\partial_{z'}w^{(m)}) +\\
&\qquad \partial_{z'}^2 w^{(m)} + (C^{(m)})^2(k^{(m)})^2 w^{(m)}\\
&= C^{(m)}\Big(C^{(m)}\partial_{x'}^2 w^{(m)} - E^{(m)}\partial_{z'}(\partial_{x'}w^{(m)})\Big) + C^{(m)}(\partial_{x'}C^{(m)})(\partial_{x'}w^{(m)}) -\\
&\qquad E^{(m)}\Big(C^{(m)}\partial_{x'}(\partial_{z'}w^{(m)}) - E^{(m)}\partial_{z'}^2 w^{(m)}\Big) - (\partial_{z'}w^{(m)})\Big(C^{(m)}\partial_{x'}E^{(m)} - E^{(m)}\partial_{z'}E^{(m)}\Big) -\\
&\qquad (\partial_{x'}C^{(m)})C^{(m)}(\partial_{x'}w^{(m)}) + (\partial_{x'}C^{(m)})E^{(m)}(\partial_{z'}w^{(m)}) + \partial_{z'}^2 w^{(m)} + (C^{(m)})^2(k^{(m)})^2 w^{(m)}\\
&= (C^{(m)})^2(k^{(m)})^2 w^{(m)} + B^{(m)}\cdot\nabla' w^{(m)} + \Big((C^{(m)})^2\partial_{x'}^2 w^{(m)} + C^{(m)}(\partial_{x'}C^{(m)})(\partial_{x'}w^{(m)}) -\\
&\qquad C^{(m)}E^{(m)}\partial_{x'}(\partial_{z'}w^{(m)})\Big) + \Big((E^{(m)})^2\partial_{z'}^2 w^{(m)} + \partial_{z'}^2 w^{(m)} - C^{(m)}E^{(m)}\partial_{z'}(\partial_{x'}w^{(m)}) -\\
&\qquad C^{(m)}(\partial_{x'}E^{(m)})(\partial_{z'}w^{(m)}) + E^{(m)}(\partial_{z'}E^{(m)}(\partial_{z'}w^{(m)})\Big)\\
&= (C^{(m)})^2(k^{(m)})^2 w^{(m)} + B^{(m)}\cdot\nabla' w^{(m)} + \partial_{x'}\Big((C^{(m)})^2\partial_{x'}w^{(m)}\Big) + C^{(m)}(\partial_{x'}C^{(m)})(\partial_{x'}w^{(m)}) +\\
&\qquad \partial_{x'}\Big(-C^{(m)}E^{(m)}\partial_{z'}w^{(m)}\Big) + (\partial_{x'}C^{(m)})E^{(m)}(\partial_{z'}w^{(m)}) + \partial_{z'}\Big((E^{(m)})^2\partial_{z'}w^{(m)} + \partial_{z'}w^{(m)}\Big) +\\
&\qquad \partial_{z'}\Big(-C^{(m)}E^{(m)}\partial_{x'}w^{(m)}\Big) - E^{(m)}(\partial_{z'}E^{(m)})(\partial_{z'}w^{(m)}) + C^{(m)}(\partial_{z'}E^{(m)})(\partial_{x'}w^{(m)})\\
&= (C^{(m)})^2(k^{(m)})^2 w^{(m)} + B^{(m)}\cdot\nabla' w^{(m)} + \nabla'\cdot\begin{bmatrix}(C^{(m)})^2\partial_{x'}w^{(m)} - C^{(m)}E^{(m)}\partial_{z'}w^{(m)}\\ -C^{(m)}E^{(m)}\partial_{x'}w^{(m)} + (1+(E^{(m)})^2)\partial_{z'}w^{(m)}\end{bmatrix} -\\
&\qquad C^{(m)}(\partial_{x'}C^{(m)})(\partial_{x'}w^{(m)}) + (\partial_{x'}C^{(m)})E^{(m)}(\partial_{z'}w^{(m)}) - E^{(m)}(\partial_{z'}E^{(m)})(\partial_{z'}w^{(m)}) +\\
&\qquad C^{(m)}(\partial_{z'}E^{(m)})(\partial_{x'}w^{(m)})
\end{aligned}
$$

$$
\begin{aligned}
&= \nabla' \cdot \left(A^{(m)} \nabla' w^{(m)}\right) + B^{(m)} \cdot \nabla' w^{(m)} + (C^{(m)})^2 (k^{(m)})^2 w^{(m)} - C^{(m)} (\partial_{x'} C^{(m)})(\partial_{x'} w^{(m)}) + \\
&\qquad (\partial_{x'} C^{(m)}) E^{(m)} (\partial_{z'} w^{(m)}) - (\partial_{z'} w^{(m)}) E^{(m)} (\partial_{z'} E^{(m)}) + C^{(m)} (\partial_{z'} E^{(m)})(\partial_{x'} w^{(m)}) \\
&= \nabla' \cdot \left(A^{(m)} \nabla' w^{(m)}\right) + B^{(m)} \cdot \nabla' w^{(m)} + (C^{(m)})^2 (k^{(m)})^2 w^{(m)} + \\
&\qquad \left(\partial_{z'} E^{(m)} - \partial_{x'} C^{(m)}\right)\left(C^{(m)} \partial_{x'} w^{(m)} - E^{(m)} \partial_{z'} w^{(m)}\right) \\
&= \nabla' \cdot \left(A^{(m)} \nabla' w^{(m)}\right) + B^{(m)} \cdot \nabla' w^{(m)} + (C^{(m)})^2 (k^{(m)})^2 w^{(m)} + \\
&\qquad \left(\frac{(\partial_{x'} g_m - \partial_{x'} g_{m+1})}{h^{(m)}} - \frac{(\partial_{x'} g_m - \partial_{x'} g_{m+1})}{h^{(m)}}\right)\left(C^{(m)} \partial_{x'} w^{(m)} - E^{(m)} \partial_{z'} w^{(m)}\right) \\
&= \nabla' \cdot \left(A^{(m)} \nabla' w^{(m)}\right) + B^{(m)} \cdot \nabla' w^{(m)} + (C^{(m)})^2 (k^{(m)})^2 w^{(m)}.
\end{aligned}
$$

Therefore, for each $m \in \{0, 1, ..., M\}$,

$$\Delta v^{(m)} + (k^{(m)})^2 v^{(m)} = 0, \ a_{m+1} + g_{m+1} < z < a_m + g_m,$$

transforms to

$$\nabla' \cdot \left(A^{(m)} \nabla' w^{(m)}\right) + B^{(m)} \cdot \nabla' w^{(m)} + (C^{(m)})^2 (k^{(m)})^2 w^{(m)} = 0, \ a_{m+1} < z' < a_m,$$

where $A^{(m)} = \begin{bmatrix} (C^{(m)})^2 & -E^{(m)} C^{(m)} \\ -E^{(m)} C^{(m)} & 1 + (E^{(m)})^2 \end{bmatrix}$, and $B^{(m)} = \begin{bmatrix} -(\partial_{x'} C^{(m)}) C^{(m)} \\ (\partial_{x'} C^{(m)}) E^{(m)} \end{bmatrix}$. Now, by adding and subtracting $\Delta w^{(m)}$ and $(k^{(m)})^2 w^{(m)}$ to one side of the transformed equation, we have the following:

$$
\begin{aligned}
0 &= \nabla' \cdot \Big(A^{(m)} \nabla' w^{(m)} \Big) + B^{(m)} \cdot \nabla' w^{(m)} + (C^{(m)})^2 (k^{(m)})^2 w^{(m)} \\
&= \nabla' \cdot \Big(A^{(m)} \nabla' w^{(m)} \Big) + B^{(m)} \cdot \nabla' w^{(m)} + (C^{(m)})^2 (k^{(m)})^2 w^{(m)} + \\
&\qquad \Delta' w^{(m)} - \Delta' w^{(m)} + (k^{(m)})^2 w^{(m)} - (k^{(m)})^2 w^{(m)} \\
&= \Delta' w^{(m)} + (k^{(m)})^2 w^{(m)} + \nabla' \cdot \Big(\Big(A^{(m)} - I \Big) \nabla' w^{(m)} \Big) + B^{(m)} \cdot \nabla' w^{(m)} + \\
&\qquad \Big((C^{(m)})^2 - 1 \Big) (k^{(m)})^2 w^{(m)}.
\end{aligned}
$$

Now, for each $m \in \{0, 1, ..., M\}$, define $F^{(m)} = \nabla' \cdot \Big(\Big(I - A^{(m)} \Big) \nabla' w^{(m)} \Big) - B^{(m)} \cdot \nabla' w^{(m)} + (k^{(m)})^2 \Big(1 - (C^{(m)})^2 \Big) w^{(m)}$, so that we have

$$
\Delta' w^{(m)} + (k^{(m)})^2 w^{(m)} = F^{(m)}, \ a_{m+1} < z' < a_m.
$$

Note that $F^{(m)}$ is $O(g^{(m)})$, so that it is "order one" or greater.

We also need to rewrite the boundary conditions in terms of the change of variables. First, let's note that at $z' = a_m$, $E^{(m)}(x', a_m) = \partial_{x'} g_m(x')$, and at $z' = a_{m+1}$, $E^{(m)}(x', a_{m+1}) = \partial_{x'} g_{m+1}(x')$. For the boundary condition $\dfrac{\partial v^{(m)}}{\partial \mathbf{n}^{(m)}} - i\eta v^{(m)} = U^{(m)}$ at $z = a_m + g_m(\xi; x)$, for $m = 1, 2, ..., M$, we can now write the boundary condition in terms of the change of variables by multiplying both sides of the equation by $C^{(m)}$. This gives the following:

$$\begin{aligned}
C^{(m)}U^{(m)} &= C^{(m)}\Big(\frac{\partial v^{(m)}}{\partial \mathbf{n}^{(m)}} - i\eta v^{(m)}\Big) \\
&= C^{(m)}\Big(\nabla v^{(m)} \cdot \mathbf{n}^{(m)} - i\eta v^{(m)}\Big) \\
&= C^{(m)}\Big(- (\partial_{x'} g_m)(\partial_x v^{(m)}) + \partial_z v^{(m)} - i\eta v^{(m)}\Big) \\
&= -(\partial_x g_m)\Big(C^{(m)}\partial_x v^{(m)}\Big) + C^{(m)}\partial_z v^{(m)} - i\eta C^{(m)} v^{(m)} \\
&= -(\partial_{x'} g_m)\Big(C^{(m)}\partial_{x'} w^{(m)} - E^{(m)}\partial_{z'} w^{(m)}\Big) + \partial_{z'} w^{(m)} - i\eta C^{(m)} w^{(m)}.
\end{aligned}$$

So at $z' = a_m$, we have

$$\begin{aligned}
-(\partial_{x'} a_m)\Big(1 + \frac{g_m - g_{m+1}}{h^{(m)}}\Big)(\partial_{x'} w^{(m)}) + (\partial_{x'} g_m)^2(\partial_{z'} w^{(m)}) \\
+\partial_{z'} w^{(m)} - i\eta\Big(1 + \frac{g_m - g_{m+1}}{h^{(m)}}\Big) w^{(m)} = \Big(1 + \frac{g_m - g_{m+1}}{h^{(m)}}\Big) U^{(m)},
\end{aligned}$$

which gives

$$\partial_{z'} w^{(m)} - i\eta w^{(m)} = U^{(m)} + J^{(m),u},$$

where

$$\begin{aligned}
J^{(m),u} = \Bigg[&\Big(\frac{g_m - g_{m+1}}{h^{(m)}}\Big) U^{(m)} + i\eta\Big(\frac{g_m - g_{m+1}}{h^{(m)}}\Big) w^{(m)} + (\partial_{x'} g_m)(\partial_{x'} w^{(m)}) + \\
&(\partial_{x'} g_m)\Big(\frac{g_m - g_{m+1}}{h^{(m)}}\Big)(\partial_{x'} w^{(m)}) - (\partial_{x'} g_m)^2(\partial_{z'} w^{(m)})\Bigg]\Bigg|_{z'=a_m}.
\end{aligned}$$

Similarly, for $m \in \{0, 1, ..., M-1\}$, the boundary condition $-\dfrac{\partial v^{(m)}}{\partial \mathbf{n}^{(m+1)}} - i\eta v^{(m)} = L^{(m)}$ at $z = a_{m+1} + g_{m+1}(\xi; x)$ in terms of the change of variables is given by

$$-\partial_{z'} w^{(m)} - i\eta w^{(m)} = L^{(m)} + J^{(m),l}, \; z' = a_{m+1},$$

where

$$J^{(m),l} = \Bigg[\Big(\frac{g_m - g_{m+1}}{h^{(m)}}\Big) L^{(m)} + i\eta \Big(\frac{g_m - g_{m+1}}{h^{(m)}}\Big) w^{(m)} - (\partial_{x'} g_{m+1})(\partial_{x'} w^{(m)}) - \\ (\partial_{x'} g_{m+1}) \Big(\frac{g_m - g_{m+1}}{h^{(m)}}\Big)(\partial_{x'} w^{(m)}) + (\partial_{x'} g_{m+1})^2 (\partial_{z'} w^{(m)}) \Bigg] \Big|_{z'=a_{m+1}}.$$

The boundary conditions at the artificial boundaries, $\partial_z v^{(0)} - T^{(0)}[v^{(0)}] = 0, \;\; z = a$, and $\partial_z v^{(M)} - T^{(M)}[v^{(M)}] = 0, \;\; z = b$, can similarly be rewritten in terms of the change of variables by first multiplying on both sides of the equations by $C^{(0)}$ and $C^{(M)}$, respectively, as follows:

$$\begin{aligned} 0 &= C^{(0)} \Big(\partial_z v^{(0)} - T^{(0)}[v^{(0)}] \Big) \\ &= C^{(0)} \partial_z v^{(0)} - C^{(0)} T^{(0)}[v^{(0)}] \\ &= \partial_{z'} w^{(0)} - \Big(1 + \frac{g_0 - g_1}{h^{(0)}}\Big) T^{(0)}[w^{(0)}] \end{aligned}$$

and

$$\begin{aligned} 0 &= C^{(M)} \Big(\partial_z v^{(M)} - T^{(M)}[v^{(M)}] \Big) \\ &= C^{(M)} \partial_z v^{(M)} - C^{(M)} T^{(M)}[v^{(M)}] \\ &= \partial_{z'} w^{(M)} - \Big(1 + \frac{g_M - g_{M+1}}{h^{(M)}}\Big) T^{(M)}[w^{(M)}]. \end{aligned}$$

Therefore, the boundary conditions at the artificial boundaries in terms of the change of variables are given by

$$\partial_{z'} w^{(0)} - T^{(0)}[w^{(0)}] = D^{(0)},\ z' = a_0$$

and

$$\partial_{z'} w^{(M)} - T^{(M)}[w^{(M)}] = D^{(M)},\ z' = a_{M+1},$$

where

$$D^{(0)} = \left[\Big(\frac{g_0 - g_1}{h^{(0)}}\Big)T^{(0)}[w^{(0)}]\right]\Big|_{z'=a_0} = \left[\Big(\frac{-g_1}{h^{(0)}}\Big)T^{(0)}[w^{(0)}]\right]\Big|_{z'=a}$$

and

$$D^{(M)} = \left[\Big(\frac{g_M - g_{M+1}}{h^{(M)}}\Big)T^{(M)}[w^{(M)}]\right]\Big|_{z'=a_{M+1}} = \left[\Big(\frac{g_M}{h^{(M)}}\Big)T^{(M)}[w^{(M)}]\right]\Big|_{z'=b}.$$

Finally, we need to write the IIOs in terms of the change of variables. Again, we must multiply both sides of the equations

$$Q[L^{(0)}] = \Big(-\frac{\partial v^{(0)}}{\partial n^{(1)}} + i\eta v^{(0)}\Big)\Big|_{z=a_1+g_1(\xi;x)},$$

$$R^{(m)} \begin{bmatrix} U^{(m)} \\ L^{(m)} \end{bmatrix} = \begin{bmatrix} \Big(\frac{\partial v^{(m)}}{\partial n^{(m)}} + i\eta v^{(m)}\Big)\Big|_{z=a_m+g_m(\xi;x)} \\ \Big(-\frac{\partial v^{(m)}}{\partial n^{(m+1)}} + i\eta v^{(m)}\Big)\Big|_{z=a_{m+1}+g_{m+1}(\xi;x)} \end{bmatrix},$$

and

$$S[U^{(M)}] = \Big(\frac{\partial v^{(M)}}{\partial n^{(M)}} + i\eta v^{(M)}\Big)\Big|_{z=a_M+g_M(\xi;x)}$$

by $C^{(0)}$, $C^{(m)}$ for $m \in \{1, 2, ..., M-1\}$, and $C^{(M)}$, respectively. Doing so gives the following for the upper layer:

$$\begin{aligned}
C^{(0)}Q[L^{(0)}] &= C^{(0)}\Big(-\frac{\partial v^{(0)}}{\partial \mathbf{n}^{(1)}} + i\eta v^{(0)}\Big)\Big|_{z=a_1+g_1} \\
&= C^{(0)}\Big(-\nabla v^{(0)} \cdot \mathbf{n}^{(1)} + i\eta v^{(0)}\Big)\Big|_{z=a_1+g_1} \\
&= C^{(0)}\Big(-\partial_z v^{(0)} + (\partial_x g_1)(\partial_x v^{(0)}) + i\eta v^{(0)}\Big)\Big|_{z=a_1+g_1} \\
&= \Big(-\partial_{z'} w^{(0)} + (\partial_{x'} g_1)\Big(C^{(0)}\partial_{x'} w^{(0)} - (\partial_{x'} g_1)(\partial_{z'} w^{(0)})\Big) + \\
&\qquad i\eta\Big(1 + \frac{g_0 - g_1}{h^{(0)}}\Big)w^{(0)}\Big)\Big|_{z'=a_1}.
\end{aligned}$$

Since $C^{(0)}Q[L^{(0)}] = \Big(1 + \frac{g_0 - g_1}{h^{(0)}}\Big)Q[L^{(0)}]$, we have

$$\begin{aligned}
Q[L^{(0)}] &= \Big(-\partial_{z'} w^{(0)} + i\eta w^{(0)}\Big)\Big|_{z'=a_1} - \Big(\frac{g_0 - g_1}{h^{(0)}}\Big)Q[L^{(0)}] \\
&\quad + \Bigg[(\partial_{x'} g_1)\Big(1 + \frac{g_0 - g_1}{h^{(0)}}\Big)(\partial_{x'} w^{(0)}) - (\partial_{x'} g_1)^2(\partial_{z'} w^{(0)}) \\
&\quad + i\eta\Big(\frac{g_0 - g_1}{h^{(0)}}\Big)w^{(0)}\Bigg]\Bigg|_{z'=a_1}.
\end{aligned}$$

So the IIO in the upper layer in terms of the change of variables is given by

$$Q[L^{(0)}] = \Big(-\partial_{z'} w^{(0)} + i\eta w^{(0)}\Big)\Big|_{z'=a_1} + K^{(0),l},$$

where

$$K^{(0),l} = \left[(\partial_{x'} g_1)\Big(1 + \frac{g_0 - g_1}{h^{(0)}}\Big)(\partial_{x'} w^{(0)}) - (\partial_{x'} g_1)^2 (\partial_{z'} w^{(0)}) + i\eta\Big(\frac{g_0 - g_1}{h^{(0)}}\Big) w^{(0)} \right]\Big|_{z'=a_1}$$
$$- \Big(\frac{g_0 - g_1}{h^{(0)}}\Big) Q[L^{(0)}]$$
$$= \left[(\partial_{x'} g_1)\Big(1 - \frac{g_1}{h^{(0)}}\Big)(\partial_{x'} w^{(0)}) - (\partial_{x'} g_1)^2 (\partial_{z'} w^{(0)}) - i\eta\Big(\frac{g_1}{h^{(0)}}\Big) w^{(0)} \right]\Big|_{z'=a_1}$$
$$+ \Big(\frac{g_1}{h^{(0)}}\Big) Q[L^{(0)}].$$

Similarly, the IIO in the lower layer in terms of the change of variables is given by

$$S[U^{(M)}] = \Big(\partial_{z'} w^{(M)} + i\eta w^{(M)}\Big)\Big|_{z'=a_M} + K^{(M),u},$$

where

$$K^{(M),u} = \Bigg[-(\partial_{x'} g_M)\Big(1 + \frac{g_M - g_{M+1}}{h^{(M)}}\Big)(\partial_{x'} w^{(M)}) + (\partial_{x'} g_M)^2 (\partial_{z'} w^{(M)}) +$$
$$i\eta\Big(\frac{g_M - g_{M+1}}{h^{(M)}}\Big) w^{(M)} \Bigg]\Big|_{z'=a_M} - \Big(\frac{g_M - g_{M+1}}{h^{(M)}}\Big) S[U^{(M)}]$$
$$= \Bigg[-(\partial_{x'} g_M)\Big(1 + \frac{g_M}{h^{(M)}}\Big)(\partial_{x'} w^{(M)}) + (\partial_{x'} g_M)^2 (\partial_{z'} w^{(M)}) +$$
$$i\eta\Big(\frac{g_M}{h^{(M)}}\Big) w^{(M)} \Bigg]\Big|_{z'=a_M} - \Big(\frac{g_M}{h^{(M)}}\Big) S[U^{(M)}]$$

Now, for the inner layers, let's first write

$$R^{(m)} \begin{bmatrix} U^{(m)} \\ L^{(m)} \end{bmatrix} = \begin{bmatrix} \Big(\frac{\partial v^{(m)}}{\partial \mathbf{n}^{(m)}} + i\eta v^{(m)}\Big)\Big|_{z=a_m+g_m(\xi;x)} \\ \Big(-\frac{\partial v^{(m)}}{\partial \mathbf{n}^{(m+1)}} + i\eta v^{(m)}\Big)\Big|_{z=a_{m+1}+g_{m+1}(\xi;x)} \end{bmatrix}$$

as

$$\begin{bmatrix} R^{(m),u}[U^{(m)}, L^{(m)}] \\ R^{(m),l}[U^{(m)}, L^{(m)}] \end{bmatrix} = \begin{bmatrix} \left(\frac{\partial v^{(m)}}{\partial \mathbf{n}^{(m)}} + i\eta v^{(m)}\right)\Big|_{z=a_m+g_m(\xi;x)} \\ \left(-\frac{\partial v^{(m)}}{\partial \mathbf{n}^{(m+1)}} + i\eta v^{(m)}\right)\Big|_{z=a_{m+1}+g_{m+1}(\xi;x)} \end{bmatrix}.$$

Similar to the upper and lower layers, after multiplying both sides of the equation by $C^{(m)}$, the IIOs in the middle layers in terms of the change of variables are given by

$$\begin{bmatrix} R^{(m),u}[U^{(m)}, L^{(m)}] \\ R^{(m),l}[U^{(m)}, L^{(m)}] \end{bmatrix} = \begin{bmatrix} \left(\partial_{z'} w^{(m)} + i\eta w^{(m)}\right)\Big|_{z'=a_m} \\ \left(-\partial_{z'} w^{(m)} + i\eta w^{(m)}\right)\Big|_{z'=a_{m+1}} \end{bmatrix} + \begin{bmatrix} K^{(m),u} \\ K^{(m),l} \end{bmatrix},$$

where

$$\begin{aligned} K^{(m),u} = \Bigg[& (-\partial_{x'} g_m)(\partial_{x'} w^{(m)}) + \left(\frac{g_m - g_{m+1}}{h^{(m)}}\right)(-\partial_{x'} g_m)(\partial_{x'} w^{(m)}) + (\partial_{x'} g_m)^2 (\partial_{z'} w^{(m)}) + \\ & i\eta \left(\frac{g_m - g_{m+1}}{h^{(m)}}\right) w^{(m)} \Bigg]\Bigg|_{z'=a_m} - \left(\frac{g_m - g_{m+1}}{h^{(m)}}\right) R^{(m),u}[U^{(m)}, L^{(m)}] \end{aligned}$$

and

$$\begin{aligned} K^{(m),l} = \Bigg[& (\partial_{x'} g_{m+1})(\partial_{x'} w^{(m)}) + \left(\frac{g_m - g_{m+1}}{h^{(m)}}\right)(\partial_{x'} g_{m+1})(\partial_{x'} w^{(m)}) - (\partial_{x'} g_{m+1})^2 (\partial_{z'} w^{(m)}) + \\ & i\eta \left(\frac{g_m - g_{m+1}}{h^{(m)}}\right) w^{(m)} \Bigg]\Bigg|_{z'=a_{m+1}} - \left(\frac{g_m - g_{m+1}}{h^{(m)}}\right) R^{(m),l}[U^{(m)}, L^{(m)}]. \end{aligned}$$

Therefore, the governing equations in terms of the domain-flattening change of variables in each layer are given by

$$\begin{cases} \Delta w^{(0)} + (k^{(0)})^2 w^{(0)} = F^{(0)},\ a_1 < z' < a \\ \partial_{z'} w^{(0)} - T^{(0)}[w^{(0)}] = D^{(0)},\ z' = a \\ -\partial_{z'} w^{(0)} - i\eta w^{(0)} = L^{(0)} + J^{(0),l},\ z' = a_1 \end{cases} \tag{3.5}$$

$$\begin{cases} \Delta w^{(m)} + (k^{(m)})^2 w^{(m)} = F^{(m)},\ a_{m+1} < z' < a_m, \text{ for } m = 1, ..., M-1 \\ \partial_{z'} w^{(m)} - i\eta w^{(m)} = U^{(m)} + J^{(m),u},\ z' = a_m, \text{ for } m = 1, ..., M-1 \\ -\partial_{z'} w^{(m)} - i\eta w^{(m)} = L^{(m)} + J^{(m),l},\ z' = a_{m+1}, \text{ for } m = 1, ..., M-1 \end{cases} \tag{3.6}$$

$$\begin{cases} \Delta w^{(M)} + (k^{(M)})^2 w^{(M)} = F^{(M)},\ b < z' < a_M \\ \partial_{z'} w^{(M)} - i\eta w^{(M)} = U^{(M)} + J^{(M),u},\ z' = a_M \\ \partial_{z'} w^{(m)} - T^{(M)}[w^{(M)}] = D^{(M)},\ z' = b. \end{cases} \tag{3.7}$$

3.2.2 High Order Perturbation of Surfaces

Recall that the deviations of the surface from "flat" are parameterized by ε, i.e.

$$g_m(\xi; x) = \varepsilon \tilde{g}_m(\xi; x)$$

for $m = 1, ..., M$, where $\varepsilon \in (0, 1)$. This parameterization of the surface leads to a Taylor expansion of the solutions

$$w^{(m)} = w^{(m)}(\xi; x', z'; \varepsilon) = \sum_{n=0}^{\infty} w_n^{(m)}(\xi; x', z')\varepsilon^n \tag{3.8}$$

for $m = 0, ..., M$ [6, 13, 39]. Work done by Nicholls, Reitich, and Shen have shown that for deterministic profiles, the solutions $w^{(m)}$ depend analytically upon ε, which leads to the convergence of the series [17, 32, 38]. Since the unknown surface quantities $L^{(m)}$, $U^{(m)}$, $\tilde{L}^{(m)}$, and $\tilde{U}^{(m)}$ are defined in terms of the solutions of the scattered fields, we may also expand the surface quantities and the IIOs as

$$L^{(m)}(\xi;x) = \sum_{n=0}^{\infty} L_n^{(m)}(\xi;x)\varepsilon^n \text{ for } m = 0, ..., M-1 \tag{3.9}$$

$$U^{(m)}(\xi;x) = \sum_{n=0}^{\infty} U_n^{(m)}(\xi;x)\varepsilon^n, \text{ for } m = 1, ..., M \tag{3.10}$$

$$Q[L^{(0)}] = \sum_{n=0}^{\infty} Q_n[L^{(0)}]\varepsilon^n \tag{3.11}$$

$$S[U^{(M)}] = \sum_{n=0}^{\infty} S_n[U^{(M)}]\varepsilon^n \tag{3.12}$$

$$\begin{pmatrix} R^{(m),u}[U^{(m)}, L^{(m)}] \\ R^{(m),l}[U^{(m)}, L^{(m)}] \end{pmatrix} = \sum_{n=0}^{\infty} \begin{pmatrix} R_n^{(m),u}[U^{(m)}, L^{(m)}] \\ R_n^{(m),l}[U^{(m)}, L^{(m)}] \end{pmatrix} \varepsilon^n \text{ for } m = 1, ..., M-1. \tag{3.13}$$

After inserting the expansions (3.8), (3.9), (3.10), (3.11), (3.12), and (3.13) into the governing equations, we see that at each perturbation order, n, we have the following set of equations for the upper layer ($m = 0$), middle layers ($m = 1, ..., M-1$), and the lower layer ($m = M$), respectively:

$$\begin{cases} \Delta w_n^{(0)} + (k^{(0)})^2 w_n^{(0)} = F_n^{(0)},\ a_1 < z' < a \\ \partial_{z'} w_n^{(0)} - T^{(0)}[w_n^{(0)}] = D_n^{(0)},\ z' = a \\ -\partial_{z'} w_n^{(0)} - i\eta w_n^{(0)} = L_n^{(0)} + J_n^{(0),l},\ z' = a_1 \end{cases} \tag{3.14}$$

$$\begin{cases} \Delta w_n^{(m)} + (k^{(m)})^2 w_n^{(m)} = F_n^{(m)},\ a_{m+1} < z' < a_m, \text{ for } m = 1, ..., M-1 \\ \partial_{z'} w_n^{(m)} - i\eta w_n^{(m)} = U_n^{(m)} + J_n^{(m),u},\ z' = a_m, \text{ for } m = 1, ..., M \\ -\partial_{z'} w_n^{(m)} - i\eta w_n^{(m)} = L_n^{(m)} + J_n^{(m),l},\ z' = a_{m+1}, \text{ for } m = 1, ..., M-1 \end{cases} \tag{3.15}$$

$$
\begin{cases}
\Delta w_n^{(M)} + (k^{(M)})^2 w_n^{(M)} = F_n^{(M)},\ b < z' < a_M \\
\partial_{z'} w_n^{(M)} - i\eta w_n^{(M)} = U_n^{(M)} + J_n^{(M),u},\ z' = a_M \\
\partial_{z'} w_n^{(M)} - T^{(M)}[w_n^{(M)}] = D_n^{(M)},\ z' = b
\end{cases}
\tag{3.16}
$$

where

$$
\begin{aligned}
F_n^{(m)} = \nabla' \cdot \Big(& - A_{1,0}^{(m)} \nabla' w_{n-1}^{(m)} - A_{0,1}^{(m)} \nabla' w_{n-1}^{(m)} - A_{2,0}^{(m)} \nabla' w_{n-2}^{(m)} - A_{1,1}^{(m)} \nabla' w_{n-2}^{(m)} - A_{0,2}^{(m)} \nabla' w_{n-2}^{(m)} \Big) - \\
& \Big(B_{1,0}^{(m)} \cdot \nabla' w_{n-1}^{(m)} + B_{0,1}^{(m)} \cdot \nabla' w_{n-1}^{(m)} + B_{1,1}^{(m)} \cdot \nabla' w_{n-2}^{(m)} + B_{2,0}^{(m)} \cdot \nabla' w_{n-2}^{(m)} + B_{0,2}^{(m)} \cdot \nabla' w_{n-2}^{(m)} \Big) - \\
& (k^{(m)})^2 \Big((C^{(1)})^2_{1,0} w_{n-1}^{(m)} + (C^{(1)})^2_{0,1} w_{n-1}^{(m)} + (C^{(1)})^2_{1,1} w_{n-2}^{(m)} + (C^{(1)})^2_{2,0} w_{n-2}^{(m)} + (C^{(1)})^2_{0,2} w_{n-2}^{(m)} \Big),
\end{aligned}
$$

$$
A_{1,0}^{(m)} = \frac{1}{h^{(m)}} \begin{bmatrix} 2\tilde{g}_m & -(\partial_{x'} \tilde{g}_m)(z' - a_{m+1}) \\ -(\partial_{x'} \tilde{g}_m)(z' - a_{m+1}) & 0 \end{bmatrix},
$$

$$
A_{0,1}^{(m)} = \frac{1}{h^{(m)}} \begin{bmatrix} -2\tilde{g}_{m+1} & -(\partial_{x'} \tilde{g}_{m+1})(a_m - z') \\ -(\partial_{x'} \tilde{g}_{m+1})(a_m - z') & 0 \end{bmatrix}
$$

$$
A_{1,1}^{(m)} = \frac{1}{(h^{(m)})^2} \begin{bmatrix} A_{1,1}^{(m),11} & A_{1,1}^{(m),12} \\ A_{1,1}^{(m),21} & A_{1,1}^{(m),22} \end{bmatrix}
$$

$$
A_{1,1}^{(m),11} = -2\tilde{g}_m \tilde{g}_{m+1}
$$

$$
A_{1,1}^{(m),12} = \tilde{g}_{m+1} (\partial_{x'} \tilde{g}_m)(z' - a_{m+1}) - \tilde{g}_m (\partial_{x'} \tilde{g}_{m+1})(a_m - z')
$$

$$
A_{1,1}^{(m),21} = \tilde{g}_{m+1} (\partial_{x'} \tilde{g}_m)(z' - a_{m+1}) - \tilde{g}_m (\partial_{x'} \tilde{g}_{m+1} (a_m - z')
$$

$$
A_{1,1}^{(m),22} = 2(\partial_{x'} \tilde{g}_m)(\partial_{x'} \tilde{g}_{m+1})(z' - a_{m+1})(a_m - z')
$$

$$
A_{2,0}^{(m)} = \frac{1}{(h^{(m)})^2} \begin{bmatrix} (\tilde{g}_m)^2 & -(\tilde{g}_m)(\partial_{x'} \tilde{g}_m)(z' - a_{m+1}) \\ -(\tilde{g}_m)(\partial_{x'} \tilde{g}_m)(z' - a_{m+1}) & (\partial_{x'} \tilde{g}_m)^2 (z' - a_{m+1})^2 \end{bmatrix}
$$

$$A_{0,2}^{(m)} = \frac{1}{(h^{(m)})^2}\begin{bmatrix} (\tilde{g}_{m+1})^2 & (\tilde{g}_{m+1})(\partial_{x'}\tilde{g}_{m+1})(a_m - z') \\ (\tilde{g}_{m+1})(\partial_{x'}\tilde{g}_{m+1})(a_m - z') & (\partial_{x'}\tilde{g}_{m+1})^2(a_m - z')^2 \end{bmatrix}$$

$$B_{1,0}^{(m)} = \frac{1}{h^{(m)}}\begin{bmatrix} -\partial_{x'}\tilde{g}_m \\ 0 \end{bmatrix}$$

$$B_{0,1}^{(m)} = \frac{1}{h^{(m)}}\begin{bmatrix} \partial_{x'}\tilde{g}_{m+1} \\ 0 \end{bmatrix}$$

$$B_{1,1}^{(m)} = \frac{1}{(h^{(m)})^2}\begin{bmatrix} (\partial_{x'}\tilde{g}_m)(\tilde{g}_{m+1}) + (\partial_{x'}\tilde{g}_{m+1})(\tilde{g}_m) \\ (\partial_{x'}\tilde{g}_m)(\partial_{x'}\tilde{g}_{m+1})((a_m - z') - (z' - a_{m+1})) \end{bmatrix}$$

$$B_{2,0}^{(m)} = \frac{1}{(h^{(m)})^2}\begin{bmatrix} -(\partial_{x'}\tilde{g}_m)(\tilde{g}_m) \\ (\partial_{x'}g_m)^2(z' - a_{m+1}) \end{bmatrix}$$

$$B_{0,2}^{(m)} = \frac{1}{(h^{(m)})^2}\begin{bmatrix} -(\partial_{x'}g_{m+1})(g_{m+1}) \\ -(\partial_{x'}g_{m+1})^2(a_m - z') \end{bmatrix}$$

$(C^{(m)})^2_{1,0} = \dfrac{2}{h^{(m)}}\tilde{g}_m$, $(C^{(m)})^2_{0,1} = -\dfrac{2}{h^{(m)}}\tilde{g}_{m+1}$, $(C^{(m)})^2_{1,1} = -\dfrac{2}{(h^{(m)})^2}\tilde{g}_m\tilde{g}_{m+1}$,
$(C^{(m)})^2_{2,0} = \dfrac{1}{(h^{(m)})^2}(\tilde{g}_m)^2$, $(C^{(m)})^2_{0,2} = \dfrac{1}{(h^{(m)})^2}(\tilde{g}_{m+1})^2$

$$D_n^{(0)} = \Big[\Big(\frac{\tilde{g}_0 - \tilde{g}_1}{h^{(0)}}\Big)T^{(0)}[w_{n-1}^{(0)}]\Big]\Big|_{z'=a_0} = \Big[\Big(\frac{-\tilde{g}_1}{h^{(0)}}\Big)T^{(0)}[w_{n-1}^{(0)}]\Big]\Big|_{z'=a},$$

$$D_n^{(M)} = \Big[\Big(\frac{\tilde{g}_M - \tilde{g}_{M+1}}{h^{(M)}}\Big)T^{(M)}[w_{n-1}^{(M)}]\Big]\Big|_{z'=a_{M+1}} = \Big[\Big(\frac{\tilde{g}_M}{h^{(M)}}\Big)T^{(M)}[w_{n-1}^{(M)}]\Big]\Big|_{z'=b},$$

$$J_n^{(m),u} = \Big(\frac{\tilde{g}_m - \tilde{g}_{m+1}}{h^{(m)}}\Big) U_{n-1}^{(m)} + \Bigg[i\eta \Big(\frac{\tilde{g}_m - \tilde{g}_{m+1}}{h^{(m)}}\Big) w_{n-1}^{(m)} + (\partial_{x'}\tilde{g}_m)(\partial_{x'} w_{n-1}^{(m)}) +$$

$$(\partial_{x'}\tilde{g}_m)\Big(\frac{\tilde{g}_m - \tilde{g}_{m+1}}{h^{(m)}}\Big)(\partial_{x'} w_{n-2}^{(m)}) - (\partial_{x'}\tilde{g}_m)^2 (\partial_{z'} w_{n-2}^{(m)}) \Bigg] \Bigg|_{z'=a_m},$$

$$J_n^{(m),l} = \Big(\frac{\tilde{g}_m - \tilde{g}_{m+1}}{h^{(m)}}\Big) L_{n-1}^{(m)} + \Bigg[i\eta \Big(\frac{\tilde{g}m - \tilde{g}_{m+1}}{h^{(m)}}\Big) w_{n-1}^{(m)} - (\partial_{x'}\tilde{g}_{m+1})(\partial_{x'} w_{n-1}^{(m)}) -$$

$$(\partial_{x'}\tilde{g}_{m+1})\Big(\frac{\tilde{g}_m - \tilde{g}_{m+1}}{h^{(m)}}\Big)(\partial_{x'} w_{n-2}^{(m)}) + (\partial_{x'}\tilde{g}_{m+1})^2 (\partial_{z'} w_{n-2}^{(m)}) \Bigg] \Bigg|_{z'=a_{m+1}},$$

The order n fields must also be quasiperiodic,

$$w_n^{(m)}(\xi; x' + d, z') = e^{i\alpha d} w_n^{(m)}(\xi; x', z') \text{ for } m = 0, ..., M.$$

The IIOs are given by

$$Q_n[L^{(0)}] = \Big(-\partial_{z'} w_n^{(0)} + i\eta w_n^{(0)} \Big)\Big|_{z'=a_1} + K_n^{(0),l},$$

$$\begin{bmatrix} R_n^{(m),u}[U^{(m)}, L^{(m)}] \\ R_n^{(m),l}[U^{(m)}, L^{(m)}] \end{bmatrix} = \begin{bmatrix} \Big(\partial_{z'} w_n^{(m)} + i\eta w_n^{(m)}\Big)\Big|_{z'=a_m} \\ \Big(-\partial_{z'} w_n^{(m)} + i\eta w_n^{(m)}\Big)\Big|_{z'=a_{m+1}} \end{bmatrix} + \begin{bmatrix} K_n^{(m),u} \\ K_n^{(m),l} \end{bmatrix},$$

and

$$S_n[U^{(M)}] = \Big(\partial_{z'} w_n^{(M)} + i\eta w_n^{(M)}\Big)\Big|_{z'=a_M} + K_n^{(M),u},$$

where

$$
\begin{aligned}
K_n^{(0),l} = &\Bigg[(\partial_{x'}\tilde{g}_1)(\partial_{x'}w_{n-1}^{(0)}) + (\partial_{x'}\tilde{g}_1)\Big(\frac{\tilde{g}_0 - \tilde{g}_1}{h^{(0)}}\Big)(\partial_{x'}w_{n-2}^{(0)}) - (\partial_{x'}\tilde{g}_1)^2(\partial_{z'}w_{n-2}^{(0)}) + \\
&\quad i\eta\Big(\frac{\tilde{g}_0 - \tilde{g}_1}{h^{(0)}}\Big)w_{n-1}^{(0)}\Bigg]\Big|_{z'=a_1} - \Big(\frac{\tilde{g}_0 - \tilde{g}_1}{h^{(0)}}\Big)Q_{n-1}[L^{(0)}] \\
= &\Bigg[(\partial_{x'}\tilde{g}_1)(\partial_{x'}w_{n-1}^{(0)}) - (\partial_{x'}\tilde{g}_1)\Big(\frac{\tilde{g}_1}{h^{(0)}}\Big)(\partial_{x'}w_{n-2}^{(0)}) - (\partial_{x'}\tilde{g}_1)^2(\partial_{z'}w_{n-2}^{(0)}) - \\
&\quad i\eta\Big(\frac{\tilde{g}_1}{h^{(0)}}\Big)w_{n-1}^{(0)}\Bigg]\Big|_{z'=a_1} + \Big(\frac{\tilde{g}_1}{h^{(0)}}\Big)Q_{n-1}[L^{(0)}],
\end{aligned}
$$

$$
\begin{aligned}
K_n^{(M),u} = &\Bigg[-(\partial_{x'}\tilde{g}_M)(\partial_{x'}w_{n-1}^{(M)}) - (\partial_{x'}\tilde{g}_M)\Big(\frac{\tilde{g}_M - \tilde{g}_{M+1}}{h^{(M)}}\Big)(\partial_{x'}w_{n-2}^{(M)}) + (\partial_{x'}\tilde{g}_M)^2(\partial_{z'}w_{n-2}^{(M)}) + \\
&\quad i\eta\Big(\frac{\tilde{g}_M - \tilde{g}_{M+1}}{h^{(M)}}\Big)w_{n-1}^{(M)}\Bigg]\Big|_{z'=a_M} - \Big(\frac{\tilde{g}_M - \tilde{g}_{M+1}}{h^{(M)}}\Big)S_{n-1}[U^{(M)}] \\
= &\Bigg[-(\partial_{x'}\tilde{g}_M)(\partial_{x'}w_{n-1}^{(M)}) - (\partial_{x'}\tilde{g}_M)\Big(\frac{\tilde{g}_M}{h^{(M)}}\Big)(\partial_{x'}w_{n-2}^{(M)}) + (\partial_{x'}\tilde{g}_M)^2(\partial_{z'}w_{n-2}^{(M)}) + \\
&\quad i\eta\Big(\frac{\tilde{g}_M}{h^{(M)}}\Big)w_{n-1}^{(M)}\Bigg]\Big|_{z'=a_M} - \Big(\frac{\tilde{g}_M}{h^{(M)}}\Big)S_{n-1}[U^{(M)}],
\end{aligned}
$$

$$
\begin{aligned}
K_n^{(m),u} = &\Bigg[(-\partial_{x'}\tilde{g}_m)(\partial_{x'}w_{n-1}^{(m)}) + \Big(\frac{\tilde{g}_m - \tilde{g}_{m+1}}{h^{(m)}}\Big)(-\partial_{x'}\tilde{g}_m)(\partial_{x'}w_{n-2}^{(m)}) + (\partial_{x'}\tilde{g}_m)^2(\partial_{z'}w_{n-2}^{(m)}) + \\
&\quad i\eta\Big(\frac{\tilde{g}_m - \tilde{g}_{m+1}}{h^{(m)}}\Big)w_{n-1}^{(m)}\Bigg]\Big|_{z'=a_m} - \Big(\frac{\tilde{g}_m - \tilde{g}_{m+1}}{h^{(m)}}\Big)R_{n-1}^{(m),u}[U^{(m)}, L^{(m)}],
\end{aligned}
$$

for $m \in \{1, ..., M-1\}$, and

$$K_n^{(m),l} = \Bigg[(\partial_{x'}\tilde{g}_{m+1})(\partial_{x'}w_{n-1}^{(m)}) + \Big(\frac{\tilde{g}_m - \tilde{g}_{m+1}}{h^{(m)}}\Big)(\partial_{x'}\tilde{g}_{m+1})(\partial_{x'}w_{n-2}^{(m)}) - (\partial_{x'}\tilde{g}_{m+1})^2(\partial_{z'}w_{n-2}^{(m)}) + i\eta\Big(\frac{\tilde{g}_m - \tilde{g}_{m+1}}{h^{(m)}}\Big)w_{n-1}^{(m)}\Bigg]\Bigg|_{z'=a_{m+1}} - \Big(\frac{\tilde{g}_m - \tilde{g}_{m+1}}{h^{(m)}}\Big)R_{n-1}^{(m),l}[U^{(m)}, L^{(m)}],$$

for $m \in \{1, ..., M-1\}$. For any $n < 0$, let $w_n^{(m)} \equiv 0$.

The linear system to solve for the impedance quantities $L_n^{(m)}$, $U_n^{(m)}$ for each perturbation order n is given by

$$A_0\bar{\mathbf{x}}_n = \mathbf{b}_n, \tag{3.17}$$

where

$$A_0 = \begin{bmatrix} D_{1,0} & U_{1,0} & 0 & 0 & 0 & 0 & \dots & 0 \\ L_{2,0} & D_{2,0} & U_{2,0} & 0 & 0 & 0 & \dots & 0 \\ 0 & L_{3,0} & D_{3,0} & U_{3,0} & 0 & 0 & \dots & 0 \\ 0 & 0 & \ddots & \ddots & \ddots & 0 & & \vdots \\ \vdots & \vdots & 0 & \ddots & \ddots & \ddots & \ddots & 0 \\ 0 & 0 & & \ddots & \ddots & \ddots & \ddots & 0 \\ 0 & 0 & \dots & 0 & 0 & L_{M-1,0} & D_{M-1,0} & U_{M-1,0} \\ 0 & 0 & \dots & 0 & 0 & 0 & L_{M,0} & D_{M,0} \end{bmatrix}$$

$$\bar{\mathbf{x}}_n = \begin{bmatrix} L_n^{(0)} \\ U_n^{(1)} \\ L_n^{(1)} \\ U_n^{(2)} \\ \vdots \\ U_n^{(M-1)} \\ L_n^{(M-1)} \\ U_n^{(M)} \end{bmatrix}$$

$$\mathbf{b}_n = \begin{bmatrix} (-2i\eta)(-v_n^{inc}(x, a_1 + g_1) \\ (-2)\Big(- \big(\frac{\partial v^{inc}}{\partial \mathbf{n}^{(1)}}(x, a_1 + g_1) \big)_n \Big) \\ 0 \\ 0 \\ \vdots \\ 0 \\ 0 \\ 0 \end{bmatrix}$$

$$+ \begin{bmatrix} \sum_{m=0}^{n-1} Q_{n-m}[L_m^{(0)}] - \sum_{m=0}^{n-1} R_{n-m}^{(1),u}[U_m^{(1)}, L_m^{(1)}] \\ - \sum_{m=0}^{n-1} Q_{n-m}[L_m^{(0)}] - \sum_{m=0}^{n-1} R_{n-m}^{(1),u}[U_m^{(1)}, L_m^{(1)}] \\ \sum_{m=0}^{n-1} R_{n-m}^{(1),l}[U_m^{(1)}, L_m^{(1)}] - \sum_{m=0}^{n-1} R_{n-m}^{(2),u}[U_m^{(2)}, L_m^{(2)}] \\ - \sum_{m=0}^{n-1} R_{n-m}^{(1),l}[U_m^{(1)}, L_m^{(1)}] - \sum_{m=0}^{n-1} R_{n-m}^{(2),u}[U_m^{(2)}, L_m^{(2)}] \\ \vdots \\ - \sum_{m=0}^{n-1} R_{n-m}^{(M-2),l}[U_m^{(M-2)}, L_m^{(M-2)}] - \sum_{m=0}^{n-1} R_{n-m}^{(M-1),u}[U_m^{(M-1)}, L_m^{(M-1)}] \\ \sum_{m=0}^{n-1} R_{n-m}^{(M-1),l}[U_m^{(M-1)}, L_m^{(M-1)}] - \sum_{m=0}^{n-1} S_{n-m}[U_m^{(M)}] \\ - \sum_{m=0}^{n-1} R_{n-m}^{(M-1),l}[U_m^{(M-1)}, L_m^{(M-1)}] - \sum_{m=0}^{n-1} S_{n-m}[U_m^{(M)}] \end{bmatrix}$$

$$D_{1,0} = \begin{bmatrix} I - Q_0 & -I + R_0^{(1),uu} \\ I + Q_0 & I + R_0^{(1),uu} \end{bmatrix}$$

$$D_{M,0} = \begin{bmatrix} I - R_0^{(M-1),ll} & -I + S_0 \\ I + R_0^{(M-1),ll} & I + S_0 \end{bmatrix}$$

$$D_{m,0} = \begin{bmatrix} I - R_0^{(m-1),ll} & -I + R_0^{(m),uu} \\ I + R_0^{(m-1),ll} & I + R_0^{(m),uu} \end{bmatrix}, \text{ for } m = 2, ..., M-1$$

$$U_{m,0} = \begin{bmatrix} R_0^{(m),ul} & 0 \\ R_0^{(m),ul} & 0 \end{bmatrix}, \text{ for } m = 1, ..., M-1$$

$$L_{m,0} = \begin{bmatrix} 0 & -R_0^{(m-1),lu} \\ 0 & R_0^{(m-1),lu} \end{bmatrix}, \text{ for } m = 2, ..., M.$$

Note that we can expand the incident wave as a Maclaurin series in the z-direction

$$\begin{aligned} v^{inc}(x,z) &= e^{i\alpha x - i\gamma^{(0)} z} \\ &= e^{i\alpha x} e^{-i\gamma^{(0)} z} \\ &= e^{i\alpha x} \sum_{n=0}^{\infty} \frac{(-i\gamma^{(0)})^n}{n!} z^n. \end{aligned}$$

Then we have that $\partial_z v^{inc}(x,z) = e^{i\alpha x} \sum_{n=1}^{\infty} \frac{(-i\gamma^{(0)})^n}{(n-1)!} z^{n-1} = (-i\gamma^{(0)}) e^{i\alpha x} \sum_{n=1}^{\infty} \frac{(-i\gamma^{(0)})^{n-1}}{(n-1)!} z^{n-1}$. Define

$$v_n^{inc}(x, a_1 + g_1) = e^{i\alpha x} \frac{(-i\gamma^{(0)})^n}{n!} (a_1 + g_1)^n$$

and

$$\left(\frac{\partial v^{inc}}{\partial \mathbf{n}^{(1)}} (x, a_1 + g_1) \right)_n = -(i\alpha)(\partial_x g_1) v_n^{inc}(x, a_1 + g_1) + (-i\gamma^{(0)}) v_{n-1}^{inc}(x, a_1 + g_1),$$

for $n = 0, 1, ..., N$, where we will define $v_{-1}^{inc}(x, a_1 + g_1) = 0$.

It is significant to note that the IIO linear system and the boundary value problem in each layer are now recursively defined. With that in mind, it is of great importance that we examine the order $n = 0$ solution, which may be solved analytically. After all, every solution of order $n \geq 1$ will now depend on this crucial starting point.

3.2.3 Impedance-Impedance Operators: Order $n = 0$ Case

The order $n = 0$ scenario corresponds to having "flat" interfaces $z = a_m$, $m = 1, ..., M$ separating each layer. First, consider the order $n = 0$ boundary value problem in the upper layer:

$$\begin{cases} \Delta w_0^{(0)} + (k^{(0)})^2 w_0^{(0)} = F_0^{(0)}, \ a_1 < z' < a \\ \partial_{z'} w_0^{(0)} - T^{(0)}[w_n^{(0)}] = D_0^{(0)}, \ z' = a \\ -\partial_{z'} w_0^{(0)} - i\eta w_0^{(0)} = L_0^{(0)} + J_0^{(0),l}, \ z' = a_1, \end{cases}$$

where $F_0^{(0)} = 0$, $D_0^{(0)} = 0$, and $J_0^{(0),l} = 0$. Then by separation of variables, we have

$$w_0^{(0)}(x', z') = \sum_{p=-\infty}^{\infty} a_p^{(0)} e^{i\alpha_p x' + i\gamma_p^{(0)} z'} + \sum_{p=-\infty}^{\infty} b_p^{(0)} e^{i\alpha_p x' - i\gamma_p^{(0)} z'}.$$

for the second summation in the solution for $w_0^{(0)}$, we can see that if $p \in P^{(0)}$, we have a downward propagating wave, and if $p \notin P^{(0)}$, we have an unbounded solution. Since we require an upward propagating wave in the upper layer and bounded solutions, we must omit the term $\sum_{p=-\infty}^{\infty} b_p^{(0)} e^{i\alpha_p x' - i\gamma_p^{(0)} z'}$ from the solution for $w_0^{(0)}$. Now, we can consider the boundary conditions to solve for the constants $a_p^{(0)}$.

The boundary condition $-\partial_{z'} w_0^{(0)} - i\eta w_0^{(0)} = L_0^{(0)} + J_0^{(0),l}$, $z' = a_1$ gives the following:

$$\begin{aligned} L_0^{(0)}(x) &= -\partial_{z'} w_0^{(0)}(x, a_1) - i\eta w_0^{(0)}(x, a_1) \\ &= -\sum_{p=-\infty}^{\infty} (i\gamma_p^{(0)}) a_p^{(0)} e^{i\alpha_p x'} e^{i\gamma_p^{(0)} a_1} - i\eta \sum_{p=-\infty}^{\infty} a_p^{(0)} e^{i\alpha_p x'} e^{i\gamma_p^{(0)} a_1}. \end{aligned}$$

Due to quasiperiodicity of the solutions, we may write $L_0^{(0)}$ using its Fourier expansion,

$$\begin{aligned} \sum_{p=-\infty}^{\infty} \hat{L}_{0,p}^{(0)} e^{i\alpha_p x'} &= -\sum_{p=-\infty}^{\infty} (i\gamma_p^{(0)}) a_p^{(0)} e^{i\alpha_p x'} e^{i\gamma_p^{(0)} a_1} - i\eta \sum_{p=-\infty}^{\infty} a_p^{(0)} e^{i\alpha_p x'} e^{i\gamma_p^{(0)} a_1} \\ &= \sum_{p=-\infty}^{\infty} (-i\gamma_p^{(0)} - i\eta) e^{i\gamma_p^{(0)} a_1} a_p^{(0)} e^{i\alpha_p x'}, \end{aligned}$$

so that we may see that $a_p^{(0)} = \dfrac{e^{-i\gamma_p^{(0)} a_1}}{-i\gamma_p^{(0)} - i\eta} \hat{L}_{0,p}^{(0)}$. Therefore,

$$w_0^{(0)}(x', z') = \sum_{p=-\infty}^{\infty} \frac{\hat{L}_{0,p}^{(0)}}{-i\gamma_p^{(0)} - i\eta} e^{i\alpha_p x' + i\gamma_p^{(0)}(z' - a_1)},$$

where $\hat{L}_{0,p}^{(0)}$ are the Fourier coefficients of $L_0^{(0)}$. Now, we may use this order $n = 0$ solution to determine the form of the order $n = 0$ IIO Q_0. Recall that

$$Q_0[L^{(0)}] = \Big(-\partial_{z'} w_0^{(0)} + i\eta w_0^{(0)} \Big)\Big|_{z'=a_1},$$

so that

$$
\begin{aligned}
Q_0[L^{(0)}] &= \Big(-\partial_{z'} w_0^{(0)} + i\eta w_0^{(0)}\Big)\Big|_{z'=a_1} \\
&= -\sum_{p=-\infty}^{\infty} (i\gamma_p^{(0)}) \frac{\hat{L}_{0,p}^{(0)}}{-i\gamma_p^{(0)} - i\eta} e^{i\alpha_p x'} + i\eta \sum_{p=-\infty}^{\infty} \frac{\hat{L}_{0,p}^{(0)}}{-i\gamma_p^{(0)} - i\eta} e^{i\alpha_p x'} \\
&= \sum_{p=-\infty}^{\infty} \Big(\frac{-i\gamma_p^{(0)} + i\eta}{-i\gamma_p^{(0)} - i\eta}\Big) \hat{L}_{0,p}^{(0)} e^{i\alpha_p x'}.
\end{aligned}
$$

Similarly, in the lower layer, via separation of variables, we find that the solution of the boundary value problem

$$
\begin{cases}
\Delta w_0^{(M)} + (k^{(M)})^2 w_0^{(M)} = F_0^{(M)}, \; b < z' < a_M \\
\partial_{z'} w_0^{(M)} - i\eta w_0^{(M)} = U_0^{(M)} + J_0^{(M),u}, \; z' = a_M \\
\partial_{z'} w_0^{(M)} - T^{(M)}[w_0^{(M)}] = D_0^{(M)}, \; z' = b,
\end{cases}
$$

where $F_0^{(M)} = 0$, $J_n^{(M),u} = 0$, and $D_n^{(M)} = 0$, is given by

$$
w_0^{(M)}(x', z') = \sum_{p=-\infty}^{\infty} a_p^{(M)} e^{i\alpha_p x' + i\gamma_p^{(M)} z'} + \sum_{p=-\infty}^{\infty} b_p^{(M)} e^{i\alpha_p x' - i\gamma_p^{(M)} z'}.
$$

In the first summation of the solution for $w_0^{(M)}$, we see that if $p \in P^{(M)}$, we have an upward propagating wave, and if $p \notin P^{(M)}$, the solution is unbounded. Because we require that $w_0^{(M)}$ be downward propagating and bounded, we omit the first summation.

Now, we may use the boundary condition $\partial_{z'} w_0^{(M)} - i\eta w_0^{(M)} = U_0^{(M)} + J_0^{(M),u}$, $z' = a_M$

to solve for the constants $b_p^{(M)}$:

$$U_0^{(M)}(x') = \partial_{z'} w_0^{(M)}(x', a_M) - i\eta w_0^{(M)}(x', a_M)$$
$$= \sum_{p=-\infty}^{\infty} (-i\gamma_p^{(M)}) b_p^{(M)} e^{i\alpha_p x'} e^{-i\gamma_p^{(M)} a_M} - i\eta \sum_{p=-\infty}^{\infty} b_p^{(M)} e^{i\alpha_p x'} e^{-i\gamma_p^{(M)} a_M}.$$

Due to quasiperiodicity of the solutions, we may write $U_0^{(M)}$ as its Fourier expansion,

$$\sum_{p=-\infty}^{\infty} \hat{U}_{0,p}^{(M)} e^{i\alpha_p x'} = \sum_{p=-\infty}^{\infty} (-i\gamma_p^{(M)}) b_p^{(M)} e^{i\alpha_p x'} e^{-i\gamma_p^{(M)} a_M} - i\eta \sum_{p=-\infty}^{\infty} b_p^{(M)} e^{i\alpha_p x'} e^{-i\gamma_p^{(M)} a_M}$$
$$= \sum_{p=-\infty}^{\infty} (-i\gamma_p^{(M)} - i\eta) e^{-i\gamma_p^{(M)} a_M} b_p^{(M)} e^{i\alpha_p x'},$$

so that we may see that $b_p^{(M)} = \dfrac{e^{i\gamma_p^{(M)} a_M}}{-i\gamma_p^{(M)} - i\eta} \hat{U}_{0,p}^{(M)}$. Therefore,

$$w_0^{(M)}(x', z') = \sum_{p=-\infty}^{\infty} \frac{\hat{U}_{0,p}^{(M)}}{-i\gamma_p^{(M)} - i\eta} e^{i\alpha_p x' - i\gamma_p^{(M)}(z' - a_M)},$$

where $\hat{U}_{0,p}^{(M)}$ are the Fourier coefficients of $U_0^{(M)}$. Now we may use this order $n = 0$ solution to determine the form of the order $n = 0$ IIO S_0. Recall that

$$S_0[U^{(M)}] = \left(\partial_{z'} w_0^{(M)} + i\eta w_0^{(M)} \right)\Big|_{z'=a_M},$$

so that

$$
\begin{aligned}
S_0[U^{(m)}] &= \Big(\partial_{z'} w_0^{(M)} + i\eta w_0^{(M)}\Big)\Big|_{z'=a_M} \\
&= \sum_{p=-\infty}^{\infty} (-i\gamma_p^{(M)}) \frac{\hat{U}_{0,p}^{(M)}}{-i\gamma_p^{(M)} - i\eta} e^{i\alpha_p x'} + i\eta \sum_{p=-\infty}^{\infty} \frac{\hat{U}_{0,p}^{(M)}}{-i\gamma_p^{(M)} - i\eta} e^{i\alpha_p x'} \\
&= \sum_{p=-\infty}^{\infty} \Big(\frac{-i\gamma_p^{(M)} + i\eta}{-i\gamma_p^{(M)} - i\eta}\Big) \hat{U}_{0,p}^{(M)} e^{i\alpha_p x'}.
\end{aligned}
$$

Finally, we turn our attention to the middle layers

$$
\begin{cases}
\Delta w_0^{(m)} + (k^{(m)})^2 w_0^{(m)} = F_0^{(m)}, \ a_{m+1} < z' < a_m, \text{ for } m = 1, ..., M-1 \\
\partial_{z'} w_0^{(m)} - i\eta w_0^{(m)} = U_0^{(m)} + J_0^{(m),u}, \ z' = a_m, \text{ for } m = 1, ..., M-1 \\
-\partial_{z'} w_0^{(m)} - i\eta w_0^{(m)} = L_0^{(m)} + J_0^{(m),l}, \ z' = a_{m+1}, \text{ for } m = 1, ..., M-1,
\end{cases}
$$

where $F_0^{(m)} = 0$, $J_0^{(m),u} = 0$, and $J_0^{(m),l} = 0$. To simplify the calculations a bit, let us make another convenient change of variables given by

$$\tilde{x} = x'$$

$$\tilde{z} = -\bar{h}^{(m)}\Big(\frac{a_m - z'}{a_m - a_{m+1}}\Big) + \bar{h}^{(m)}\Big(\frac{z' - a_{m+1}}{a_m - a_{m+1}}\Big),$$

where $\bar{h}^{(m)} = \dfrac{a_m - a_{m+1}}{2}$. This change of variables maps $\{a_{m+1} < z' < a_m\}$ to $\{-\bar{h}^{(m)} < \tilde{z} < \bar{h}^{(m)}\}$. Let $u_0^{(m)}(\tilde{x}, \tilde{z}) := w_0^{(m)}(x'(\tilde{x}, \tilde{z}), z'(\tilde{x}, \tilde{z}))$. This change of variables gives the derivative rules

$$\partial_{\tilde{x}} = \partial_{x'}$$

$$\partial_{\tilde{z}} = \partial_{z'},$$

so that the boundary value problems in the middle layers are given by

$$\begin{cases} \Delta u_0^{(m)} + (k^{(m)})^2 u_0^{(m)} = 0, \ -\bar{h}^{(m)} < \tilde{z} < \bar{h}^{(m)} \text{ for } m = 1, ..., M-1 \\ \partial_{\tilde{z}} u_0^{(m)} - i\eta u_0^{(m)} = U_0^{(m)}, \ \tilde{z} = \bar{h}^{(m)} \text{ for } m = 1, ..., M-1 \\ -\partial_{\tilde{z}} u_0^{(m)} - i\eta u_0^{(m)} = L_0^{(m)}, \ \tilde{z} = -\bar{h}^{(m)} \text{ for } m = 1, ..., M-1. \end{cases}$$

By separation of variables, we find that the solutions of the boundary value problem in the middle layers are given by

$$u_0^{(m)}(\tilde{x}, \tilde{z}) = \sum_{p=-\infty}^{\infty} \Big(a_p^{(m)} \cosh(i\gamma_p^{(m)} \tilde{z}) + b_p^{(m)} \frac{\sinh(i\gamma_p^{(m)} \tilde{z})}{i\gamma_p^{(m)}} \Big) e^{i\alpha_p \tilde{x}},$$

where

$$\cosh(i\gamma_p^{(m)} \tilde{z}) := \begin{cases} \cos(\gamma_p^{(m)} \tilde{z}) \text{ if } \operatorname{Im}(\gamma_p^{(m)}) = 0 \\ 1 \text{ if } \gamma_p^{(m)} = 0 \\ \cosh(\operatorname{Im}(\gamma_p^{(m)}) \tilde{z}) \text{ if } \operatorname{Re}(\gamma_p^{(m)}) = 0 \end{cases}$$

and

$$\frac{\sinh(i\gamma_p^{(m)} \tilde{z})}{i\gamma_p^{(m)}} := \begin{cases} \frac{\sin(\gamma_p^{(m)} \tilde{z})}{\gamma_p^{(m)}} \text{ if } \operatorname{Im}(\gamma_p^{(m)}) = 0 \\ \tilde{z} \text{ if } \gamma_p^{(m)} = 0 \\ \frac{\sinh(\operatorname{Im}(\gamma_p^{(m)}) \tilde{z})}{\operatorname{Im}(\gamma_p^{(m)})} \text{ if } \operatorname{Re}(\gamma_p^{(m)}) = 0. \end{cases}$$

Recall that

$$\gamma_p^{(m)} = \sqrt{(k^{(m)})^2 - \alpha_p^2}, \ \operatorname{Im}(\gamma_p^{(m)}) \geq 0$$

for $m = 1, ..., M-1$.

Now we must consider the boundary conditions to solve for the coefficients $a_p^{(m)}$ and $b_p^{(m)}$. The boundary conditions give

$$\begin{aligned}
\hat{U}_{0,p}^{(m)} &= \Big(a_p^{(m)}(i\gamma_p^{(m)})\sinh{(i\gamma_p^{(m)}\bar{h}^{(m)})} + b_p^{(m)}\cosh{(i\gamma_p^{(m)}\bar{h}^{(m)})}\Big) - \\
&\qquad i\eta\Big(a_p^{(m)}\cosh{(i\gamma_p^{(m)}\bar{h}^{(m)})} + b_p^{(m)}\frac{\sinh{(i\gamma_p^{(m)}\bar{h}^{(m)})}}{i\gamma_p^{(m)}}\Big) \\
&= \Big((i\gamma_p^{(m)})\sinh{(i\gamma_p^{(m)}\bar{h}^{(m)})} - i\eta\cosh{(i\gamma_p^{(m)}\bar{h}^{(m)})}\Big)a_p^{(m)} + \\
&\qquad \Big(\cosh{(i\gamma_p^{(m)}\bar{h}^{(m)})} - i\eta\frac{\sinh{(i\gamma_p^{(m)}\bar{h}^{(m)})}}{i\gamma_p^{(m)}}\Big)b_p^{(m)}
\end{aligned}$$

$$\begin{aligned}
\hat{L}_{0,p}^{(m)} &= -\Big(a_p^{(m)}(i\gamma_p^{(m)})\sinh{(i\gamma_p^{(m)}(-\bar{h}^{(m)}))} + b_p^{(m)}\cosh{(i\gamma_p^{(m)}(-\bar{h}^{(m)}))}\Big) - \\
&\qquad i\eta\Big(a_p^{(m)}\cosh{(i\gamma_p^{(m)}(-\bar{h}^{(m)}))} + b_p^{(m)}\frac{\sinh{(i\gamma_p^{(m)}(-\bar{h}^{(m)}))}}{i\gamma_p^{(m)}}\Big) \\
&= \Big((i\gamma_p^{(m)})\sinh{(i\gamma_p^{(m)}\bar{h}^{(m)})} - i\eta\cosh{(i\gamma_p^{(m)}\bar{h}^{(m)})}\Big)a_p^{(m)} + \\
&\qquad \Big(-\cosh{(i\gamma_p^{(m)}\bar{h}^{(m)})} + i\eta\frac{\sinh{(i\gamma_p^{(m)}\bar{h}^{(m)})}}{i\gamma_p^{(m)}}\Big)b_p^{(m)}
\end{aligned}$$

Let

$$
\begin{aligned}
a_{m,p} &= (i\gamma_p^{(m)})^2 \frac{\sinh(i\gamma_p^{(m)}\bar{h}^{(m)})}{i\gamma_p^{(m)}} - i\eta\cosh(i\gamma_p^{(m)}\bar{h}^{(m)}) \\
&= -(\gamma_p^{(m)})^2 sh_{m,p} - i\eta ch_{m,p}, \\
b_{m,p} &= \cosh(i\gamma_p^{(m)}\bar{h}^{(m)}) - i\eta\frac{\sinh(i\gamma_p^{(m)}\bar{h}^{(m)})}{i\gamma_p^{(m)}} \\
&= ch_{m,p} - i\eta sh_{m,p}, \\
ch_{m,p} &= \cosh(i\gamma_p^{(m)}\bar{h}^{(m)}), \\
sh_{m,p} &= \frac{\sinh(i\gamma_p^{(m)}\bar{h^{(m)}})}{i\gamma_p^{(m)}}
\end{aligned}
$$

so that

$$
\begin{bmatrix} a_{m,p} & b_{m,p} \\ a_{m,p} & -b_{m,p} \end{bmatrix} \begin{bmatrix} a_p^{(m)} \\ b_p^{(m)} \end{bmatrix} = \begin{bmatrix} \hat{U}_{0,p}^{(m)} \\ \hat{L}_{0,p}^{(m)} \end{bmatrix}.
$$

Since

$$
\begin{aligned}
\det \begin{bmatrix} a_{m,p} & b_{m,p} \\ a_{m,p} & -b_{m,p} \end{bmatrix} &= -2a_{m,p}b_{m,p} \\
&= i\Big(\frac{(\gamma_p^{(m)})^2 + \eta^2}{\gamma_p^{(m)}}\Big)\sinh(i\gamma_p^{(m)}\bar{h}^{(m)})\cosh(i\gamma_p^{(m)}\bar{h}^{(m)}) - \\
&\qquad i\eta\Big(\sinh^2(i\gamma_p^{(m)}\bar{h}^{(m)}) + \cosh^2(i\gamma_p^{(m)}\bar{h}^{(m)})\Big) \\
&\neq 0,
\end{aligned}
$$

we may always find unique solutions $\begin{bmatrix} a_p^{(m)} \\ b_p^{(m)} \end{bmatrix} = \begin{bmatrix} a_{m,p} & b_{m,p} \\ a_{m,p} & -b_{m,p} \end{bmatrix}^{-1} \begin{bmatrix} \hat{U}_{0,p}^{(m)} \\ \hat{L}_{0,p}^{(m)} \end{bmatrix}$.

Now we must use the order $n = 0$ solutions to determine the form of the order $n = 0$ IIO R_0. Recall that

$$R_0^{(m)} \begin{bmatrix} U^{(m)} \\ L^{(m)} \end{bmatrix} = \begin{bmatrix} R_0^{(m),uu} & R_0^{(m),ul} \\ R_0^{(m),lu} & R_0^{(m),ll} \end{bmatrix} \begin{bmatrix} U^{(m)} \\ L^{(m)} \end{bmatrix}$$
$$= \begin{bmatrix} \left(\partial_{z'} w_0^{(m)} + i\eta w_0^{(m)} \right)\Big|_{z'=a_m} \\ \left(-\partial_{z'} w_0^{(m)} + i\eta w_0^{(m)} \right)\Big|_{z'=a_{m+1}} \end{bmatrix}$$
$$= \begin{bmatrix} \left(\partial_{\tilde{z}} u_0^{(m)} + i\eta u_0^{(m)} \right)\Big|_{\tilde{z}=\bar{h}^{(m)}} \\ \left(-\partial_{\tilde{z}} u_0^{(m)} + i\eta u_0^{(m)} \right)\Big|_{\tilde{z}=-\bar{h}^{(m)}}. \end{bmatrix}$$

Then for fixed p,

$$R_{0,p}^{(m)} \begin{bmatrix} \hat{U}_{0,p}^{(m)} \\ \hat{L}_{0,p}^{(m)} \end{bmatrix} = \begin{bmatrix} \bar{a}_{m,p} & \bar{b}_{m,p} \\ \bar{a}_{m,p} & -\bar{b}_{m,p} \end{bmatrix} \begin{bmatrix} a_p^{(m)} \\ b_p^{(m)} \end{bmatrix}$$
$$= \begin{bmatrix} \bar{a}_{m,p} & \bar{b}_{m,p} \\ \bar{a}_{m,p} & -\bar{b}_{m,p} \end{bmatrix} \begin{bmatrix} a_{m,p} & b_{m,p} \\ a_{m,p} & -b_{m,p} \end{bmatrix}^{-1} \begin{bmatrix} \hat{U}_{0,p}^{(m)} \\ \hat{L}_{0,p}^{(m)} \end{bmatrix}.$$

Now, we can see that $R_{0,p}^{(m)} = \dfrac{1}{2} \begin{bmatrix} \frac{\bar{a}_{m,p}}{a_{m,p}} + \frac{\bar{b}_{m,p}}{b_{m,p}} & \frac{\bar{a}_{m,p}}{a_{m,p}} - \frac{\bar{b}_{m,p}}{b_{m,p}} \\ \frac{\bar{a}_{m,p}}{a_{m,p}} - \frac{\bar{b}_{m,p}}{b_{m,p}} & \frac{\bar{a}_{m,p}}{a_{m,p}} + \frac{\bar{b}_{m,p}}{b_{m,p}} \end{bmatrix}$. By simply carrying out the calculations $R_{0,p}^{(m)}(R_{0,p}^{(m)})^*$ and $(R_{0,p}^{(m)})^* R_{0,p}^{(m)}$, we will see that $R_{0,p}^{(m)}(R_{0,p}^{(m)})^* = (R_{0,p}^{(m)})^* R_{0,p}^{(m)} = I$ and therefore, $R_{0,p}^{(m)}$ is a unitary operator (here, * represents the conjugate transpose). Note that, more generally, it can be shown that $R_0^{(m)}$ is unitary for interfaces that are not "flat", as well [10, 16, 39].

Now that we have the order $n = 0$ solutions for each layer, we can note that the fields in each layer are quasiperiodic. To see this, note that, for $p \in \mathbb{Z}$,

$$\begin{aligned} e^{i\alpha_p d} &= e^{i(\alpha+(2\pi/d)p)d} \\ &= e^{i\alpha d}e^{i2\pi p} \\ &= e^{i\alpha d}\Big(\cos(2\pi p) + i\sin(2\pi p)\Big) \\ &= e^{i\alpha d}. \end{aligned}$$

Then for the upper, lower, and middle layers, respectively,

$$\begin{aligned} w_0^{(0)}(x'+d,z') &= \sum_{p=-\infty}^{\infty} \frac{\hat{L}_{0,p}^{(0)}}{-i\gamma_p^{(0)} - i\eta} e^{i\alpha_p(x'+d)+i\gamma_p^{(0)}(z'-a_1)} \\ &= \sum_{p=-\infty}^{\infty} e^{i\alpha_p d} \frac{\hat{L}_{0,p}^{(0)}}{-i\gamma_p^{(0)} - i\eta} e^{i\alpha_p x'+i\gamma_p^{(0)}(z'-a_1)} \\ &= e^{i\alpha d} \sum_{p=-\infty}^{\infty} \frac{\hat{L}_{0,p}^{(0)}}{-i\gamma_p^{(0)} - i\eta} e^{i\alpha_p x'+i\gamma_p^{(0)}(z'-a_1)} \\ &= e^{i\alpha d} w_0^{(0)}(x',z') \end{aligned}$$

$$\begin{aligned} w_0^{(M)}(x'+d,z') &= \sum_{p=-\infty}^{\infty} \frac{\hat{U}_{0,p}^{(M)}}{-i\gamma_p^{(M)} - i\eta} e^{i\alpha_p(x'+d)-i\gamma_p^{(M)}(z'-a_M)} \\ &= \sum_{p=-\infty}^{\infty} e^{i\alpha_p d} \frac{\hat{U}_{0,p}^{(M)}}{-i\gamma_p^{(M)} - i\eta} e^{i\alpha_p x'-i\gamma_p^{(M)}(z'-a_M)} \\ &= e^{i\alpha d} \sum_{p=-\infty}^{\infty} \frac{\hat{U}_{0,p}^{(M)}}{-i\gamma_p^{(M)} - i\eta} e^{i\alpha_p x'-i\gamma_p^{(M)}(z'-a_M)} \\ &= e^{i\alpha d} w_0^{(M)}(x',z') \end{aligned}$$

$$
\begin{aligned}
w_0^{(m)}(x'+d,z') &= \sum_{p=-\infty}^{\infty} \Big(a_p^{(m)} \cosh{(i\gamma_p^{(m)} z')} + b_p^{(m)} \frac{\sinh{(i\gamma_p^{(m)} z')}}{i\gamma_p^{(m)}}\Big) e^{i\alpha_p(x'+d)} \\
&= \sum_{p=-\infty}^{\infty} e^{i\alpha_p d}\Big(a_p^{(m)} \cosh{(i\gamma_p^{(m)} z')} + b_p^{(m)} \frac{\sinh{(i\gamma_p^{(m)} z')}}{i\gamma_p^{(m)}}\Big) e^{i\alpha_p x'} \\
&= e^{i\alpha d} \sum_{p=-\infty}^{\infty} \Big(a_p^{(m)} \cosh{(i\gamma_p^{(m)} z')} + b_p^{(m)} \frac{\sinh{(i\gamma_p^{(m)} z')}}{i\gamma_p^{(m)}}\Big) e^{i\alpha_p x'} \\
&= e^{i\alpha_d} w_0^{(m)}(x',z').
\end{aligned}
$$

3.3 Reduce to an Ordinary Differential Equation

Because the fields are quasiperiodic, i.e. $w^{(m)}(\xi; x'+d, z'; \varepsilon) = e^{i\alpha d} w^{(m)}(\xi; x', z'; \varepsilon)$, for $m = 0, 1, ..., M$, we may expand the fields as generalized Fourier series (also called Floquet series)

$$
w^{(m)}(\xi;, x', z'; \varepsilon) = \sum_{n=0}^{\infty} \sum_{p=-\infty}^{\infty} \hat{w}_{n,p}^{(m)}(\xi; z') e^{i\alpha_p x'} \varepsilon^n,
$$

where $\hat{w}_{n,p}^{(m)}$ are the Fourier coefficients. So we have that in each m^{th} layer, for each perturbation order n,

$$
w_n^{(m)}(\xi; x', z') = \sum_{p=-\infty}^{\infty} \hat{w}_{n,p}^{(m)}(\xi, z') e^{i\alpha_p x}. \tag{3.18}
$$

Since the IIO surface quantities are defined in terms of the fields, we may also expand the IIO surface quantities as Fourier series

$$
L^{(m)}(\xi; x') = \sum_{n=0}^{\infty} \sum_{p=-\infty}^{\infty} \hat{L}_{n,p}^{(m)} e^{i\alpha_p x'} \varepsilon^n, \text{ for } m = 0, 1, ..., M-1
$$

$$
U^{(m)}(\xi; x') = \sum_{n=0}^{\infty} \sum_{p=-\infty}^{\infty} \hat{U}_{n,p}^{(m)} e^{i\alpha_p x'} \varepsilon^n, \text{ for } m = 1, 2, ..., M.
$$

Then for each perturbation order n,

$$L_n^{(m)}(\xi; , x') = \sum_{p=-\infty}^{\infty} \hat{L}_{n,p}^{(m)} e^{i\alpha_p x'}, \text{ for } m = 0, 1, ..., M-1 \tag{3.19}$$

$$U_n^{(m)}(\xi; , x') = \sum_{p=-\infty}^{\infty} \hat{U}_{n,p}^{(m)} e^{i\alpha_p x'}, \text{ for } m = 1, 2, ..., M, \tag{3.20}$$

where $\hat{U}_{n,p}^{(m)}$ and $\hat{L}_{n,p}^{(m)}$ are the Fourier coefficients.

After inserting the Fourier expansions (3.18), (3.19), (3.20) into the boundary value problems for each layer (3.14), (3.15), (3.16), we have the following ordinary differential equations for the upper layer ($m = 0$), middle layers ($m = 1, ..., M-1$), and the lower layer ($m = M$), respectively:

$$\begin{cases} \partial_{z'}^2 \hat{w}_{n,p}^{(0)} + (\gamma_p^{(0)})^2 \hat{w}_{n,p}^{(0)} = F_{n,p}^{(0)}, \ \ a_1 < z' < a \\ \partial_{z'} \hat{w}_{n,p}^{(0)} - (i\gamma_p^{(0)}) \hat{w}_{n,p}^{(0)} = D_{n,p}^{(0)}, \ \ z' = a \\ -\partial_{z'} \hat{w}_{n,p}^{(0)} - i\eta \hat{w}_{n,p}^{(0)} = \hat{L}_{n,p}^{(0)} + J_{n,p}^{(0),l}, \ \ z' = a_1 \end{cases} \tag{3.21}$$

$$\begin{cases} \partial_{z'}^2 \hat{w}_{n,p}^{(m)} + (\gamma_p^{(m)})^2 \hat{w}_{n,p}^{(m)} = F_{n,p}^{(m)}, \ \ a_{m+1} < z' < a_m \\ \partial_{z'} \hat{w}_{n,p}^{(m)} - i\eta \hat{w}_{n,p}^{(m)} = \hat{U}_{n,p}^{(m)} + J_{n,p}^{(m),l}, \ \ z' = a_m \\ -\partial_{z'} \hat{w}_{n,p}^{(m)} - i\eta \hat{w}_{n,p}^{(m)} = \hat{L}_{n,p}^{(m)} + J_{n,p}^{(m),l}, \ \ z' = a_{m+1} \end{cases} \quad \text{for } m = 1, ..., M-1 \tag{3.22}$$

$$\begin{cases} \partial_{z'}^2 \hat{w}_{n,p}^{(M)} + (\gamma_p^{(M)})^2 \hat{w}_{n,p}^{(M)} = F_{n,p}^{(M)}, \ \ b < z' < a_M \\ \partial_{z'} \hat{w}_{n,p}^{(M)} + (i\gamma_p^{(M)}) \hat{w}_{n,p}^{(M)} = D_{n,p}^{(M)}, \ \ z' = b \\ \partial_{z'} \hat{w}_{n,p}^{(M)} - i\eta \hat{w}_{n,p}^{(M)} = \hat{U}_{n,p}^{(M)} + J_{n,p}^{(M),l}, \ \ z' = a_M, \end{cases} \tag{3.23}$$

where

$$D_{n,p}^{(0)} = (i\gamma_p^{(0)})\Big(\frac{\tilde{g}_0 - \tilde{g}_1}{h^{(0)}}\Big)\hat{w}_{n-1,p}^{(0)}\Big|_{z'=a_0} = (i\gamma_p^{(0)})\Big(\frac{-\tilde{g}_1}{h^{(0)}}\Big)\hat{w}_{n-1,p}^{(0)}\Big|_{z'=a},$$

$$D_{n,p}^{(M)} = (-i\gamma_p^{(M)})\Big(\frac{\tilde{g}_M - \tilde{g}_{M+1}}{h^{(M)}}\Big)\hat{w}_{n-1,p}^{(M)}\Big|_{z'=a_{M+1}} = (-i\gamma_p^{(M)})\Big(\frac{\tilde{g}_M}{h^{(M)}}\Big)\hat{w}_{n-1,p}^{(M)}\Big|_{z'=b},$$

$$\begin{aligned}
F_{n,p}^{(m)} = \nabla' \cdot \Bigg[&- A_{1,0}^{(m)} \begin{bmatrix} (i\alpha_p)\hat{w}_{n-1,p}^{(m)} \\ \partial_{z'}\hat{w}_{n-1,p}^{(m)} \end{bmatrix} - A_{0,1}^{(m)} \begin{bmatrix} (i\alpha_p)\hat{w}_{n-1,p}^{(m)} \\ \partial_{z'}\hat{w}_{n-1,p}^{(m)} \end{bmatrix} - A_{2,0}^{(m)} \begin{bmatrix} (i\alpha_p)\hat{w}_{n-2,p}^{(m)} \\ \partial_{z'}\hat{w}_{n-2,p}^{(m)} \end{bmatrix} - \\
& A_{1,1}^{(m)} \begin{bmatrix} (i\alpha_p)\hat{w}_{n-2,p}^{(m)} \\ \partial_{z'}\hat{w}_{n-2,p}^{(m)} \end{bmatrix} - A_{0,2}^{(m)} \begin{bmatrix} (i\alpha_p)\hat{w}_{n-2,p}^{(m)} \\ \partial_{z'}\hat{w}_{n-2,p}^{(m)} \end{bmatrix} \Bigg] - \Bigg[B_{1,0}^{(m)} \cdot \begin{bmatrix} (i\alpha_p)\hat{w}_{n-1,p}^{(m)} \\ \partial_{z'}\hat{w}_{n-1,p}^{(m)} \end{bmatrix} + \\
& B_{0,1}^{(m)} \cdot \begin{bmatrix} (i\alpha_p)\hat{w}_{n-1,p}^{(m)} \\ \partial_{z'}\hat{w}_{n-1,p}^{(m)} \end{bmatrix} + B_{1,1}^{(m)} \cdot \begin{bmatrix} (i\alpha_p)\hat{w}_{n-2,p}^{(m)} \\ \partial_{z'}\hat{w}_{n-2,p}^{(m)} \end{bmatrix} + B_{2,0}^{(m)} \cdot \begin{bmatrix} (i\alpha_p)\hat{w}_{n-2,p}^{(m)} \\ \partial_{z'}\hat{w}_{n-2,p}^{(m)} \end{bmatrix} + \\
& B_{0,2}^{(m)} \cdot \begin{bmatrix} (i\alpha_p)\hat{w}_{n-2,p}^{(m)} \\ \partial_{z'}\hat{w}_{n-2,p}^{(m)} \end{bmatrix} \Bigg] - (k^{(m)})^2 \Bigg[(C^{(m)})_{1,0}^2 \hat{w}_{n-1,p}^{(m)} + (C^{(m)})_{0,1}^2 \hat{w}_{n-1,p}^{(m)} + \\
& (C^{(m)})_{1,1}^2 \hat{w}_{n-2,p}^{(m)} + (C^{(m)})_{2,0}^2 \hat{w}_{n-2,p}^{(m)} + (C^{(m)})_{0,2}^2 \hat{w}_{n-2,p}^{(m)} \Bigg]
\end{aligned}$$

$$\begin{aligned}
J_{n,p}^{(m),u} = &\Big(\frac{\tilde{g}_m - \tilde{g}_{m+1}}{h^{(m)}}\Big)\hat{U}_{n-1,p}^{(m)} + i\eta\Big(\frac{\tilde{g}_m - \tilde{g}_{m+1}}{h^{(m)}}\Big)\hat{w}_{n-1,p}^{(m)} + (\partial_{x'}\tilde{g}_m)(i\alpha_p)\hat{w}_{n-1,p}^{(m)} + \\
&(\partial_{x'}\tilde{g}_m)\Big(\frac{\tilde{g}_m - \tilde{g}_{m+1}}{h^{(m)}}\Big)(i\alpha_p)\hat{w}_{n-2,p}^{(m)} - (\partial_{x'}\tilde{g}_m)^2(\partial_{z'}\hat{w}_{n-2,p}^{(m)})
\end{aligned}$$

$$\begin{aligned}
J_{n,p}^{(m),l} = &\Big(\frac{\tilde{g}_m - \tilde{g}_{m+1}}{h^{(m)}}\Big)\hat{L}_{n-1,p}^{(m)} + i\eta\Big(\frac{\tilde{g}_m - \tilde{g}_{m+1}}{h^{(m)}}\Big)\hat{w}_{n-1,p}^{(m)} - (\partial_{x'}\tilde{g}_{m+1})(i\alpha_p)\hat{w}_{n-1,p}^{(m)} - \\
&(\partial_{x'}\tilde{g}_{m+1})\Big(\frac{\tilde{g}_m - \tilde{g}_{m+1}}{h^{(m)}}\Big)(i\alpha_p)\hat{w}_{n-2,p}^{(m)} + (\partial_{x'}\tilde{g}_{m+1})^2\partial_{z'}\hat{w}_{n-2,p}^{(m)}.
\end{aligned}$$

Note that for each random sample ξ and for each Taylor order n, we have the same deterministic differential operator. We will be able to use this fact to save computationally [13, 17].

3.4 Discretization

To discretize and ultimately solve the boundary value problems, we will approximate the fields, $w^{(m)}(\xi; x', z'; \varepsilon)$, using the Chebyshev polynomials

$$w^{(m)}(\xi; x', z'; \varepsilon) \approx \sum_{n=0}^{N} \sum_{p=-N_x/2}^{N_x/2-1} \sum_{l=0}^{N_z} \hat{w}_{n,p,l}^{(m)} e^{i\alpha_p x'} T_l\Big(\frac{2z' - a_m - a_{m+1}}{a_m - a_{m+1}}\Big)\varepsilon^n,$$

where T_l is the l^{th} Chebyshev polynomial [39]. Let

$$x'_j = \frac{dj}{N_x} \text{ for } j = 0, ..., N_x - 1,$$

where N_x is the total number of Fourier modes in the x-direction, and let the collocation points in the z direction be the Chebyshev points given by

$$z'_l = \Big(\frac{a_m - a_{m+1}}{2}\Big)\Big(\cos\Big(\frac{l\pi}{N_z}\Big) - 1\Big) + a_m \text{ for } l = 0, ..., N_z,$$

where $N_z + 1$ is the total number of collocation points in the z-direction.Note that these are the Chebyshev points that have been transformed to the interval $[a_{m+1}, a_m]$.

Now, we will approximate $w_n^{(m)}(\xi_r; x'_j, z'_l)$ for each r^{th} Monte Carlo sample, n^{th} Taylor order, and m^{th} layer, for $j = 0, 1, ..., N_x - 1$ and $l = 0, 1, ..., N_z$. Here, $r = 1, 2, ..., R$, $n = 0, 1, ..., N$, and $m = 0, 1, ..., M$. Now, we can express the differential operator using the Chebyshev differentiation matrix, D_{N_z}, and solve the boundary value problem via Chebyshev collocation [53]. Note that the second derivative is approximated by $\Big(D_{N_z}\Big)^2$ [53].

Before describing the discretized boundary value problem for each layer, a brief description of Chebyshev differentiation matrices is helpful [2, 53]. As an example, suppose the polynomial $p(z) = \sum_{n=0}^{N_z} a_n T_n(z)$ approximates the function $f(z)$ on the interval $[-1, 1]$ at the Chebyshev points $z_j = \cos\left(\frac{j\pi}{N_z}\right)$, so that $p(z_j) = f(z_j)$. Then the $(N_z + 1) \times (N_z + 1)$ Chebyshev differentiation matrix D_{N_z}, is such that

$$D_{N_z} \begin{bmatrix} p(z_0) \\ \vdots \\ p(z_{N_z}) \end{bmatrix} = \begin{bmatrix} p'(z_0) \\ \vdots \\ p'(z_{N_z}) \end{bmatrix}.$$

In particular, the $(N_z + 1) \times (N_z + 1)$ Chebyshev differentiation matrix D_{N_z} has entries

$$(D_{N_z})_{00} = \frac{2{N_z}^2 + 1}{6}$$

$$(D_{N_z})_{N_z N_z} = -\frac{2N_z^2 + 1}{6}$$

$$(D_{N_z})_{ii} = \frac{-z_i}{2(1 - z_i)^2},\ i = 1, ..., N_z - 1$$

$$(D_{N_z})_{ij} = \left(\frac{c_i}{c_j}\right) \frac{(-1)^{i+j}}{(z_i - z_j)},\ i \neq j,\ i, j = 1, ..., N_z - 1,$$

$$\text{where } c_i = \begin{cases} 2,\ i = 0, N_z \\ 1,\ i = 1, ..., N_z - 1 \end{cases},$$

where $z_j = \cos\left(\frac{j\pi}{N_z}\right)$, $j = 0, 1, ..., N_z$ are the Chebyshev points [53].

Now, returning to our problem, the discretized problem in the upper layer, $m = 0$, for fixed p is given by

$$A_p^{(0)} \tilde{\mathbf{w}}_{n,p}^{(0)} = \tilde{\mathbf{f}}_{n,p}^{(0)}, \tag{3.24}$$

where

$$A_p^{(0)} = \left(\frac{2}{h^{(0)}} D_{N_z}\right)^2 + \left(\gamma_p^{(0)}\right)^2 I,$$

I is the $(N_z+1)\times(N_z+1)$ identity matrix, $\tilde{\mathbf{w}}_{n,p}^{(0)}$ is the $(N_z+1)\times 1$ vector of unknown approximate values for $w_n^{(0)}(\xi_r; x_j', z_l')$, and $\tilde{\mathbf{f}}_{n,p}^{(0)}$ is the $(N_z+1)\times 1$ vector of the right hand side values of the boundary value problem (3.21). Then the boundary condition at the upper artificial boundary is enforced by [53] replacing the first entry of $\tilde{\mathbf{f}}_{n,p}^{(0)}$ with $D_{n,p}^{(0)}$, replacing the first row of $A_p^{(0)}$ with the first row $\frac{2}{h^{(0)}}D_{N_z}$ and then changing the entry $\left(A_p^{(0)}\right)_{1,1}$ to

$$\left(A_p^{(0)}\right)_{1,1} - \left(i\gamma_p^{(0)}\right).$$

The boundary condition at the $z' = a_1$ is enforced by replacing the last entry of $\tilde{\mathbf{f}}_{n,p}^{(0)}$ with $\hat{L}_{n,p}^{(0)} + J_{n,p}^{(0),l}$, the last row of $A_p^{(0)}$ with the last row of $-\frac{2}{h^{(0)}}D_{N_z}$ and then changing the entry $\left(A_p^{(0)}\right)_{N_z+1,N_z+1}$ to

$$\left(A_p^{(0)}\right)_{N_z+1,N_z+1} - (i\eta).$$

The discretized problems in the middle layers, $m = 1, ..., M-1$, for fixed p are given by

$$A_p^{(m)}\tilde{\mathbf{w}}_{n,p}^{(m)} = \tilde{\mathbf{f}}_{n,p}^{(m)}, \tag{3.25}$$

where

$$A_p^{(m)} = \left(\frac{2}{h^{(m)}}D_{N_z}\right)^2 + \left(\gamma_p^{(m)}\right)^2 I,$$

I is the $(N_z+1)\times(N_z+1)$ identity matrix, $\tilde{\mathbf{w}}_{n,p}^{(m)}$ is the $(N_z+1)\times 1$ vector of unknown approximate values for $w_n^{(m)}(\xi_r; x_j', z_l')$, and $\tilde{\mathbf{f}}_{n,p}^{(m)}$ is the $(N_z+1)\times 1$ vector of the right hand side values of the boundary value problems (3.22). Then the boundary condition at the upper boundary of the m^{th} layer, $z' = a_m$, is enforced by [53] replacing the first entry of $\tilde{\mathbf{f}}_{n,p}^{(m)}$ with $\hat{U}_{n,p}^{(m)} + J_{n,p}^{(m),u}$, replacing the first row of $A_p^{(m)}$ with the first row $\frac{2}{h^{(m)}}D_{N_z}$ and then changing the entry $\left(A_p^{(m)}\right)_{1,1}$ to

$$\left(A_p^{(m)}\right)_{1,1} - (i\eta).$$

The boundary condition at the lower boundary of the m^{th} layer, $z' = a_{m+1}$, is enforced by replacing the last entry of $\tilde{\mathbf{f}}_{n,p}^{(m)}$ with $\hat{L}_{n,p}^{(m)} + J_{n,p}^{(m),l}$, the last row of $A_p^{(m)}$ with the last row of $-\frac{2}{h^{(m)}} D_{N_z}$ and then changing the entry $\left(A_p^{(m)}\right)_{N_z+1,N_z+1}$ to

$$\left(A_p^{(m)}\right)_{N_z+1,N_z+1} - (i\eta).$$

The discretized problem in the lower layer, $m = M$, for fixed p is given by

$$A_p^{(M)} \tilde{\mathbf{w}}_{n,p}^{(M)} = \tilde{\mathbf{f}}_{n,p}^{(M)}, \tag{3.26}$$

where

$$A_p^{(M)} = \left(\frac{2}{h^{(M)}} D_{N_z}\right)^2 + \left(\gamma_p^{(M)}\right)^2 I,$$

I is the $(N_z+1) \times (N_z+1)$ identity matrix, $\tilde{\mathbf{w}}_{n,p}^{(M)}$ is the $(N_z+1) \times 1$ vector of unknown approximate values for $w_n^{(M)}(\xi_r; x'_j, z'_l)$, and $\tilde{\mathbf{f}}_{n,p}^{(M)}$ is the $(N_z+1) \times 1$ vector of the right hand side values of the boundary value problems (3.23). Then the boundary condition at the upper boundary of the M^{th} layer, $z' = a_M$, is enforced by [53] replacing the first entry of $\tilde{\mathbf{f}}_{n,p}^{(M)}$ with $\hat{U}_{n,p}^{(M)} + J_{n,p}^{(M),u}$, replacing the first row of $A_p^{(M)}$ with the first row $\frac{2}{h^{(m)}} D_{N_z}$ and then changing the entry $\left(A_p^{(M)}\right)_{1,1}$ to

$$\left(A_p^{(M)}\right)_{1,1} - (i\eta).$$

The boundary condition at the lower artificial boundary is enforced by replacing the last entry of $\tilde{\mathbf{f}}_{n,p}^{(M)}$ with $D_{n,p}^{(M)}$, the last row of $A_p^{(M)}$ with the last row of $\frac{2}{h^{(M)}} D_{N_z}$ and then changing the entry $\left(A_p^{(M)}\right)_{N_z+1,N_z+1}$ to

$$\left(A_p^{(M)}\right)_{N_z+1,N_z+1} + \left(i\gamma_p^{(M)}\right).$$

It is quite important to note that for fixed p, the deterministic differential operators $A_p^{(m)}$, $m = 0, 1, .., M$, are the same for each Monte Carlo sample and for each Taylor order. We may take advantage of this fact by finding and storing the LU decomposition for $A_p^{(m)}$ for each mode p, for $m = 0, 1, ..., M$. Then, when solving the discretized boundary value problems (3.24), (3.25), and (3.26), we can use the stored LU decomposition of the differential operators along with backward and forward substitution. Being able to use forward and backward substitution when solving the boundary value problem requires only $O(N_z^2)$ computational cost compared to $O(N_z^3)$ computational cost required when using a full direct linear solver.

3.5 Monte Carlo Sampling

To sample the probability space of random interfaces, classic Monte Carlo sampling is used. For a large number of random samples, the boundary value problem will be solved for each random sample and the statistics (mean and variance) of the solution to the boundary value problem will then be computed. The Monte Carlo method is quite simple, but also quite slow with a convergence rate of approximately $O\left(R^{-1/2}\right)$, where R is the total number of samples [7].

We turn to [27] to describe the Monte Carlo method in context of solving differential equations with some sort of random input. In our case, this random input is the random interface separating each layer which gives the boundary in each boundary value problem. After implementing the Transformed Field Equations method, the domain of each boundary value problem is "flattened," and in turn the boundary value problems become non-homogeneous (nonzero right hand sides) with the right hand sides depending on the random interfaces. To understand the convergence of the Monte Carlo method, we must recall the Strong Law of Large Numbers and the Central Limit Theorem [12, 20].

For i.i.d. random variables $X_1, ..., X_R$ with finite mean μ, the Strong Law of Large Numbers says that as $R \to \infty$, there is a probability of one that

$$\left|\frac{X_1 + ... + X_R}{R} - \mu\right| < \epsilon$$

for any $\epsilon > 0$ [20] and the Central Limit Theorem says that as $R \to \infty$, the distribution of $\{\frac{1}{R}\sum_{j=1}^{R} X_j\}$ is approximately a normal distribution [12]. The Strong Law of Large Numbers ensures convergence of the Monte Carlo Method and the Central Limit Theorem is used to describe the rate of convergence [27].

The Monte Carlo Method is simple, easy to use, and will converge. The choice to use the Monte Carlo Method in our numerical algorithm was made based on the simplicity and clarity of the method. With that being said, it is important to note that more efficient sampling techniques could be used instead, such as the quasi-Monte Carlo method or variance reduction techniques. Caflisch gives a detailed description of the quasi-Monte Carlo method in [7] and a short description and example of a variance reduction technique can be found in [27].

Briefly, the quasi-Monte Carlo method uses a sequence of quasi-random numbers, also known as a low-discrepancy sequence, instead of using a random number generator to generate random samples as would be done in the Monte Carlo method. The term "quasi-random" is a bit misleading in that the sequence of quasi-random numbers is actually a deterministic sequence. A sequence of quasi-random numbers is distributed more uniformly, which leads to a faster rate of convergence than the Monte Carlo Method [7, 27]. Variance reduction techniques are exactly as their name describes. The goal of a variance reduction technique is to attain the same computation that the Monte Carlo method would, but in a way that results in a smaller variance. If the variance is able to be reduced, then the error in using the Monte Carlo method would be reduced, as well [27].

3.6 The Numerical Algorithm and Computational Costs

Below is pseudocode describing the numerical algorithm. Following the pseudocode, the approximate computational cost associated with the various parts of the algorithm will be given. Recall that N_x is the number of Fourier modes in the x direction, N_z+1 is the number of collocation points in the z direction, N is the number of Taylor orders, and R is the number of Monte Carlo samples.

3.6.1 Pseudocode of the Numerical Algorithm

For $p = -\frac{N_x}{2}, ..., \frac{N_x}{2} - 1$ (for each mode p)

  Find and store the LU decomposition of the BVP differential operators $A_p^{(m)}$.

End.

For $r = 1, ..., R$ (for each MC sample)

  For $n = 0, ..., N$ (for each Taylor order)

    Solve the linear system (3.17) for $U_n^{(m)}$, $L_n^{(m)}$.

    For $s = 0, ..., N - n$

      Solve for the fields $w_s^{(m)}$ using impedance data $L^{(m)} = L_n^{(m)}$ and $U^{(m)} = U_n^{(m)}$:

        If $s = 0$, solve for the order $s = 0$ fields analytically.

        If $1 \leq s \leq N - n$, solve the discretized boundary value problem for the fields $w_s^{(m)}$ by forward and backward substitution.

      Calculate the IIO's $Q_s[L_n^{(0)}]$, $R_s^{(m),u}[U_n^{(m)}, L_n^{(m)}]$, $R_s^{(m),l}[U_n^{(m)}, L_n^{(m)}]$, and $S_s[U_n^{(m)}]$

    End.

  End.

  For $n = 0, ..., N$

    Solve for the fields $w_n^{(m)}$ using impedance data $L^{(m)} = \sum_{n=0}^{N} L_n^{(m)} \varepsilon^n$ and $U^{(m)} = \sum_{n=0}^{N} U_n^{(m)} \varepsilon^n$:

      If $n = 0$, solve for the order $n = 0$ fields analytically.

      If $1 \leq n \leq N$, solve the discretized boundary value problem for the fields $w_n^{(m)}$ by forward and backward substitution.

  End.

End.

Calculate the average field values $\bar{w}^{(m)}(\cdot) = \dfrac{1}{R}\sum_{r=1}^{R} \bar{w}^{(m)}(\cdot)$.

Calculate the variance of the field values $\sigma^2_{w^{(m)}(\cdot)} = \dfrac{1}{R}\sum_{r=1}^{R}\left(w^{(m)}(\cdot) - \bar{w}^{(m)}(\cdot)\right)^2$.

3.6.2 Computational Costs

The approximate computational costs are discussed for the key parts of the algorithm. Recall that N_x is the number of Fourier modes in the x direction, $N_z + 1$ is the number of collocation points in the z direction, N is the number of Taylor orders, and R is the number of Monte Carlo samples.

The approximate computational cost to find and store the LU decomposition of the differential operators $A_p^{(m)}$ of the boundary value problems for each m^{th} layer is $O(N_x N_z^3)$.

To solve the linear system (3.17) for $U_n^{(m)}$, $L_n^{(m)}$, the Fast Fourier Transform of the right hand side of (3.17) is taken, so that the Fourier coefficients $\hat{U}_{n,p}^{(m)}$ and $\hat{L}_{n,p}^{(m)}$ can be found by solving the linear system. The linear system is solved by inverting the $(M+1)\times(M+1)$ matrix containing the order $n = 0$ IIOs. From there, the Inverse Fast Fourier Transform is taken to ultimately find the values $U_n^{(m)}(\xi_r; x'_j)$ and $L_n^{(m)}(\xi_r; x'_j)$. This entire process ultimately results in a computational cost of approximately $O(MRNN_x \log(N_x))$.

Next, for $s = 0, 1, ..., N - n$, the fields $w_s^{(m)}$ are found using impedance data $L^{(m)} = L_n^{(m)}$ and $U^{(m)} = U_n^{(m)}$. This is done by first solving for the order $s = 0$ fields analytically which results in a computational cost of approximately $O(RN^2 N_x \log(N_x) N_z)$. Then for $s = 1, ..., N - n$, the fields $w_s^{(m)}$ are found by solving the boundary value problems (3.24), (3.25), and (3.26). This is where significant computational savings occur! When solving the boundary value problems, being able to use forward and backward substitution results in a computational cost of approximately $O(N_z^2)$ versus a computational cost of $O(N_z^3)$ that would have been required when using a full direct linear solver. Once the fields $w_s^{(m)}$ are found for $s = 0, 1, ..., N - n$, the IIOs $Q_s[L_n^{(0)}]$, $R_s^{(m),u}[U_n^{(m)}, L_n^{(m)}]$, $R_s^{(m),l}[U_n^{(m)}, L_n^{(m)}]$, and $S_s[U_n^{(m)}]$ are calculated using the newly found fields $w_s^{(m)}$. Overall, this portion of the algorithm results in a computational cost of approximately $O(RN^2 N_x N_z^2) + O(RNN_x \log(N_x)(N + N_z))$.

Finally, once all of the impedance data is known, for each $n = 0, 1, ..., N$, the solutions to the fields $w_n^{(m)}$ using impedance data $L^{(m)} = \sum_{n=0}^{N} L_n^{(m)} \varepsilon^n$ and $U^{(m)} = \sum_{n=0}^{N} U_n^{(m)} \varepsilon^n$ can be found. This is done using the same process as in the previous step. Therefore this portion of the algorithm results in a computational cost of approximately $O(RNN_x N_z^2) + O(RN_x \log(N_x)(N + N_z))$.

Thus, the computational complexity of the numerical algorithm when using the LU decomposition along with forward and backward substitution to solve the boundary value problems is approximately $O(RN_x N^2 N_z^2)$. As a comparison, the computational complexity when using a full direct linear solver to solve the boundary value problems is approximately $O(RN_x N^2 N_z^3)$. A major benefit of the numerical algorithm is its significant reduction in computational costs.

3.7 The Padé Approximation

In order to improve the radius of convergence for the Taylor summation (3.8), we investigate the summation by Padé approximation. This section explores the details of Padé approximations by following the relevant parts of the all-encompassing book of Baker and Graves-Morris *Padé Approximants* [3]. In particular, a description of the Padé approximation will be given followed by a discussion on the convergence of the approximation.

Consider an analytic function $f(z)$. Then $f(z)$ has the Taylor series

$$f(z) = \sum_{n=0}^{\infty} c_n z^n$$

with disk of convergence $|z| < R$. Often, for practical purposes, we must use a truncated Taylor series to approximate the function

$$f(z) \approx \sum_{n=0}^{N} c_n z^n.$$

It is well known that as N approaches infinity, $\displaystyle\sum_{n=0}^{N} c_n z_0^n$ approaches $f(z_0)$, for $|z_0| < R$ (for points inside the disk of convergence), exponentially fast [2]. The truncated Taylor series works magnificently for points of analyticity of the function that are inside the disk of convergence. The Padé approximation may provide a way to approximate the function $f(z)$ for points of analyticity that are outside the disk of convergence of the Taylor series. The Padé approximant is defined as the rational function

$$[L/M](z) = \frac{a_0 + a_1 z + ... + a_L z^L}{b_0 + b_1 z + ... + b_M z^M} = \frac{\sum_{l=0}^{L} a_l z^l}{\sum_{m=0}^{M} b_m z^m},$$

where

$$[L/M](z) = \sum_{n=0}^{N} c_n z^n + O(z^{L+M+1}),$$

$L+M = N$, and it is standard to let $b_0 = 1$. In particular, let us consider the equi-order Padé approximant $[M/M](z)$, where, for simplicity, we assume that N is even (so that $M = N/2$). Now, to find the coefficients $a_0, a_1, ..., a_M$ and $b_1, b_2, ..., b_M$, we can use the following:

$$\frac{\sum_{l=0}^{M} a_l z^l}{\sum_{m=0}^{M} b_m z^m} = \sum_{n=0}^{N} c_n z^n + O(z^{2M+1}).$$

Multiplying both sides of the equation by $\displaystyle\sum_{m=0}^{M} b_m z^m$ gives

$$\Big(\sum_{m=0}^{M} b_m z^m\Big)\Big(\sum_{n=0}^{2M} c_n z^n\Big) = \Big(\sum_{l=0}^{M} a_l z^l\Big) + O(z^{2M+1}).$$

Now, matching the coefficients in front of z^{M+1}, z^{M+2}, ..., z^{2M} on the left and right of the equation, we have

$$b_M c_1 + b_{M-1} c_2 + ... + b_0 c_{M+1} = 0$$

$$b_M c_2 + b_{M-1} c_3 + ... + b_0 c_{M+2} = 0$$

$$\vdots$$

$$b_M c_M + b_{M-1} c_{M+1} + ... + b_0 c_{2M} = 0.$$

Since $b_0 = 1$, we have

$$b_M c_1 + b_{M-1} c_2 + ... + b_1 c_M = -c_{M+1}$$

$$b_M c_2 + b_{M-1} c_3 + ... + b_1 c_{M+1} = -c_{M+2}$$

$$\vdots$$

$$b_M c_M + b_{M-1} c_{M+1} + ... + b_1 c_{2M-1} = -c_{2M},$$

which we can write as the linear system

$$\begin{bmatrix} c_1 & c_2 & ... & c_M \\ c_2 & c_3 & ... & c_{M+1} \\ \vdots & \vdots & \ddots & \vdots \\ c_M & c_{M+1} & ... & c_{2M-1} \end{bmatrix} \begin{bmatrix} b_M \\ b_{M-1} \\ \vdots \\ b_1 \end{bmatrix} = \begin{bmatrix} -c_{M+1} \\ -c_{M+2} \\ \vdots \\ -c_{2M} \end{bmatrix}$$

and use to solve for b_1, b_2, ..., b_M. Now, we may turn our attention to the coefficients in front of $z^0, z^1, ..., z^M$ to see that

$$a_0 = c_0$$

$$a_1 = b_0 c_1 + b_1 c_0$$

$$\vdots$$

$$a_m = \sum_{i=0}^{m} b_i c_{m-i}$$

$$\vdots$$

$$a_M = \sum_{i=0}^{M} b_i c_{M-i}.$$

Naturally, the next question that needs to be addressed is convergence and what is required to achieve convergence. Before discussing convergence, it is necessary to highlight some lemmas and theorems found in Baker and Graves-Morris's *Padé Approximants* [3]. First, consider the Theorem 1.1.2 in [3] credited to Jacobi in [22], which gives a way to define the Padé approximant $[L/M](z)$.

Theorem 3.1. *The* $[L/M](z)$ *Padé approximant of* $\sum_{n=0}^{\infty} c_n z^n$ *is given by*

$$[L/M](z) = \frac{P_L(z)}{Q_M(z)}$$

provided $Q(0) \neq 0$*, where*

$$Q_M(z) = \begin{vmatrix} c_{L-M+1} & c_{L-M+2} & \cdots & c_{L+1} \\ c_{L-M+2} & c_{L-M+3} & \cdots & c_{L+2} \\ \vdots & \vdots & \ddots & \vdots \\ c_L & c_{L+1} & \cdots & c_{L+M} \\ z^M & z^{M-1} & \dots & 1 \end{vmatrix}$$

and

$$P_L(z) = \begin{vmatrix} c_{L-M+1} & c_{L-M+2} & \cdots & c_{L+1} \\ c_{L-M+2} & c_{L-M+3} & \cdots & c_{L+2} \\ \vdots & \vdots & \ddots & \vdots \\ c_L & c_{L+1} & \cdots & c_{L+M} \\ \sum_{i=0}^{L-M} c_i z^{M+i} & \sum_{i=0}^{L-M+1} c_i z^{M-1+i} & \dots & \sum_{i=0}^{L} c_i z^i \end{vmatrix}.$$

Next, consider the Corollary from Section 6.3 of [3], which gives an error formula for a Padé approximation.

Corollary 3.1. *Suppose that $f(z)$ is analytic in and continuous on a contour Γ which encloses both z and the origin. Let $R_M(z)$ be an arbitrary polynomial of degree at most M which is not identically zero. Then*

$$f(z) - [L/M](z) = \frac{z^{L+M+1}}{2\pi i Q_M(z)R_M(z)} \int_\Gamma \frac{f(v)Q_M(v)R_M(v)}{v^{L+M+1}(v-z)} dv.$$

Below is the proof as accounted by Baker in [3].

Proof. Consider the function $\phi(z) = R_M(z)(f(z)Q_M(z) - P_L(z))z^{-L-M-1}$.
Let Γ be any simple closed contour which encloses z and the origin.
By Cauchy's Theorem,

$$\phi(z) = \frac{1}{2\pi i} \int_\Gamma \frac{\phi(v)}{v-z} dv.$$

Now, note that

$$\frac{\phi(z)z^{L+M+1}}{Q_M(z)R_M(z)} = f(z) - [L/M](z).$$

Now we have

$$\begin{aligned}
f(z) - [L/M](z) &= \frac{\phi(z)z^{L+M+1}}{Q_M(z)R_M(z)} \\
&= \frac{z^{L+M+1}}{2\pi i Q_M(z)R_M(z)} \int_\Gamma \frac{\phi(v)}{v-z} dv \\
&= \frac{z^{L+M+1}}{2\pi i Q_M(z)R_M(z)} \int_\Gamma \frac{R_M(z)(f(z)Q_M(z) - P_L(z))}{(v-z)v^{L+M+1}} dv \\
&= \frac{z^{L+M+1}}{2\pi i Q_M(z)R_M(z)} \left(\int_\Gamma \frac{R_M(z)Q_M(z)f(z)}{(v-z)v^{L+M+1}} dv - \int_\Gamma \frac{R_M(z)P_L(z)}{(v-z)v^{L+M+1}} dv \right).
\end{aligned}$$

Now we need to show that $\displaystyle\int_\Gamma \frac{R_M(z)P_L(z)}{(v-z)v^{L+M+1}} dv = 0$, where Γ is any simple closed contour that encloses z and the origin.

Note that for $|v| > |z|$, $\dfrac{R_M(z)P_L(z)}{(v-z)v^{L+M+1}}$ is analytic.

Recall that $R_M(v)$ is a polynomial of degree at most M and $P_L(v)$ is a polynomial of degree at most L. So $R_M(v)P_M(v)$ is a polynomial of degree at most $L+M$.

So $\dfrac{R_M(z)P_L(z)}{(v-z)v^{L+M+1}}$ is of order $\dfrac{1}{v^2}$.

Then as $|v|$ approaches ∞, $\displaystyle\int_\Gamma \frac{R_M(z)P_L(z)}{(v-z)v^{L+M+1}}dv = \int_{|v|>|z|} \frac{R_M(z)P_L(z)}{(v-z)v^{L+M+1}}dv$ approaches 0.

Therefore,

$$f(z) - [L/M](z) = \frac{z^{L+M+1}}{2\pi i Q_M(z)R_M(z)} \int_\Gamma \frac{f(v)Q_M(v)R_M(v)}{v^{L+M+1}(v-z)}dv.$$

□

Next, we must draw our attention to a lemma by Szegö [41, 45] as stated in the paper "Convergence of Padé Approximants in the General Case" by Zinn-Justin [56].

Lemma 3.1. *Suppose the inequality*

$$\prod_{i=1}^{n} |(z - z_i)| < \alpha^n,$$

holds for $z \in D$, where $\alpha > 0$. Then the set D has measure of at most $\delta = \pi\alpha^2$.

A proof of this Lemma can be found in [41].

The above results will be used in the proof of the primary convergence result of interest, which is credited to Nutall [41] and Zinn-Justin [56]. The proof of the following theorem (Theorem 6.5.3 in [3]) follows that of Zinn-Justin as stated in [3].

Theorem 3.2. *Let $f(z)$ be a meromorphic function and let $\varepsilon, \delta > 0$ be given. Then there exists M_0 such that for any $M > M_0$, any $[M/M](z)$ Padé approximant satisfies*

$$|f(z) - [M/M](z)| < \varepsilon$$

on any compact set of the z-plane except for a set E_M of measure less than δ.

Instead of considering a meromorphic function, let us instead consider an analytic function.

Proof. Suppose f is an analytic function. Let's show convergence for $|z| < R_0$ except on a set E_M of measure less than δ. Let $\varepsilon, \delta > 0$ be given and define $\eta = \frac{1}{2}\sqrt{\frac{\delta}{\pi}}$. Without loss of generality, assume $0 < \eta < R_0$. Define $R_{min} \equiv \frac{3}{\eta}R_0^2$. Since f is analytic, for some δ_0, where $0 < \delta_0 < 1$, there exists R such that $R > R_{min}$ and $f(z)$ is analytic in $|z - R| < \delta_0$ [1].

For simplicity, let $R_M(z) \equiv 1$. By Corollary 3.1 we have

$$\begin{aligned} |f(z) - [M/M](z)| &= \Big| \frac{z^{2M+1}}{2\pi i R_M(z) Q_M(z)} \oint_{|t|=R} \frac{f(t) R_M(t) Q_M(t)}{t^{2M+1}(t-z)} dt \Big| \\ &\le \frac{R_0^{2M+1}}{2\pi |Q_M(z)|} \oint_{|t|=R} \Big| \frac{f(t) Q_M(t)}{t^{2M+1}(t-z)} \Big| dt. \end{aligned}$$

Let $K = \sup_{|t|=R} |f(t)|$. Then

$$|f(z) - [M/M](z)| \le \frac{R_0^{2M+1} K}{2\pi} \sup_{|t|=R} \frac{|Q_M(t)|}{|Q_M(z)|} \oint_{|t|=R} \Big| \frac{1}{t^{2M+1}(t-z)} \Big| dt.$$

Now,

$$
\begin{aligned}
\oint_{|t|=R} \left| \frac{1}{t^{2M+1}(t-z)} \right| dt &= \frac{R}{R^{2M+1}} \int_0^{2\pi} \frac{1}{|Re^{i\theta} - z|} d\theta \\
&\leq \frac{R}{R^{2M+1}} \int_0^{2\pi} \frac{1}{||Re^{i\theta}| - |z||} d\theta \\
&\leq \frac{R}{R^{2M+1}} \int_0^{2\pi} \frac{1}{R - R_0} d\theta \\
&\leq \frac{R}{R^{2M+1}} \Big(\frac{2\pi}{R_{min} - R_0} \Big) \\
&= \frac{2\pi R}{R^{2M+1}} \Big(\frac{1}{3R_0^2/\eta - R_0} \Big) \\
&\leq \frac{2\pi}{R^{2M}} \Big(\frac{1}{3R_0^2/R_0 - R_0} \Big) \\
&= \frac{2\pi}{2R_0 R^{2M}}.
\end{aligned}
$$

This gives

$$
\begin{aligned}
|f(z) - [M/M](z)| &\leq \frac{R_0^{2M+1} K}{2\pi} \sup_{|t|=R} \frac{|Q_M(t)|}{|Q_M(z)|} \Big(\frac{2\pi}{2R_0 R^{2M}} \Big) \\
&= \frac{R_0^{2M} K}{2R^{2M}} \sup_{|t|=R} \frac{|Q_M(t)|}{|Q_M(z)|}.
\end{aligned}
$$

By the Fundamental Theorem of Algebra,

$$
Q_M(z) = \prod_{i=1}^{M} (z - z_i),
$$

where z_i are the roots of $Q_M(z)$. Then we can separate the roots z_i into two groups:

$$
\{z_i : |z_i| < 2R\} \text{ and } \{z_i : |z_i| \geq 2R\}.
$$

Then for some $M' \leq M$, we can index them as follows

$$\{z_i : |z_i| < 2R\} = z_1, z_2, ..., z_{M'}$$

$$\{z_i : |z_i| \geq 2R\} = z_{M'+1}, z_{M'+2}, ..., z_M.$$

Now, we can write

$$\sup_{|t|=R} \frac{|Q_M(t)|}{|Q_M(z)|} = \sup_{|t|=R} \prod_{i=1}^{M'} \Big| \frac{t - z_i}{z - z_i} \Big| \prod_{i=M'+1}^{M} \Big| \frac{t - z_i}{z - z_i} \Big|.$$

Let us take a closer look at $\sup\limits_{|t|=R} \prod\limits_{i=M'+1}^{M} \Big| \frac{t - z_i}{z - z_i} \Big|$.

$$\begin{aligned}
\sup_{|t|=R} \prod_{i=M'+1}^{M} \Big| \frac{t - z_i}{z - z_i} \Big| &\leq \prod_{i=M'+1}^{M} \sup_{|t|=R} \Big| \frac{t - z_i}{z - z_i} \Big| \\
&\leq \prod_{i=M'+1}^{M} \sup_{|t|=R} \frac{|t| + |z_i|}{||z| - |z_i||} \\
&= \prod_{i=M'+1}^{M} \frac{|z_i| + R}{|z_i| - |z|} \\
&\leq \prod_{i=M'+1}^{M} \frac{|z_i| + R}{|z_i| - R} \\
&= \prod_{i=M'+1}^{M} \frac{1 + R/|z_i|}{1 - R/|z_i|} \\
&\leq \prod_{i=M'+1}^{M} \frac{1 + R/(2R)}{1 - R/(2R)} \\
&= 3^{M-M'}.
\end{aligned}$$

Also, note that

$$\begin{aligned}
\sup_{|t|=R}\prod_{i=1}^{M'}\left|\frac{t-z_i}{z-z_i}\right| &\le \prod_{i=1}^{M'}\sup_{|t|=R}\left|\frac{t-z_i}{z-z_i}\right| \\
&\le \prod_{i=1}^{M'}\sup_{|t|=R}\frac{|t|+|z_i|}{|z-z_i|} \\
&= \prod_{i=1}^{M'}\frac{R+|z_i|}{|z-z_i|} \\
&\le \prod_{i=1}^{M'}\frac{R+2R}{|z-z_i|} \\
&= \frac{(3R)^{M'}}{\prod_{i=1}^{M'}|z-z_i|}.
\end{aligned}$$

Let E_M be the set for which $\displaystyle\prod_{i=1}^{M'}|z-z_i| < \eta^{M'}$ for any $z \in E_M$. By Szegö's lemma, the measure of E_M is less than $\pi\eta^2 = \dfrac{\delta}{4} < \delta$. This implies that for any $z \notin E_M$, $\displaystyle\prod_{i=1}^{M'}|z-z_i| \ge \eta^{M'}$. Now we can see that, for any $z \notin E_M$ such that $|z| \le R_0$,

$$\sup_{|t|=R}\frac{|Q_M(t)|}{|Q_M(z)|} \le \frac{(3R)^{M'}3^{M-M'}}{\eta^{M'}} = \frac{3^M R^{M'}}{\eta^{M'}}.$$

Therefore, since $R > R_{min} = \dfrac{3}{\eta}R_0^2$ and $\dfrac{R}{\eta} > \dfrac{3R_0^2}{\eta^2} > \dfrac{3R_0^2}{R_0^2} = 3 > 1$,

$$\begin{aligned}
|f(z) - [M/M](z)| &\leq \frac{R_0^{2M}K}{2R^{2M}}\Big(\frac{3^M R^{M'}}{\eta^{M'}}\Big) \\
&= \frac{KR_0^{2M}3^M}{2R^{2M}}\Big(\frac{R}{\eta}\Big)^{M'} \\
&\leq \frac{KR_0^{2M}3^M}{2R^{2M}}\Big(\frac{R}{\eta}\Big)^{M} \\
&= \frac{K}{2}\Big(\frac{3R_0^2}{\eta}\Big)^M\Big(\frac{1}{R}\Big)^M \\
&< \varepsilon.
\end{aligned}$$

$\square$

Chapter 4

Numerical Results

In this chapter, numerical results will be presented to demonstrate the accuracy and convergence of the numerical algorithm. To test the accuracy of the method, the mean and variance of the energy defect will be calculated. There will be a derivation of the energy defect and then numerical results will be shown.

4.1 The Energy Defect

The energy defect is a result of the conservation of energy and says that the total amount of energy, which consists of the energy reflected and the energy transmitted, should be conserved. Recall that for $m = 0, ..., M$

$$w^{(m)}(\xi; x', z') = \sum_{p=-\infty}^{\infty} \sum_{n=0}^{\infty} \hat{w}_{n,p}^{(0)}(\xi; z') e^{i\alpha_p x'} \varepsilon^n.$$

Then the energy defect is given by

$$e(\xi) = \sum_{p \in P^{(0)}} \frac{\gamma_p^{(0)}}{\gamma_0^{(0)}} \Big| \sum_{n=0}^{\infty} \hat{w}_{n,p}^{(0)}(\xi; a) \varepsilon^n \Big|^2 + \sum_{p \in P^{(M)}} \frac{\gamma_p^{(M)}}{\gamma_0^{(0)}} \Big| \sum_{n=0}^{\infty} \hat{w}_{n,p}^{(M)}(\xi; b) \varepsilon^n \Big|^2 - 1, \qquad (4.1)$$

where the first sum is the amount of energy reflected and the second sum is the amount of energy transmitted [43]. By the conservation of energy, the energy defect should be 0.

The following is a derivation of (4.1) with guidance from [43]. Recall that for $z > a$, $v^{(0)}(x, z) = \sum_{p=-\infty}^{\infty} \hat{v}_p^{(0)} e^{i\alpha_p x + i\gamma_p^{(0)}(z-a)}$ and for $z < b$, $v^{(M)}(x, z) = \sum_{p=-\infty}^{\infty} \hat{v}_p^{(M)} e^{i\alpha_p x - i\gamma_p^{(0)}(z-b)}$ and that v is the total field. For $z > a_1 + g_1(\xi; x)$, $v = v^{inc} + v^{(0)}$ and for $z < a_M + g_M(\xi, x)$, $v = v^{(M)}$.

The domain of the governing equations is given by $\Omega = \Omega_0(\xi) \cup \Omega_1(\xi) \cup ... \cup \Omega_M(\xi)$ and let the boundary of the domain be given by $\partial\Omega = C_1 \cup C_2 \cup C_3 \cup C_4$. Let C_1 be given by $\{(x,z) : 0 \leq x \leq d, z = b\}$, C_2 be given by $\{(x,z) : x = 0, b \leq z \leq a\}$, C_3 be given by $\{(x,z) : 0 \leq x \leq d, z = a\}$, and C_4 be given by $\{(x,z) : x = d, b \leq z \leq a\}$. Note that since the total field is quasiperiodic, we are restricting the domain to one full period in the x-direction. On the domain Ω, $\Delta v + k^2 v = 0$ and $\Delta \bar{v} + k^2 \bar{v} = 0$. This gives the following

$$\begin{aligned}
0 &= (\Delta v + k^2 v)\bar{v} - (\Delta \bar{v} + k^2 \bar{v})v \\
&= \Delta v \bar{v} + k^2 v \bar{v} - \Delta \bar{v} v - k^2 \bar{v} v. \\
&= \Delta v \bar{v} - \Delta \bar{v} v.
\end{aligned}$$

Then by Green's Identity [11], we have

$$\int_{\Omega} (\Delta v \bar{v} - \Delta \bar{v} v) dx = \int_{\partial\Omega} \Big(\frac{\partial v}{\partial \mathbf{n}} \bar{v} - \frac{\partial \bar{v}}{\partial \mathbf{n}} v \Big) ds = 0.$$

Therefore,

$$\begin{aligned}
0 &= \int_{\Omega} (\Delta v \bar{v} - \Delta \bar{v} v) dx \\
&= \int_{\partial\Omega} \Big(\frac{\partial v}{\partial \mathbf{n}} \bar{v} - \frac{\partial \bar{v}}{\partial \mathbf{n}} v) ds \\
&= \int_{C_1} \Big(\frac{\partial v}{\partial \mathbf{n}} \bar{v} - \frac{\partial \bar{v}}{\partial \mathbf{n}} v \Big) ds + \int_{C_2} \Big(\frac{\partial v}{\partial \mathbf{n}} \bar{v} - \frac{\partial \bar{v}}{\partial \mathbf{n}} v \Big) ds + \\
&\qquad \int_{C_3} \Big(\frac{\partial v}{\partial \mathbf{n}} \bar{v} - \frac{\partial \bar{v}}{\partial \mathbf{n}} v \Big) ds + \int_{C_4} \Big(\frac{\partial v}{\partial \mathbf{n}} \bar{v} - \frac{\partial \bar{v}}{\partial \mathbf{n}} v \Big) ds.
\end{aligned}$$

Since C_2 and C_4 have opposite pointing normals and due to quasiperiodicty of the fields, i.e. $v(\xi; x + d, z) = e^{i\alpha d} v(\xi; x, z)$, the contributions from C_2 and C_4 cancel each other out as shown below:

$$
\begin{aligned}
\int_{C_2}\Big(\frac{\partial v}{\partial \mathbf{n}}\bar{v}-\frac{\partial \bar{v}}{\partial \mathbf{n}}v\Big)ds &= \int_b^a \Big[\Big(\nabla v\cdot \begin{bmatrix}1\\ \\0\end{bmatrix}\Big)(\xi;d,z)\bar{v}(\xi;d,z)-\Big(\nabla \bar{v}\cdot \begin{bmatrix}1\\ \\0\end{bmatrix}\Big)(\xi;d,z)v(\xi;d,z)\Big]dz \\
&= \int_b^a \Big[\partial_x v(\xi;d,z)\bar{v}(\xi;d,z)-\partial_x\bar{v}(\xi;d,z)v(\xi;d,z)\Big]dz \\
&= \int_b^a \Big[e^{i\alpha d}\partial_x v(\xi;,0,z)e^{-i\alpha d}\bar{v}(\xi;,0,z)-e^{-i\alpha d}\partial_x\bar{v}(\xi;0,z)e^{i\alpha d}v(\xi;0,z)\Big]dz \\
&= \int_b^a \Big[\partial_x v(\xi;,0,z)\bar{v}(\xi;,0,z)-\partial_x\bar{v}(\xi;0,z)v(\xi;0,z)\Big]dz
\end{aligned}
$$

and

$$
\begin{aligned}
\int_{C_4}\Big(\frac{\partial v}{\partial \mathbf{n}}\bar{v}-\frac{\partial \bar{v}}{\partial \mathbf{n}}v\Big)ds &= \int_b^a \Big[\Big(\nabla v\cdot \begin{bmatrix}-1\\ \\0\end{bmatrix}\Big)(\xi;0,z)\bar{v}(\xi;0,z)-\Big(\nabla \bar{v}\cdot \begin{bmatrix}-1\\ \\0\end{bmatrix}\Big)(\xi;0,z)v(\xi;0,z)\Big]dz \\
&= \int_b^a \Big[-\partial_x v(\xi;0,z)\bar{v}(\xi;0,z)+\partial_x\bar{v}(\xi;0,z)v(\xi;0,z)\Big]dz \\
&= -\int_b^a \Big[\partial_x v(\xi;0,z)\bar{v}(\xi;0,z)-\partial_x\bar{v}(\xi;0,z)v(\xi;0,z)\Big]dz \\
&= -\int_{C_2}\Big(\frac{\partial v}{\partial \mathbf{n}}\bar{v}-\frac{\partial \bar{v}}{\partial \mathbf{n}}v\Big)ds.
\end{aligned}
$$

Therefore,

$$
\begin{aligned}
0 &= \int_{\partial\Omega}\Big(\frac{\partial v}{\partial \mathbf{n}}\bar{v}-\frac{\partial \bar{v}}{\partial \mathbf{n}}v)ds \\
&= \int_{C_1}\Big(\frac{\partial v}{\partial \mathbf{n}}\bar{v}-\frac{\partial \bar{v}}{\partial \mathbf{n}}v\Big)ds+\int_{C_2}\Big(\frac{\partial v}{\partial \mathbf{n}}\bar{v}-\frac{\partial \bar{v}}{\partial \mathbf{n}}v\Big)ds+\int_{C_3}\Big(\frac{\partial v}{\partial \mathbf{n}}\bar{v}-\frac{\partial \bar{v}}{\partial \mathbf{n}}v\Big)ds+\int_{C_4}\Big(\frac{\partial v}{\partial \mathbf{n}}\bar{v}-\frac{\partial \bar{v}}{\partial \mathbf{n}}v\Big)ds \\
&= \int_{C_1}\Big(\frac{\partial v}{\partial \mathbf{n}}\bar{v}-\frac{\partial \bar{v}}{\partial \mathbf{n}}v\Big)ds+\int_{C_3}\Big(\frac{\partial v}{\partial \mathbf{n}}\bar{v}-\frac{\partial \bar{v}}{\partial \mathbf{n}}v\Big)ds.
\end{aligned}
$$

On C_1,

$$\frac{\partial v}{\partial \mathbf{n}}(x,b) = \frac{\partial v^{(M)}}{\partial \mathbf{n}}(x,b) = \nabla v^{(M)}(x,b) \cdot \begin{bmatrix} 0 \\ -1 \end{bmatrix} = -\sum_{p=-\infty}^{\infty} (-i\gamma_p^{(M)}) \hat{v_p}^{(M)} e^{i\alpha_p x}$$

and

$$\bar{v}(x,b) = v^{(\bar{M})}(x,b) = \sum_{q=-\infty}^{\infty} \bar{\hat{v}}_q^{(M)} e^{-i\alpha_p x},$$

so that on C_1,

$$\begin{aligned}\Big(\frac{\partial v}{\partial \mathbf{n}}\bar{v} - \frac{\partial \bar{v}}{\partial \mathbf{n}} v\Big)\Big|_{x=x,z=b} = &\sum_{p=-\infty}^{\infty}\sum_{q=-\infty}^{\infty} (i\gamma_p^{(M)}) \hat{v}_p^{(M)} \bar{\hat{v}}_q^{(M)} e^{i(\alpha_p-\alpha_q)x} + \\ &\sum_{p=-\infty}^{\infty}\sum_{q\in P^{(M)}} (i\gamma_q^{(M)}) \hat{v}_p^{(M)} \bar{\hat{v}}_q^{(M)} e^{i(\alpha_p-\alpha_q)x} + \\ &\sum_{p=-\infty}^{\infty}\sum_{q\notin P^{(M)}} (-i\gamma_q^{(M)}) \hat{v}_p^{(M)} \bar{\hat{v}}_q^{(M)} e^{i(\alpha_p-\alpha_q)x}.\end{aligned}$$

Note that $\alpha_p - \alpha_q = \Big(\alpha + \dfrac{2\pi p}{d}\Big) - \Big(\alpha + \dfrac{2\pi q}{d}\Big) = \dfrac{2\pi(p-q)}{d}$. Let $m = p - q$. Then $\alpha_p - \alpha_q = \frac{2\pi m}{d}$. Then, if $m \neq 0$,

$$\begin{aligned}\int_0^d e^{i(2\pi m/d)x} dx &= \frac{d}{2\pi m i} e^{i(2\pi m/d)x}\Big|_0^d \\ &= 0,\end{aligned}$$

and if $m = 0$

$$\int_0^d e^{i(2\pi m/d)x} dx = \int_0^d dx$$
$$= d.$$

Then $\int_{C_1} \Big(\frac{\partial v}{\partial \mathbf{n}}\bar{v} - \frac{\partial \bar{v}}{\partial \mathbf{n}} v\Big) ds \neq 0$ if $p = q$. So now we have two scenarios which avoid the trivial solution: $p, q \in P^{(M)}$ and $p = q$ or $p, q \notin P^{(M)}$ and $p = q$. Now we have the following:

$$\begin{aligned}
\int_{C_1} \Big(\frac{\partial v}{\partial \mathbf{n}}\bar{v} - \frac{\partial \bar{v}}{\partial \mathbf{n}} v\Big) ds &= \sum_{p=-\infty}^{\infty} \sum_{q=-\infty}^{\infty} (i\gamma_p^{(M)}) \hat{v}_p^{(M)} \bar{\hat{v}}_q^{(M)} \int_0^d e^{i(\alpha_p - \alpha_q)x} dx + \\
&\quad \sum_{p=-\infty}^{\infty} \sum_{q \in P^{(M)}} (i\gamma_q^{(M)}) \hat{v}_p^{(M)} \bar{\hat{v}}_q^{(M)} \int_0^d e^{i(\alpha_p - \alpha_q)x} dx + \\
&\quad \sum_{p=-\infty}^{\infty} \sum_{q \notin P^{(M)}} (-i\gamma_q^{(M)}) \hat{v}_p^{(M)} \bar{\hat{v}}_q^{(M)} \int_0^d e^{i(\alpha_p - \alpha_q)x} dx \\
&= \sum_{p \in P^{(M)}} (i\gamma_p^{(M)}) |\hat{v}_p^{(M)}|^2 (d) + \sum_{p \notin P^{(M)}} (i\gamma_p^{(M)}) |\hat{v}_p^{(M)}|^2 (d) \\
&\quad + \sum_{p \in P^{(M)}} (i\gamma_p^{(M)}) |\hat{v}_p^{(M)}|^2 (d) + \sum_{p \notin P^{(M)}} (-i\gamma_p^{(M)}) |\hat{v}_p^{(M)}|^2 (d) \\
&= 2d \sum_{p \in P^{(M)}} (i\gamma_p^{(M)}) |\hat{v}_p^{(M)}|^2 .
\end{aligned}$$

On C_3,

$$\begin{aligned}
\frac{\partial v}{\partial \mathbf{n}}(x,a) &= \frac{\partial(v^{inc}+v^{(0)})}{\partial \mathbf{n}}(x,a) \\
&= \nabla(v^{inc}(x,a)+v^{(0)}(x,a)) \cdot \begin{bmatrix} 0 \\ 1 \end{bmatrix} \\
&= \partial_z v^{inc}(x,a) + \partial_z v^{(0)}(x,a) \\
&= (-i\gamma^{(0)})e^{i\alpha x - i\gamma^{(0)}a} + \sum_{p=-\infty}^{\infty} (i\gamma_p^{(0)})\hat{v}_p^{(0)} e^{i\alpha_p x} \\
&= (-i\gamma_0^{(0)})e^{i\alpha x - i\gamma^{(0)}a} + \sum_{p=-\infty}^{\infty} (i\gamma_p^{(0)})\hat{v}_p^{(0)} e^{i\alpha_p x}
\end{aligned}$$

and

$$\bar{v}(x,a) = \bar{v}^{inc}(x,a) + \bar{v}^{(0)}(x,a) = e^{-i\alpha x + i\gamma_0^{(0)}a} + \sum_{q=-\infty}^{\infty} \bar{\hat{v}}_q^{(0)} e^{-i\alpha_q x},$$

so that on C_3,

$$
\begin{aligned}
\left(\frac{\partial v}{\partial \mathbf{n}}\bar{v} - \frac{\partial \bar{v}}{\partial \mathbf{n}}v\right)\Big|_{x=x,z=a} = & \sum_{p=-\infty}^{\infty}\sum_{q=-\infty}^{\infty}(i\gamma_p^{(0)})\hat{v}_p^{(0)}\bar{\hat{v}}_q^{(0)}e^{i(\alpha_p-\alpha_q)x}+ \\
& e^{i\gamma_0^{(0)}a}\sum_{p=-\infty}^{\infty}(i\gamma_p^{(0)})\hat{v}_p^{(0)}e^{i(2\pi p/d)x}+ \\
& (-i\gamma_0^{(0)})e^{-i\gamma_0^{(0)}a}\sum_{q=-\infty}^{\infty}\bar{\hat{v}}_q^{(0)}e^{-i(2\pi q/d)x} + (-i\gamma_0^{(0)}) \\
& + \sum_{p=-\infty}^{\infty}\sum_{q\in P^{(0)}}(i\gamma_p^{(0)})\hat{v}_p^{(0)}\bar{\hat{v}}_q^{(0)}e^{i(\alpha_p-\alpha_q)x}- \\
& \sum_{p=-\infty}^{\infty}\sum_{q\notin P^{(0)}}(i\gamma_p^{(0)})\hat{v}_p^{(0)}\bar{\hat{v}}_q^{(0)}e^{i(\alpha_p-\alpha_q)x} \\
& - (i\gamma_0^{(0)})e^{i\gamma_0^{(0)}a}\sum_{p=-\infty}^{\infty}\hat{v}_p^{(0)}e^{i(2\pi p/d)x}- \\
& e^{-i\gamma_0^{(0)}a}\sum_{q\in P^{(0)}}(-i\gamma_q^{(0)})\bar{\hat{v}}_p^{(0)}e^{-i(2\pi q/d)x} \\
& - e^{-i\gamma_0^{(0)}a}\sum_{q\notin P^{(0)}}(i\gamma_q^{(0)})\bar{\hat{v}}_p^{(0)}e^{-i(2\pi q/d)x} - (i\gamma_0^{(0)}).
\end{aligned}
$$

Again, since $\int_0^d e^{i(2\pi m/d)x}dx \neq 0$ only when $m = 0$, which corresponds to $\int_0^d e^{i(\alpha_p - \alpha_q)x}dx \neq 0$ when $p = q$, we have the following:

$$
\begin{aligned}
\int_{C_3} \Big(\frac{\partial v}{\partial \mathbf{n}}\bar{v} - \frac{\partial \bar{v}}{\partial \mathbf{n}}v\Big)ds = &\sum_{p=-\infty}^{\infty}\sum_{q=-\infty}^{\infty}(i\gamma_p^{(0)})\hat{v}_p^{(0)}\bar{\hat{v}}_q^{(0)}\int_0^d e^{i(\alpha_p-\alpha_q)x}dx+ \\
&\quad e^{i\gamma_0^{(0)}a}\sum_{p=-\infty}^{\infty}(i\gamma_p^{(0)})\hat{v}_p^{(0)}\int_0^d e^{i(2\pi p/d)x}dx \\
&\quad (-i\gamma_0^{(0)})e^{-i\gamma_0^{(0)}a}\sum_{q=-\infty}^{\infty}\bar{\hat{v}}_q^{(0)}\int_0^d e^{-i(2\pi q/d)x}dx + \int_0^d(-i\gamma_0^{(0)})dx \\
&\quad + \sum_{p=-\infty}^{\infty}\sum_{q\in P^{(0)}}(i\gamma_p^{(0)})\hat{v}_p^{(0)}\bar{\hat{v}}_q^{(0)}\int_0^d e^{i(\alpha_p-\alpha_q)x}dx- \\
&\quad \sum_{p=-\infty}^{\infty}\sum_{q\notin P^{(0)}}(i\gamma_p^{(0)})\hat{v}_p^{(0)}\bar{\hat{v}}_q^{(0)}\int_0^d e^{i(\alpha_p-\alpha_q)x}dx \\
&\quad - (i\gamma_0^{(0)})e^{i\gamma_0^{(0)}a}\sum_{p=-\infty}^{\infty}\hat{v}_p^{(0)}\int_0^d e^{i(2\pi p/d)x}dx \\
&\quad - e^{-i\gamma_0^{(0)}a}\sum_{q\in P^{(0)}}(-i\gamma_q^{(0)})\bar{\hat{v}}_p^{(0)}\int_0^d e^{-i(2\pi q/d)x}dx \\
&\quad - e^{-i\gamma_0^{(0)}a}\sum_{q\notin P^{(0)}}(i\gamma_q^{(0)})\bar{\hat{v}}_p^{(0)}\int_0^d e^{-i(2\pi q/d)x}dx - \int_0^d(i\gamma_0^{(0)})dx \\
= &\sum_{p\in P^{(0)}}(i\gamma_p^{(0)})|\hat{v}_p^{(0)}|^2(d) + \sum_{p\notin P^{(0)}}(i\gamma_p^{(0)})|\hat{v}_p^{(0)}|^2(d) + e^{i\gamma_0^{(0)}a}(i\gamma_0^{(0)})\hat{v}_0^{(0)}(d) \\
&\quad + e^{-i\gamma_0^{(0)}a}(-i\gamma_0^{(0)})\bar{\hat{v}}_0^{(0)}(d) - i\gamma_0^{(0)}d + \sum_{p\in P^{(0)}}(i\gamma_p^{(0)})|\hat{v}_p^{(0)}|^2(d)- \\
&\quad \sum_{p\notin P^{(0)}}(i\gamma_p^{(0)})|\hat{v}_p^{(0)}|^2(d) - (i\gamma_0^{(0)})e^{i\gamma_0^{(0)}a}\hat{v}_0^{(0)}(d) + e^{-i\gamma_0^{(0)}a}(i\gamma_0^{(0)})\bar{\hat{v}}_0^{(0)}(d) \\
&\quad - i\gamma_0^{(0)}d \\
= &\ 2d\sum_{p\in P^{(0)}}(i\gamma_p^{(0)})|\hat{v}_p^{(0)}|^2 - 2i\gamma_0^{(0)}d
\end{aligned}
$$

Then,

$$
\begin{aligned}
0 &= \int_\Omega (\Delta v \bar{v} - \Delta \bar{v} v) dx \\
&= \int_{\partial\Omega} \Big(\frac{\partial v}{\partial \mathbf{n}} \bar{v} - \frac{\partial \bar{v}}{\partial \mathbf{n}} v \Big) ds \\
&= \int_{C_1} \Big(\frac{\partial v}{\partial \mathbf{n}} \bar{v} - \frac{\partial \bar{v}}{\partial \mathbf{n}} v \Big) ds + \int_{C_3} \Big(\frac{\partial v}{\partial \mathbf{n}} \bar{v} - \frac{\partial \bar{v}}{\partial \mathbf{n}} v \Big) ds \\
&= 2d \sum_{p \in P^{(M)}} (i\gamma_p^{(M)}) |\hat{v}_p^{(M)}|^2 + 2d \sum_{p \in P^{(0)}} (i\gamma_p^{(0)}) |\hat{v}_p^{(0)}|^2 - 2i\gamma_0^{(0)} d,
\end{aligned}
$$

which implies

$$
0 = \sum_{p \in P^{(0)}} \gamma_p^{(0)} |\hat{v}_p^{(0)}|^2 + \sum_{p \in P^{(M)}} \gamma_p^{(M)} |\hat{v}_p^{(M)}|^2 - \gamma_0^{(0)}.
$$

Therefore $1 = \sum_{p \in P^{(0)}} \frac{\gamma_p^{(0)}}{\gamma_0^{(0)}} |\hat{v}_p^{(0)}|^2 + \sum_{p \in P^{(M)}} \frac{\gamma_p^{(M)}}{\gamma_0^{(0)}} |\hat{v}_p^{(M)}|^2$. Then we define the energy defect to be

$$
e = \sum_{p \in P^{(0)}} \frac{\gamma_p^{(0)}}{\gamma_0^{(0)}} |\hat{v}_p^{(0)}|^2 + \sum_{p \in P^{(M)}} \frac{\gamma_p^{(M)}}{\gamma_0^{(0)}} |\hat{v}_p^{(M)}|^2 - 1.
$$

Now, again, we recall that our solution on $\Omega_0(\xi)$ is given by

$$
w^{(0)}(\xi; x', z') = \sum_{p=-\infty}^{\infty} \sum_{n=0}^{\infty} \hat{w}_{n,p}^{(0)}(\xi; z') e^{i\alpha_p x'} \varepsilon^n
$$

and that our solution on $\Omega_M(\xi)$ is given by

$$
w^{(M)}(\xi; x', z') = \sum_{p=-\infty}^{\infty} \sum_{n=0}^{\infty} \hat{w}_{n,p}^{(M)}(\xi; z') e^{i\alpha_p x'} \varepsilon^n,
$$

so we can see that, with regards to the derivation of the energy defect and the form of our solutions, we have that the energy defect is given by (4.1). We will use this as a way to measure the accuracy of the algorithm. The goal is to have the mean energy defect,

$\bar{e} = \frac{1}{R}\sum_{r=1}^{R} e(\xi_r)$, and the variance of the energy defect, $\sigma_e^2 = \frac{1}{R}\sum_{r=1}^{R}(e(\xi_r) - \bar{e})^2$ as close to 0 as possible.

4.2 Numerical Results

For these results, two random interfaces were used resulting in three layers. Given an incident plane wave, $v^{inc}(x,z) = e^{i\alpha x - i\gamma^{(0)} z}$, which illuminates the structure from above, the absolute value of the mean energy defect and the variance of the energy defect were calculated to demonstrate the accuracy and convergence of the numerical algorithm. The electromagnetic fields have been assumed to have a transverse electric (TE) polarization. The following results were found with various values of ε, N_x (the number of Fourier modes in the x direction), N_z ($N_z + 1$ is the number of collocation points in the z direction), N (the number of Taylor orders), and the correlation length l_c. The following parameters were fixed. The wavenumber in the upper layer was set to $k^{(0)} = 2\pi$; the wave number in the middle layer was set to $k^{(1)} = \pi$; the wavenumber in the lower layer was set to $k^{(2)} = 2\pi$; the upper artificial boundary was set to $z = a = 1.1$; the lower artificial boundary was set to $z = b = -1.1$; the period in the x-direction was set to $d = 9$; the thickness of the inner layer after the domain-flattening change of variables was set to 2.2; the incident angle was set to $\theta = 0$; and $R = 10^4$ Monte Carlo samples were used. Let ϵ_{mach} denote machine epsilon. These results were found using a Taylor summation. Later, results will be presented which compare results using a Taylor summation versus a Padé summation.

4.2.1 Example 1: Varying N_x and N_z with Fixed $l_c = 1$, $\varepsilon = 0.1$, $N = 20$

N_x	$N_z = 2^3$	$N_z = 2^4$	$N_z = 2^5$	$N_z = 2^6$
2^3	1.0501e-03	1.0814e-03	1.0802e-03	1.0827e-03
2^4	3.8155e-05	1.1569e-06	1.1161e-06	1.1277e-06
2^5	3.9156e-05	5.3976e-10	5.5434e-10	5.5156e-10
2^6	3.9349e-05	1.1695e-11	2.3820e-13	2.4384e-13

Table 4.1: $|\bar{e}|$ calculated with $l_c = 1$, $\varepsilon = 0.1$, and $N = 20$

N_x	$N_z = 2^3$	$N_z = 2^4$	$N_z = 2^5$	$N_z = 2^6$
2^3	1.8407e-06	1.8379e-06	1.8221e-06	1.8365e-06
2^4	1.4026e-08	8.6896e-10	8.6678e-10	8.6775e-10
2^5	1.2821e-08	ϵ_{mach}	ϵ_{mach}	ϵ_{mach}
2^6	1.2812e-08	ϵ_{mach}	ϵ_{mach}	ϵ_{mach}
2^7	1.2818e-08	ϵ_{mach}	ϵ_{mach}	ϵ_{mach}

Table 4.2: σ_e^2, calculated with $l_c = 1$, $\varepsilon = 0.1$, and $N = 20$

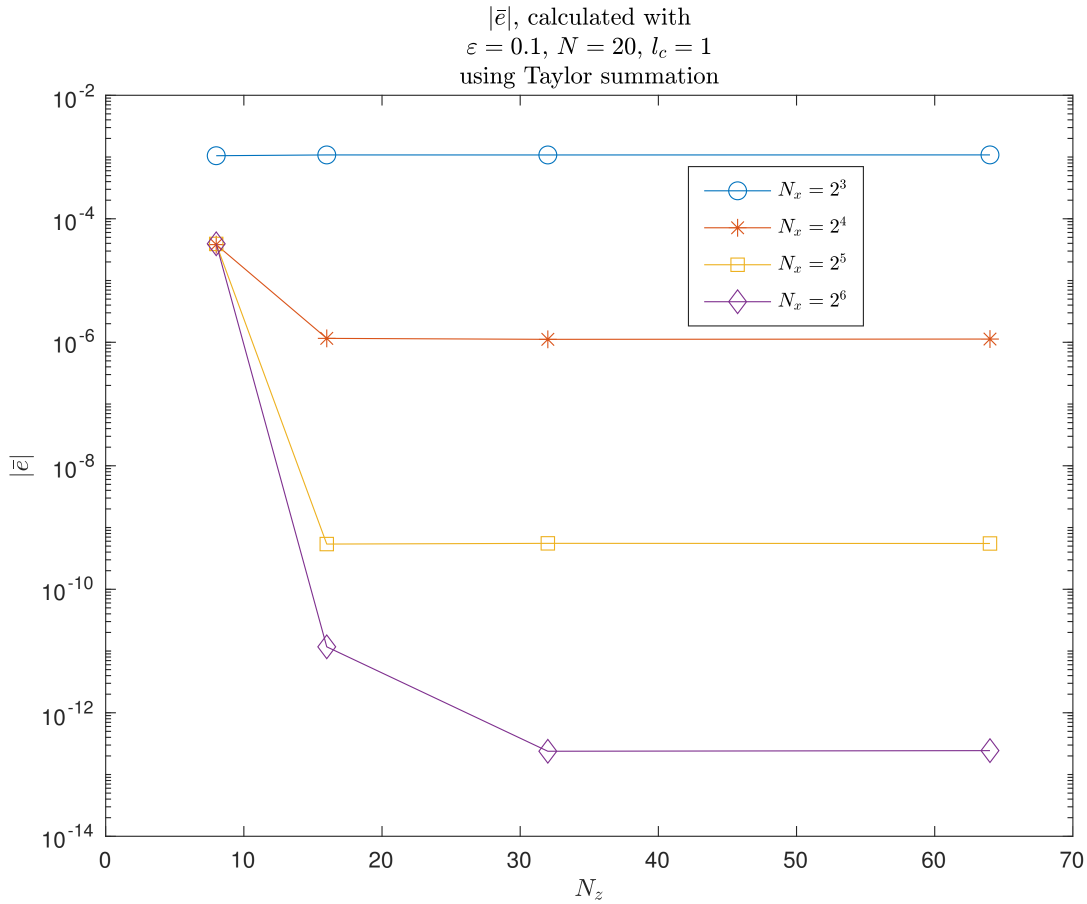

Figure 4.1: $|\bar{e}|$ for fixed values of N_x, calculated with $\varepsilon = 0.1$, $N = 20$, $l_c = 1$, and Taylor summation

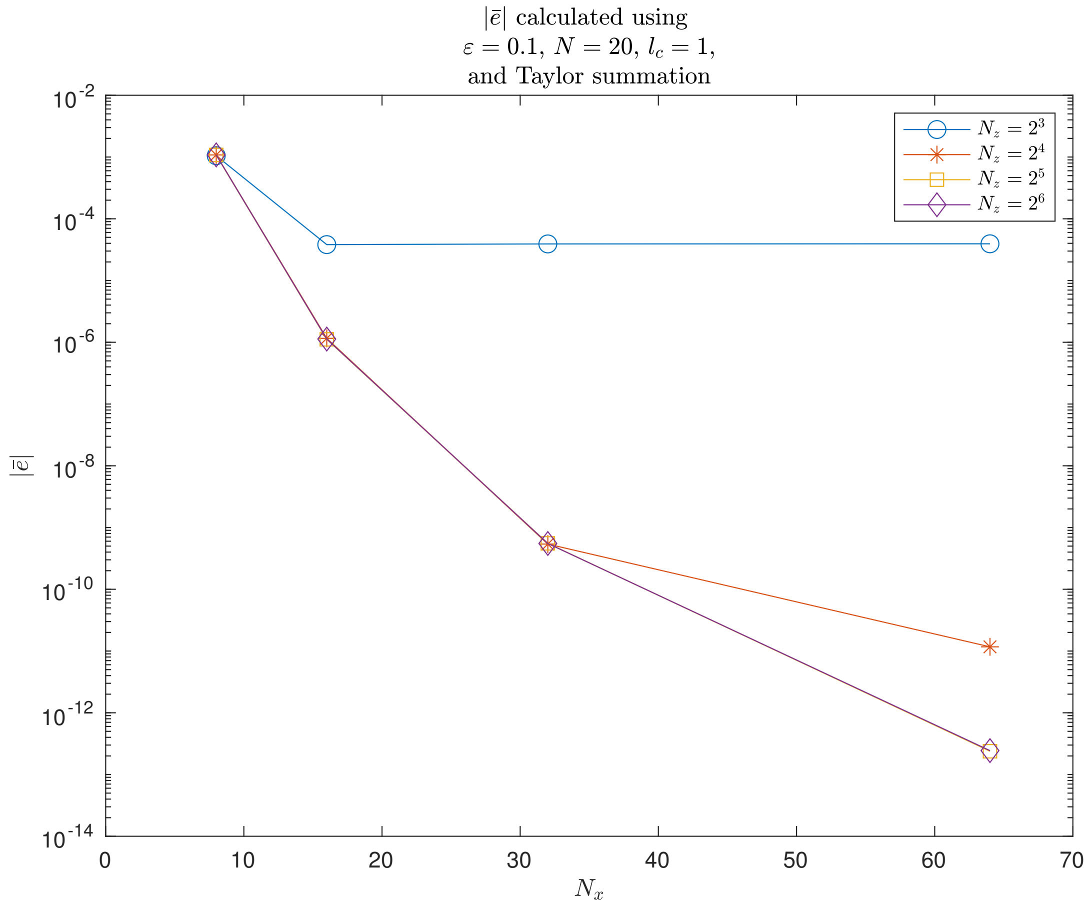

Figure 4.2: $|\bar{e}|$ for fixed values of N_z, calculated with $\varepsilon = 0.1$, $N = 20$, $l_c = 1$, and Taylor summation

In Example 1, from the results in Tables 4.1 and 4.2 and Figures 4.1 and 4.2, we can see that for a fixed N_x, as N_z increases, we have increased accuracy with spectral convergence. Similarly, for a fixed N_z, as N_x increases, we have increased accuracy with spectral convergence.

4.2.2 Example 2: Varying ε and N with Fixed $l_c = 2$, $N_x = 2^5$, $N_z = 2^5$

ε	$N=2$	$N=4$	$N=8$	$N=16$
0.01	2.5860e-07	8.9270e-11	5.8876e-12	5.8876e-12
0.05	1.8107e-04	1.8469e-06	4.0214e-09	3.9343e-09
0.1	2.8511e-03	1.0254e-04	1.3407e-07	6.2869e-08
0.2	4.6765e-02	3.2213e-03	2.5526e-05	4.6869e-06

Table 4.3: $|\bar{e}|$, calculated with $l_c = 2$, $N_x = 2^5$, and $N_z = 2^5$

ε	$N=2$	$N=4$	$N=8$	$N=16$
0.01	1.5934e-11	ϵ_{mach}	ϵ_{mach}	ϵ_{mach}
0.05	2.8624e-07	1.0078e-10	1.4301e-16	1.3036e-16
0.1	2.9170e-05	1.2568e-07	2.7749e-12	1.3858e-14
0.2	5.1089e-03	1.1718e-04	3.9580e-07	7.0365e-08

Table 4.4: σ_e^2, calculated with $l_c = 2$, $N_x = 2^5$, and $N_z = 2^5$

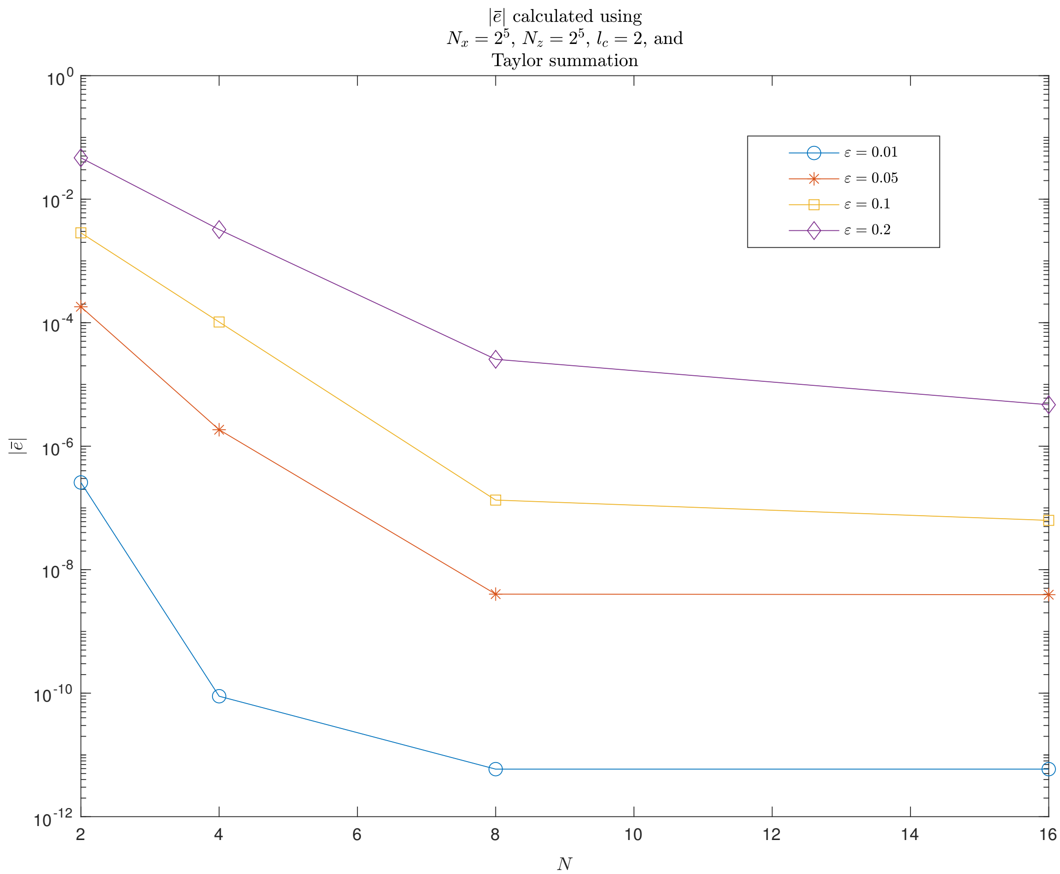

Figure 4.3: $|\bar{e}|$, calculated with $N_x = 2^5$, $N_z = 2^5$, $l_c = 2$, and Taylor summation

In Example 2, from the results in Tables 4.3 and 4.4 and Figure 4.3, we see that as ε, the perturbation of the random rough surface, is increased, higher Taylor orders are required to achieve high accuracy. For a fixed value of ε, we observe increased accuracy with spectral convergence as the number of Taylor orders are increased.

4.2.3 Example 3: Varying ε and N with Fixed $l_c = 1$, $N_x = 2^7$, $N_z = 2^7$

ε	$N = 2$	$N = 4$	$N = 8$	$N = 16$	$N = 32$
0.01	2.7959e-07	1.0623e-10	7.0483e-16	5.7461e-16	7.5618e-16
0.05	1.9164e-04	1.9641e-06	1.2516e-10	1.7223e-14	1.7578e-14
0.1	3.1013e-03	1.1381e-04	1.1027e-07	5.3063e-12	6.8486e-14
0.2	4.9897e-02	3.6524e-03	6.0578e-05	1.2516e-06	3.9608e-08

Table 4.5: $|\bar{e}|$, calculated with $l_c = 1$, $N_x = 2^7$, and $N_z = 2^7$

ε	$N = 2$	$N = 4$	$N = 8$	$N = 16$	$N = 32$
0.01	7.2569e-12	ϵ_{mach}	ϵ_{mach}	ϵ_{mach}	ϵ_{mach}
0.05	1.4451e-07	5.4612e-11	ϵ_{mach}	ϵ_{mach}	ϵ_{mach}
0.1	1.6076e-05	7.5851e-08	6.1797e-13	ϵ_{mach}	ϵ_{mach}
0.2	2.8219e-03	7.5741e-05	1.3858e-07	1.7220e-09	7.9382e-12

Table 4.6: σ_e^2, calculated with $l_c = 1$, $N_x = 2^7$, and $N_z = 2^7$

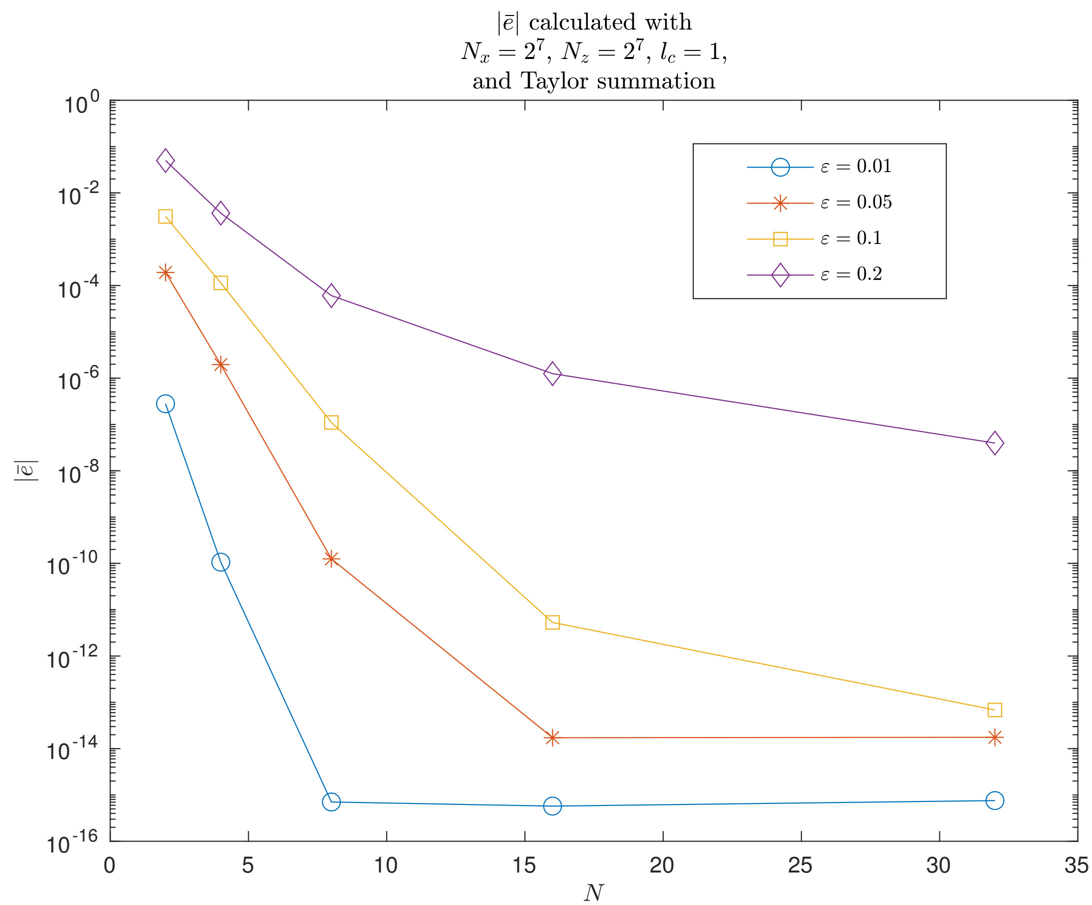

Figure 4.4: $|\bar{e}|$, calculated with $N_x = 2^7$, $N_z = 2^7$, $l_c = 1$, and Taylor summation

In Example 3, the correlation length was decreased from $l_c = 2$ (in Example 2) to $l_c = 1$, resulting in a "rougher" interface. With these rougher interfaces, in the results in Tables 4.5 and 4.6 and Figure 4.4, we observe that higher values of N_x and N_z were required to achieve a similar level of accuracy as demonstrated with a correlation length of $l_c = 2$. A visual example of how the "roughness" of the surface changes with varying values of the correlation length was shown in Figure 2.4.

4.2.4 Plots of Total Fields for a Fixed Random Sample

Below, the total fields in the upper, middle, and lower layers are calculated and plotted in transformed coordinates and in the original coordinates for a fixed random sample. The sample random interfaces which were used are shown below, as well. The parameters stated above were used with $\varepsilon = 0.1$, $N_x = 2^6$, $N_z = 2^6$, $N = 10$, and $l_c = 1$. Figure 4.5 shows the random sample of the two random interfaces separating each layer. Figure 4.6 is a close-up view of the upper random interface shown in figure 4.5. Figure 4.7 is a close-up view of the lower random interface shown in figure 4.5.

Recall that the total field is denoted by v and that the transformed fields are defined by

$$w^{(m)}(\xi; x', z') := v^{(m)}(\xi; x(x', z'), z(x', z')).$$

for $m = 0, ..., M$. Figure 4.8 is the total field in the upper layer, $v = v^{inc} + w^{(0)}$, in the transformed coordinates $(x'(x, z), z'(x, z))$. Figure 4.9 is the total field in the upper layer, $v = v^{inc} + v^{(0)}$, in the original coordinates, $(x(x', z'), z(x', z'))$. Figure 4.10 is the total field in the middle layer, $v = w^{(1)}$, in the transformed coordinates $(x'(x, z), z'(x, z))$. Figure 4.11 is the total field in the middle layer, $v = v^{(1)}$, in the original coordinates $(x(x', z'), z(x', z'))$. Figure 4.12 is the total field in the lower layer, $v = w^{(2)}$, in the transformed coordinates $(x'(x, z), z'(x, z))$. Figure 4.13 is the total field in the lower layer, $v = v^{(2)}$, in the original coordinates $(x(x', z'), z(x', z'))$.

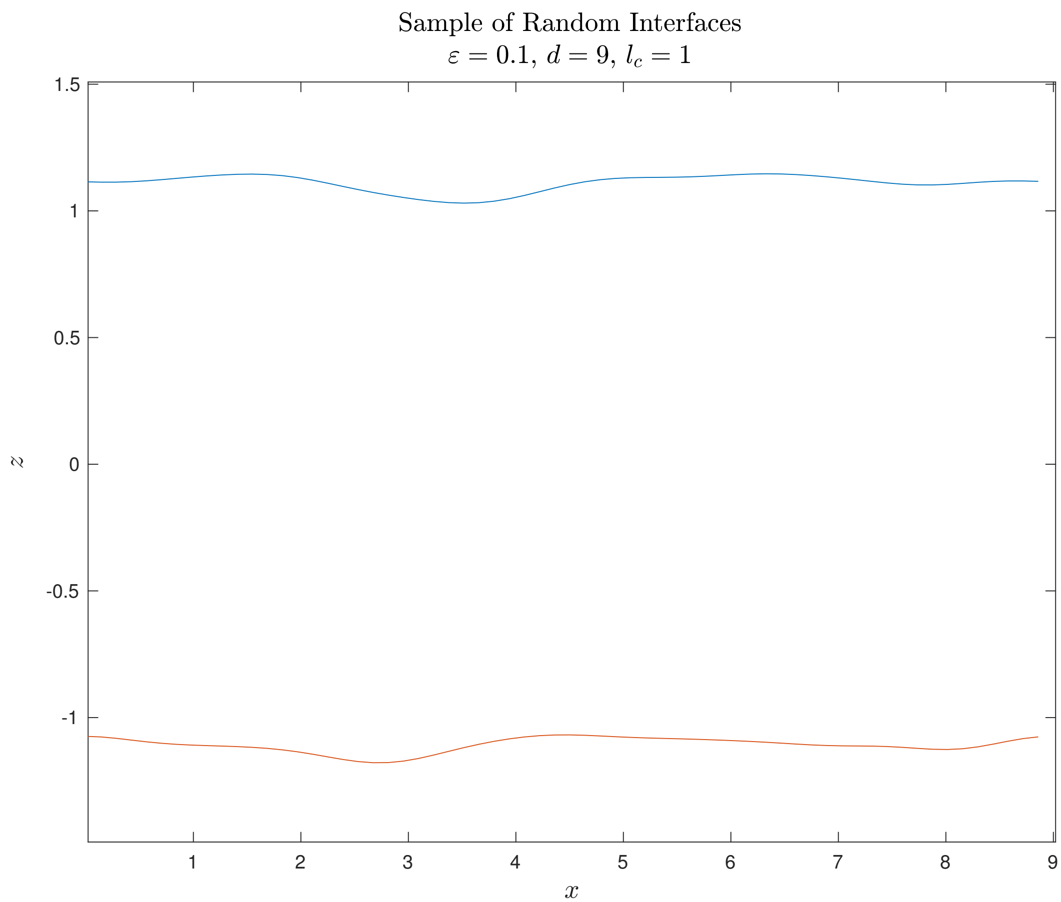

Figure 4.5: Sample Random Interfaces Separating Three Layers

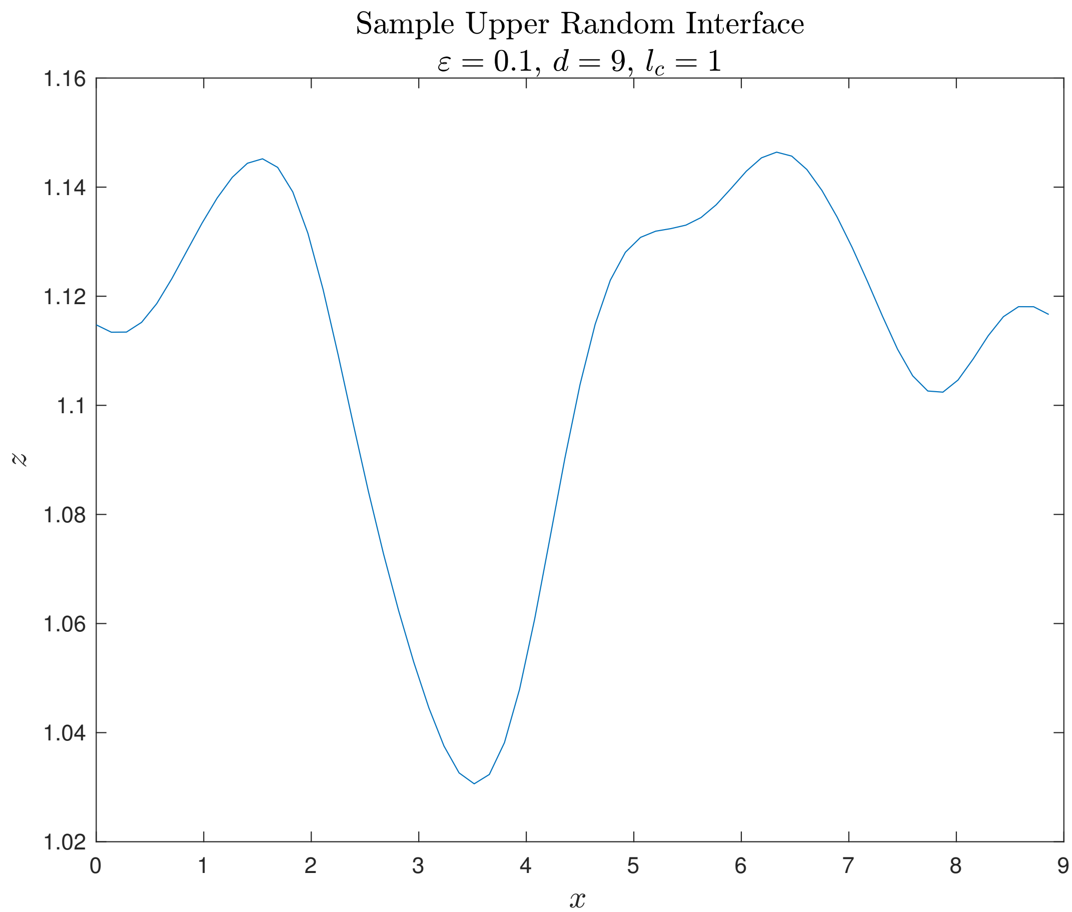

Figure 4.6: Sample Random Interfaces Separating Three Layers: Upper Interface

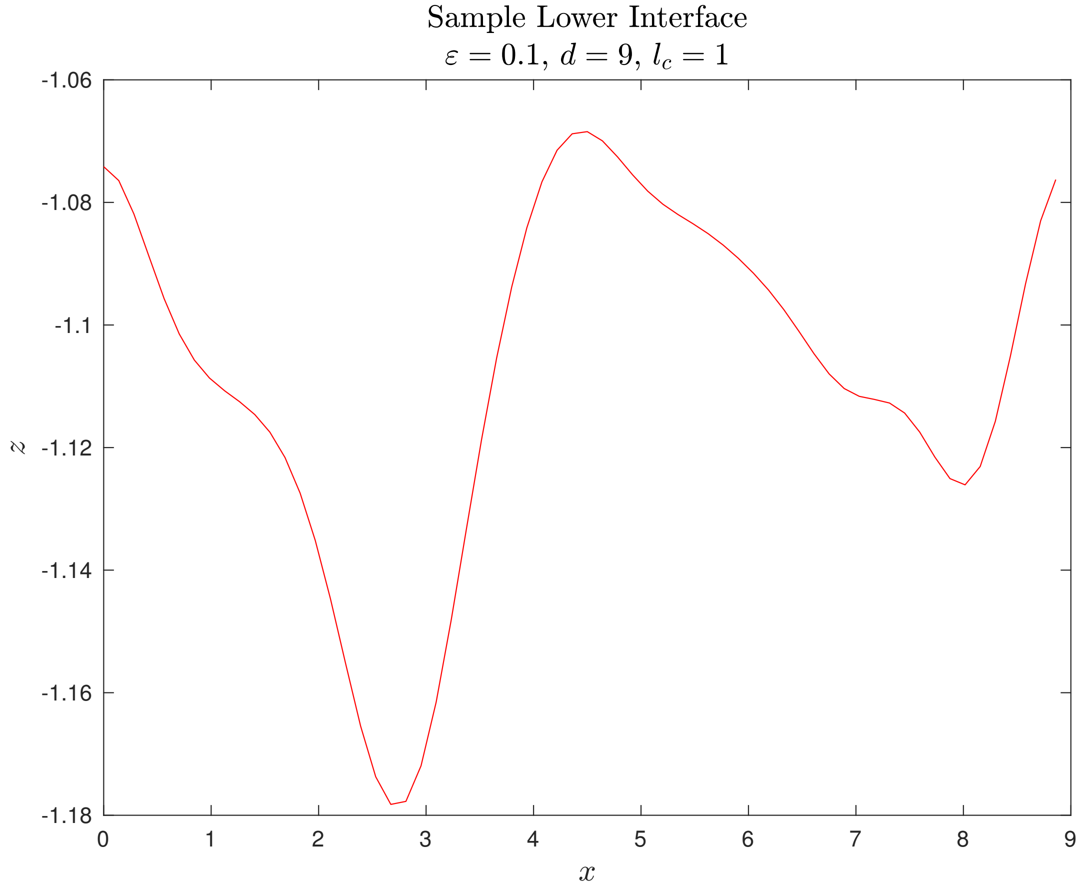

Figure 4.7: Sample Random Interfaces Separating Three Layers: Lower Interface

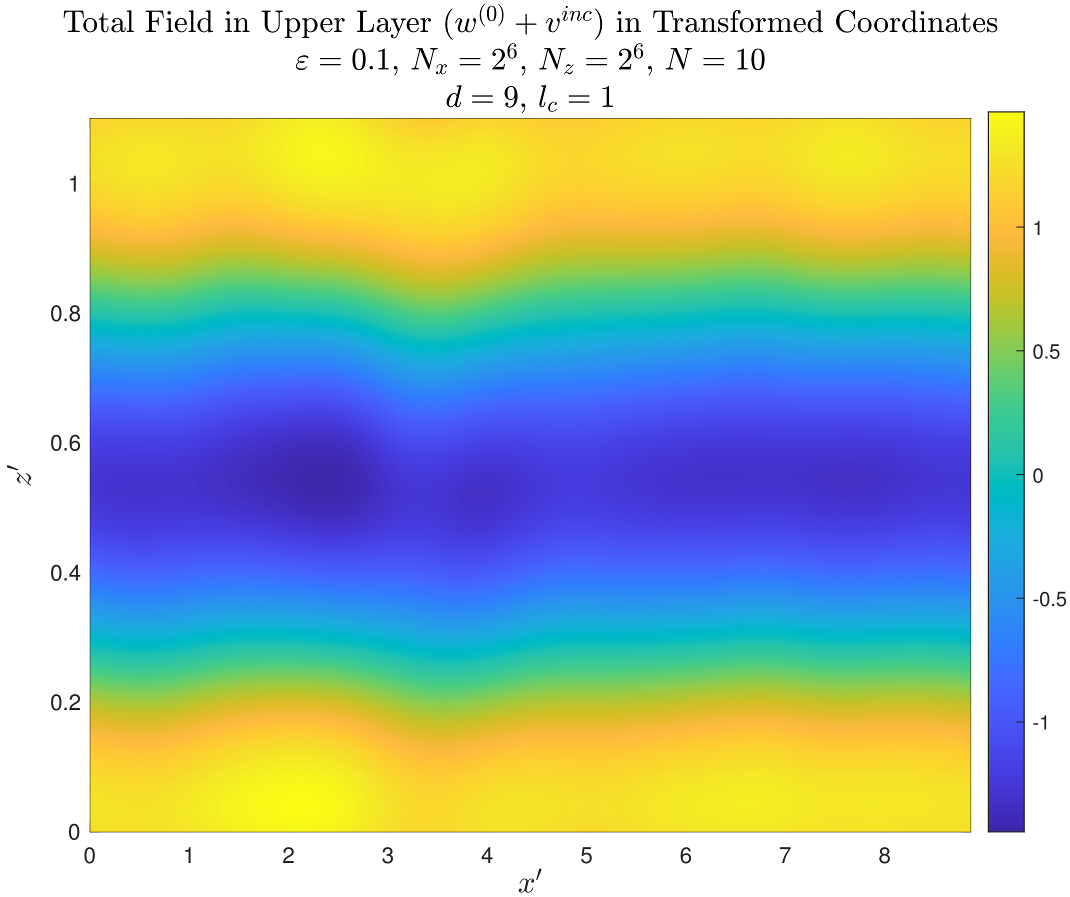

Figure 4.8: Sample Total Upper Field in Transformed Coordinates

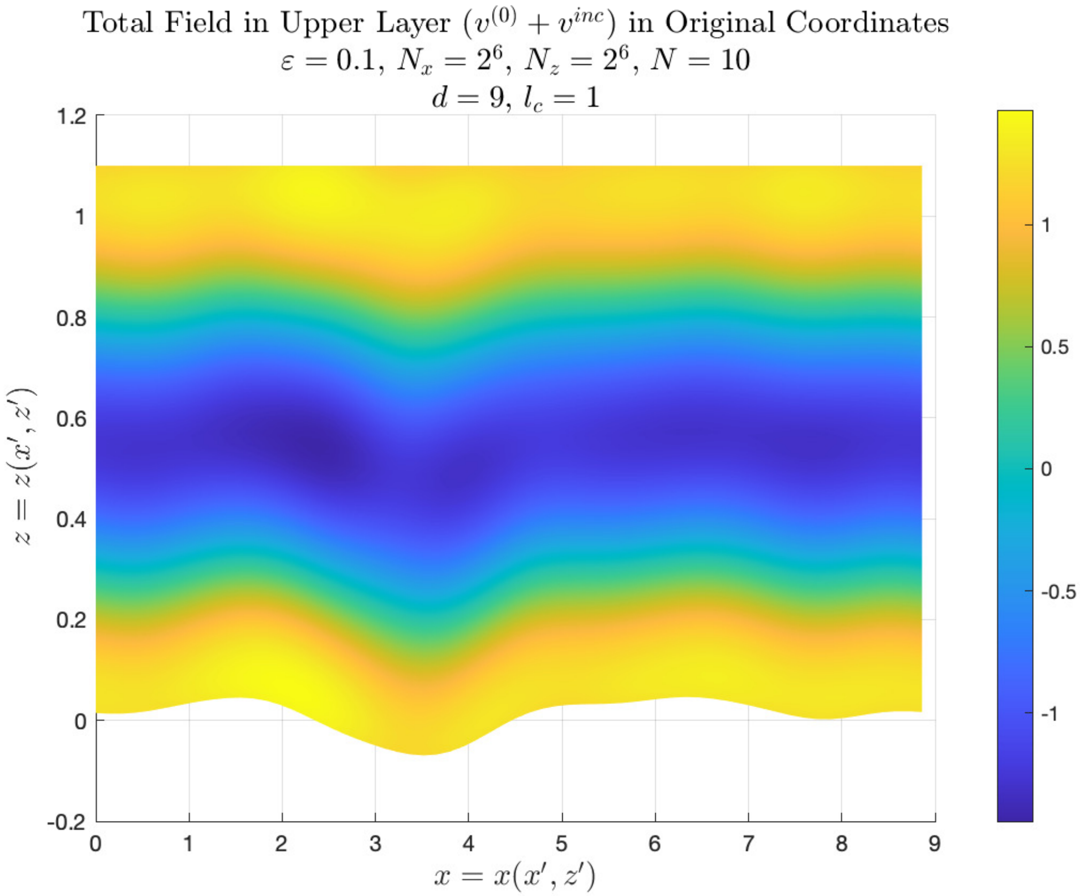

Figure 4.9: Sample Total Upper Field in Original Coordinates

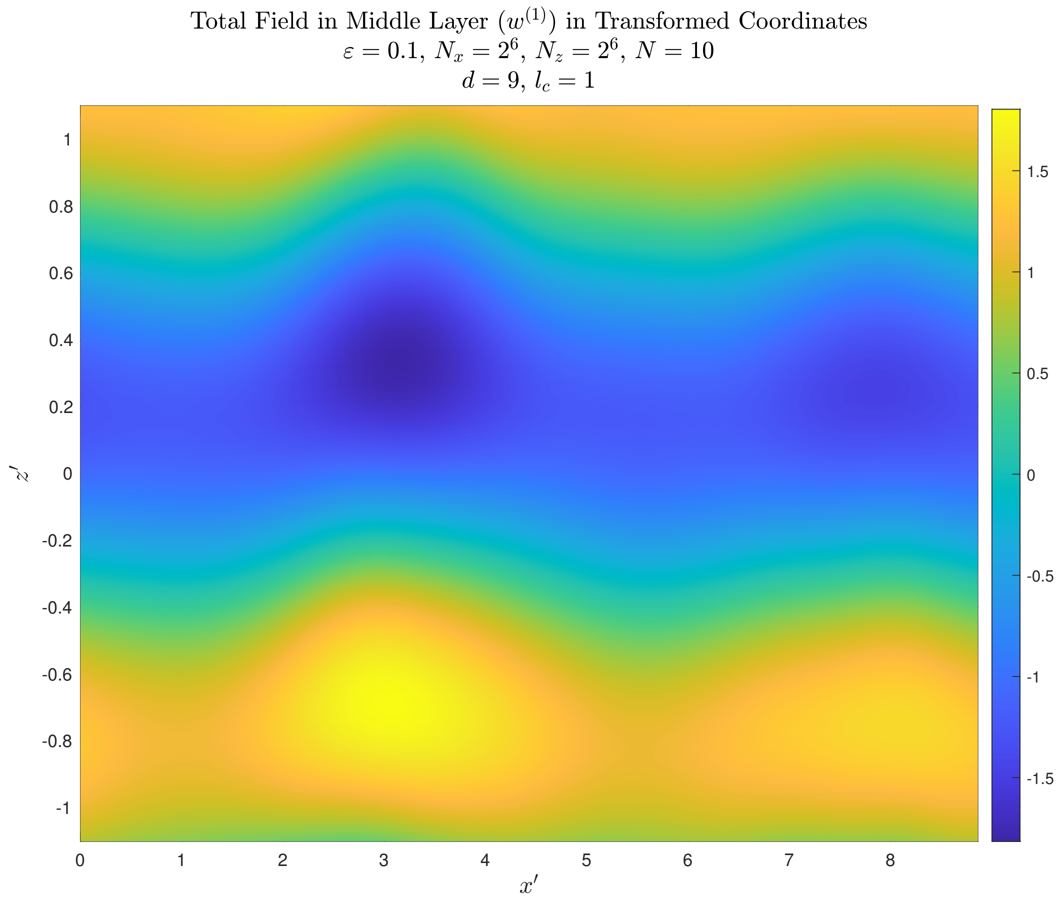

Figure 4.10: Sample Total Middle Field in Transformed Coordinates

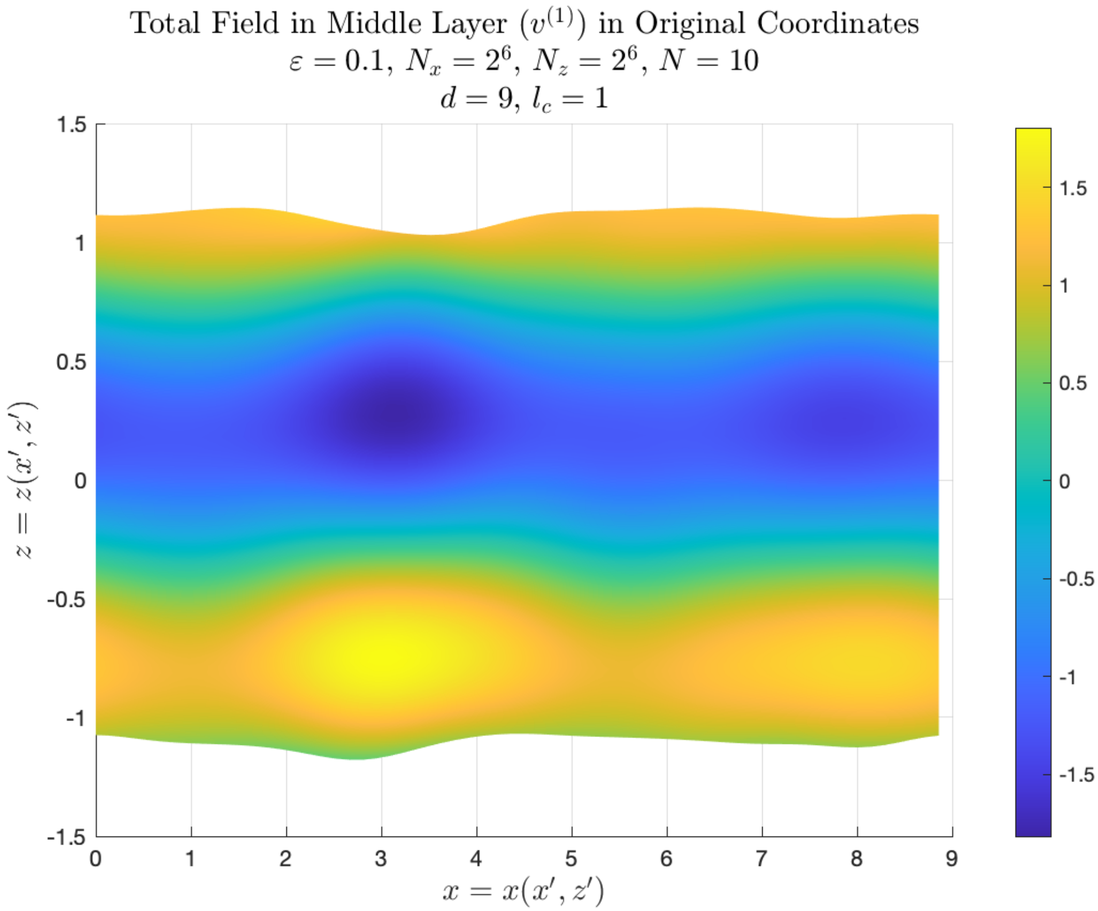

Figure 4.11: Sample Total Middle Field in Original Coordinates

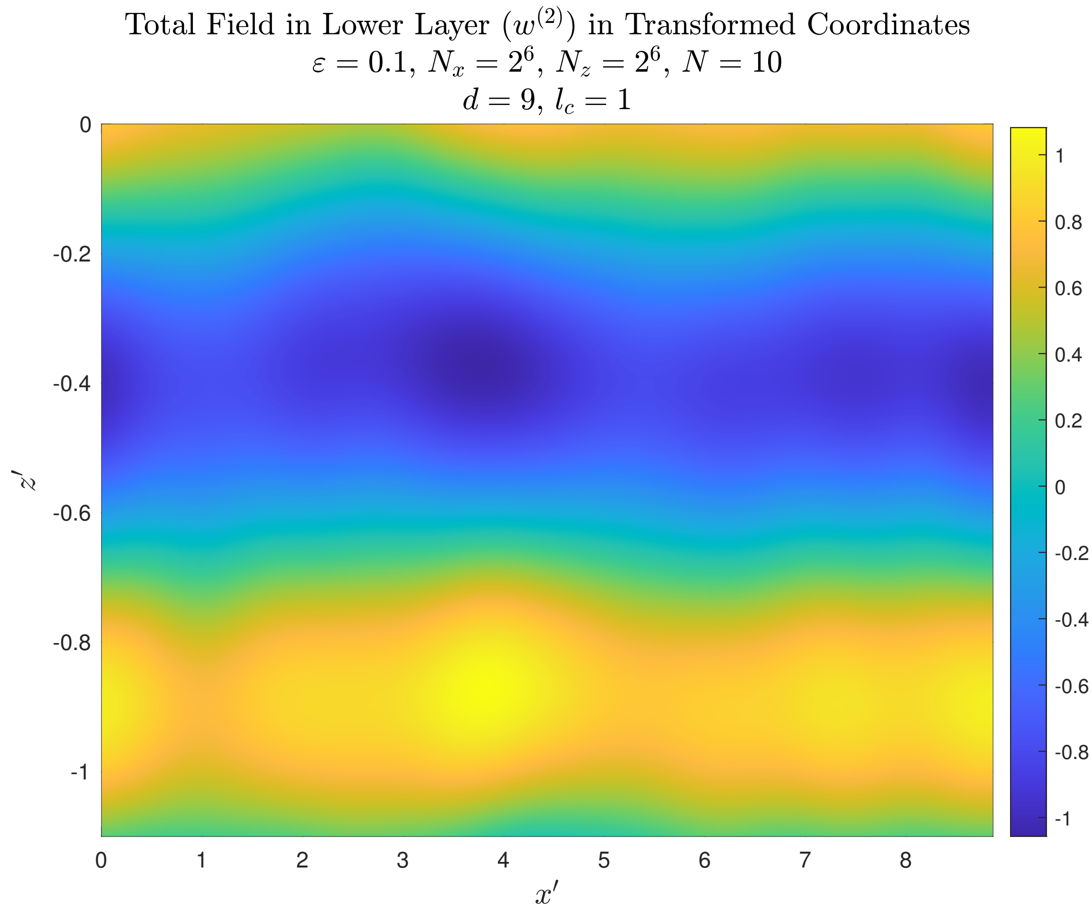

Figure 4.12: Sample Total Lower Field in Transformed Coordinates

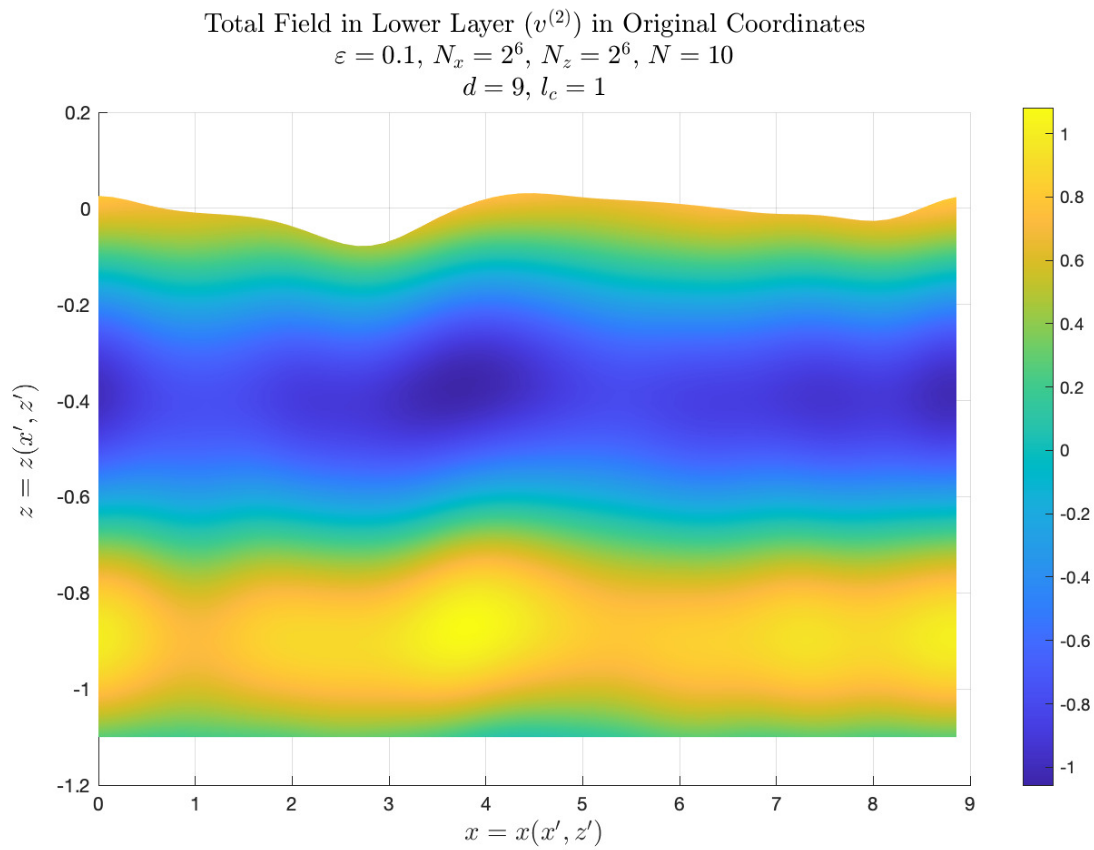

Figure 4.13: Sample Total Lower Field in Original Coordinates

4.2.5 Example 4: Varying N_x and N_z with fixed $l_c = 1$, $\varepsilon = 0.1$, $N = 10$ using Taylor and Padé Summations

The following are the absolute value of the energy defect mean and the energy defect variance using varying values of N_x, N_z, N, ε, and l_c (the correlation length) calculated using the Taylor summation as well as the Padé summation.

N_x	$N_z = 2^3$	$N_z = 2^4$	$N_z = 2^5$	$N_z = 2^6$
2^3	1.0529e-03	1.0830e-03	1.0805e-03	1.0824e-03
2^4	3.8119e-05	1.1037e-06	1.1053e-06	1.0713e-06
2^5	3.9447e-05	3.5165e-09	3.5016e-09	3.5737e-09
2^6	3.9352e-05	4.1083e-09	4.1247e-09	4.0991e-09

Table 4.7: $|\bar{e}|$, calculated with Taylor summation, $l_c = 1$, $N = 10$, and $\varepsilon = 0.1$

N_x	$N_z = 2^3$	$N_z = 2^4$	$N_z = 2^5$	$N_z = 2^6$
2^3	1.8478e-06	1.8391e-06	1.8319e-06	1.8395e-06
2^4	1.4035e-08	8.7117e-10	8.7290e-10	8.7698e-10
2^5	1.2815e-08	1.0680e-14	1.0653e-14	1.0671e-14
2^6	1.2845e-08	1.0662e-14	1.0660e-14	1.0663e-14

Table 4.8: σ_e^2, calculated with Taylor summation $l_c = 1$, $N = 10$, and $\varepsilon = 0.1$

N_x	$N_z = 2^3$	$N_z = 2^4$	$N_z = 2^5$	$N_z = 2^6$
2^3	1.0528e-03	1.0829e-03	1.0804e-03	1.0824e-03
2^4	3.8090e-05	1.1906e-06	1.1924e-06	1.1554e-06
2^5	3.9444e-05	6.2421e-10	6.4007e-10	6.3855e-10
2^6	3.9348e-05	8.0596e-11	9.1019e-11	9.1906e-11

Table 4.9: $|\bar{e}|$, calculated with Padé summation, $l_c = 1$, $N = 10$, and $\varepsilon = 0.1$

N_x	$N_z = 2^3$	$N_z = 2^4$	$N_z = 2^5$	$N_z = 2^6$
2^3	1.8481e-06	1.8393e-06	1.8321e-06	1.8398e-06
2^4	1.4085e-08	8.8877e-10	8.9048e-10	8.9432e-10
2^5	1.2813e-08	ϵ_{mach}	ϵ_{mach}	ϵ_{mach}
2^6	1.2842e-08	ϵ_{mach}	ϵ_{mach}	ϵ_{mach}

Table 4.10: σ_e^2, calculated with Padé summation, $l_c = 1$, $N = 10$, and $\varepsilon = 0.1$

In Example 4, we compare the absolute value of the mean energy defect and the variance of the energy defect for varying values of N_x and N_z when using a Taylor summation versus the Padé summation. From the numerical results shown in Tables 4.7 - 4.10, , we see that for fixed values of $\varepsilon = 0.1$, $N = 10$, and correlation length $l_c = 1$, the Taylor summation and Padé summation perform quite comparably.

4.2.6 Example 5: Varying N_x and N_z with fixed $l_c = 1$, $\varepsilon = 0.1$, $N = 20$ using Taylor and Padé Summations

N_x	$N_z = 2^3$	$N_z = 2^4$	$N_z = 2^5$	$N_z = 2^6$
2^3	1.0599e-03	1.0843e-03	1.0823e-03	1.0818e-03
2^4	3.8100e-05	1.1445e-06	1.1907e-06	1.1547e-06
2^5	3.9366e-05	5.4464e-10	5.5401e-10	5.3786e-10
2^6	3.8979e-05	1.1693e-11	1.4952e-13	2.4404e-13

Table 4.11: $|\bar{e}|$, calculated with Taylor summation, $l_c = 1$, $N = 20$, and $\varepsilon = 0.1$

N_x	$N_z = 2^3$	$N_z = 2^4$	$N_z = 2^5$	$N_z = 2^6$
2^3	1.9633e-06	1.8471e-06	1.8389e-06	1.8360e-06
2^4	1.4003e-08	8.6665e-10	8.5984e-10	8.6737e-10
2^5	1.2826e-08	ϵ_{mach}	ϵ_{mach}	ϵ_{mach}
2^6	1.3092e-08	ϵ_{mach}	ϵ_{mach}	ϵ_{mach}

Table 4.12: σ_e^2, calculated with Taylor summation, $l_c = 1$, $N = 20$, and $\varepsilon = 0.1$

N_x	$N_z = 2^3$	$N_z = 2^4$	$N_z = 2^5$	$N_z = 2^6$
2^3	1.0599e-03	1.0843e-03	1.0823e-03	1.0818e-03
2^4	3.8101e-05	1.1437e-06	1.1899e-06	1.1539e-06
2^5	3.9366e-05	5.4488e-10	5.5425e-10	5.3803e-10
2^6	3.8979e-05	1.1453e-11	1.9606e-15	4.0004e-15

Table 4.13: $|\bar{e}|$, calculated with Padé summation, $l_c = 1$, $N = 20$, and $\varepsilon = 0.1$

N_x	$N_z = 2^3$	$N_z = 2^4$	$N_z = 2^5$	$N_z = 2^6$
2^3	1.9633e-06	1.8471e-06	1.8389e-06	1.8360e-06
2^4	1.4004e-08	8.6687e-10	8.6006e-10	8.6759e-10
2^5	1.2826e-08	ϵ_{mach}	ϵ_{mach}	ϵ_{mach}
2^6	1.3092e-08	ϵ_{mach}	ϵ_{mach}	ϵ_{mach}

Table 4.14: σ_e^2, calculated with Padé summation, $l_c = 1$, $N = 20$, and $\varepsilon = 0.1$

In Example 5, we again compare the absolute value of the mean energy defect and the variance of the energy defect for varying values of N_x and N_z when using a Taylor summation versus the Padé summation. From the numerical results shown in Tables 4.11 - 4.14, we see that for fixed values of $\varepsilon = 0.1$, $N = 20$ (increased from $N = 10$ in Example 4), and correlation length $l_c = 1$, the Taylor summation and Padé summation again perform quite comparably. As expected, the results using the Taylor summation and the Padé summation both improve with the increased number of Taylor orders.

4.2.7 Example 6: Varying ε and N with fixed $l_c = 1$, $N_x = 2^6$, and $N_z = 2^6$ using Taylor and Padé Summations

ε	$N = 2$	$N = 4$	$N = 8$	$N = 16$
0.01	2.8136e-07	1.1283e-10	3.7068e-16	3.6188e-16
0.05	1.9124e-04	1.9590e-06	1.2463e-10	6.9234e-16
0.1	3.1018e-03	1.1400e-04	1.0975e-07	5.3839e-12
0.2	4.9805e-02	3.6397e-03	6.0474e-05	1.2474e-06

Table 4.15: $|\bar{e}|$, calculated with Taylor summation, $l_c = 1$, $N_x = 2^6$, and $N_z = 2^6$

ε	$N = 2$	$N = 4$	$N = 8$	$N = 16$
0.01	7.2280e-12	ϵ_{mach}	ϵ_{mach}	ϵ_{mach}
0.05	1.4367e-07	5.4369e-11	ϵ_{mach}	ϵ_{mach}
0.1	1.6105e-05	7.5887e-08	6.1719e-13	ϵ_{mach}
0.2	2.8237e-03	7.5536e-05	1.3807e-07	1.7219e-09

Table 4.16: σ_e^2, calculated with Taylor summation, $l_c = 1$, $N_x = 2^6$, and $N_z = 2^6$

ε	$N=2$	$N=4$	$N=8$	$N=16$
0.01	1.4132e-07	4.7801e-11	3.5889e-16	3.6220e-16
0.05	6.6048e-05	7.0430e-07	2.1062e-12	6.7797e-16
0.1	1.0168e-03	4.3865e-05	1.3864e-09	4.1979e-15
0.2	1.5445e-02	2.3691e-03	3.1150e-06	1.7452e-11

Table 4.17: $|\bar{e}|$, calculated with Padé summation, $l_c = 1$, $N_x = 2^6$, and $N_z = 2^6$

ε	$N=2$	$N=4$	$N=8$	$N=16$
0.01	2.0643e-11	ϵ_{mach}	ϵ_{mach}	ϵ_{mach}
0.05	3.6886e-07	2.6366e-11	ϵ_{mach}	ϵ_{mach}
0.1	1.5659e-05	2.0362e-08	7.4835e-15	ϵ_{mach}
0.2	2.5638e-02	2.4458e-05	8.7980e-10	ϵ_{mach}

Table 4.18: σ_e^2, calculated with Padé summation, $l_c = 1$, $N_x = 2^6$, and $N_z = 2^6$

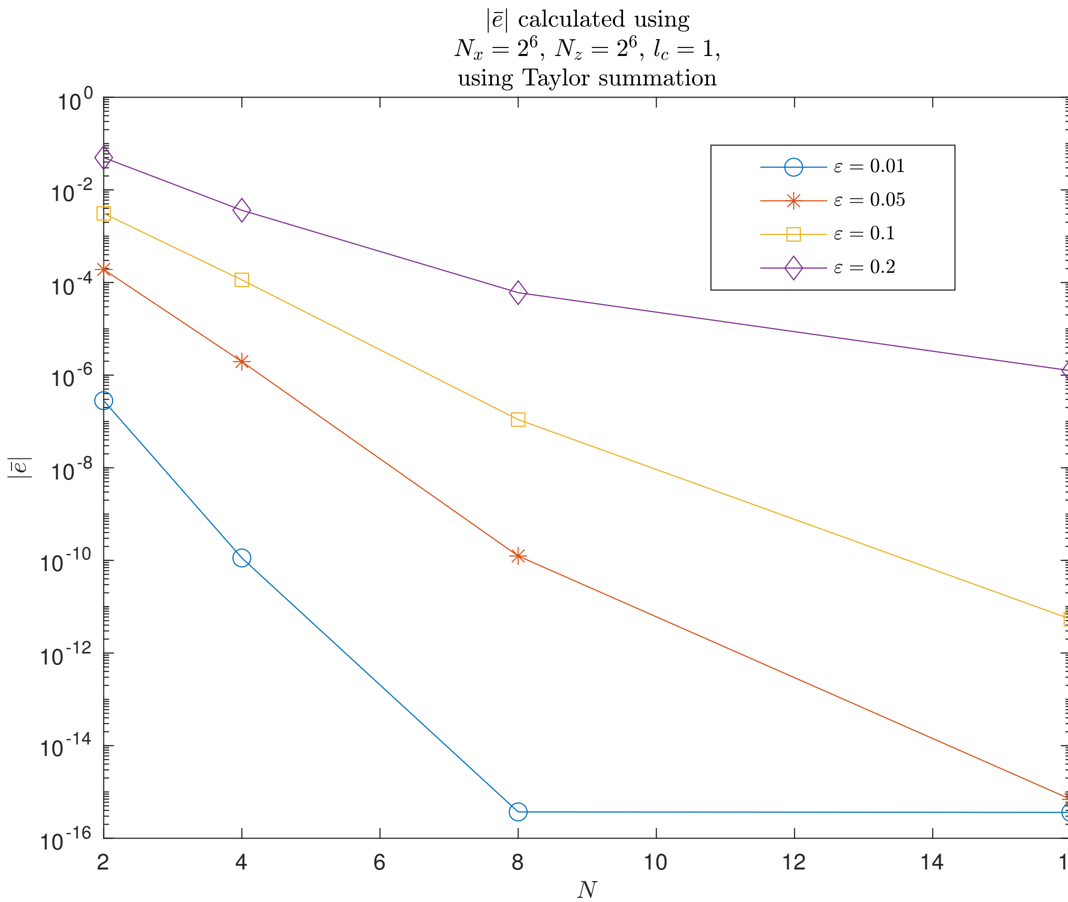

Figure 4.14: $|\bar{e}|$, calculated with $N_x = 2^6$, $N_z = 2^6$, $l_c = 1$, and Taylor summation

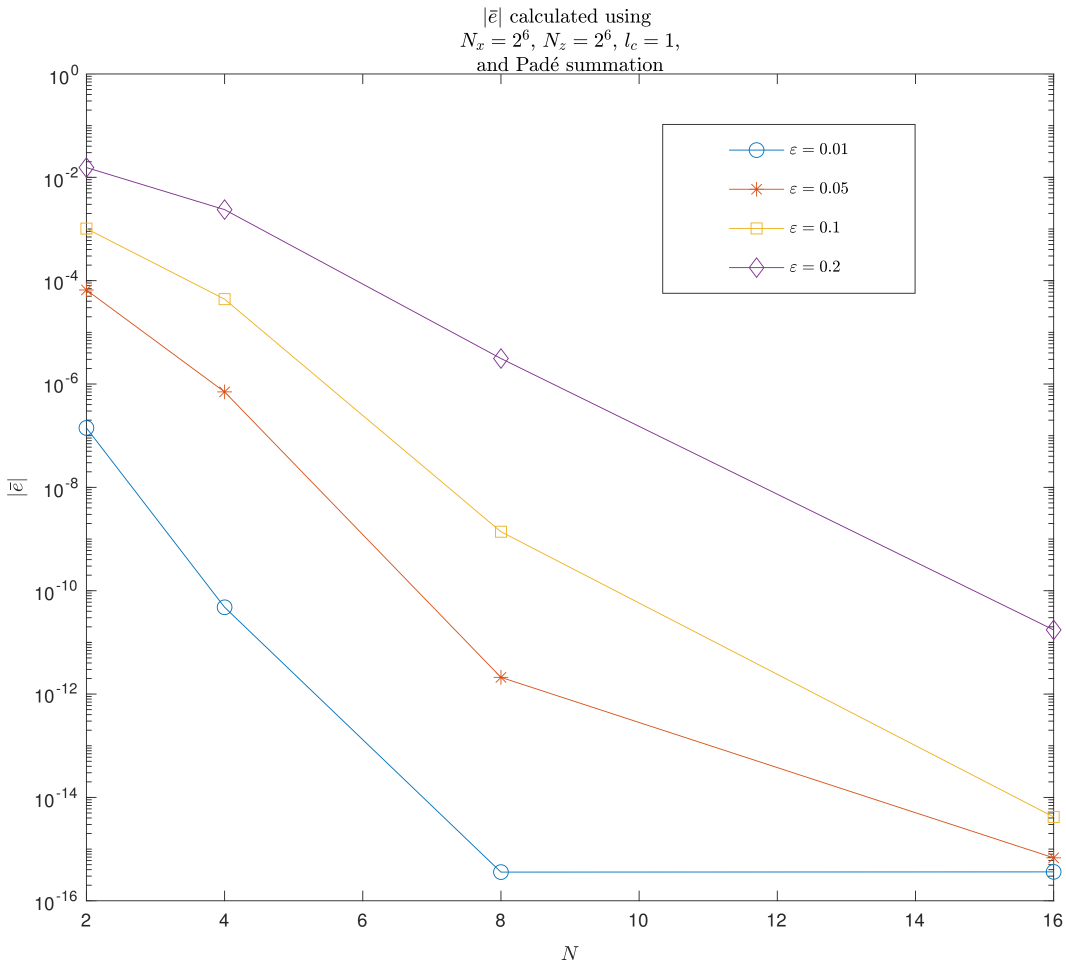

Figure 4.15: $|\bar{e}|$, calculated with $N_x = 2^6$, $N_z = 2^6$, $l_c = 1$, and Padé summation

In Example 6, we compare the absolute value of the mean energy defect and the variance of the energy defect for varying values of ε and N when using a Taylor summation versus the Padé summation. From the numerical results shown in Tables 4.15 - 4.18 and Figures 4.14 and 4.15, we see that for fixed values of $N_x = 2^6$, $N_z = 2^6$, and correlation length $l_c = 1$, as ε is increased, higher Taylor orders are required to achieve high accuracy when using both the Taylor summation and the Padé summation. We also observe that the Padé summation outperforms the Taylor summation, particularly as the value of ε is increased, starting around $\varepsilon = 0.2$. For $\varepsilon = 0.2$ and $N = 16$, the difference in the performance of the Padé summation and the Taylor summation is quite significant.

4.2.8 Example 7: Varying ε and N with fixed $l_c = 2$, $N_x = 2^6$, and $N_z = 2^6$ using Taylor and Padé Summations

ε	$N = 2$	$N = 4$	$N = 8$	$N = 16$
0.01	2.3976e-07	7.7876e-11	1.0195e-13	9.5632e-14
0.05	1.7509e-04	1.7391e-06	3.4446e-11	1.1855e-10
0.1	2.8369e-03	1.0235e-04	6.8329e-08	2.3055e-09
0.2	4.6019e-02	3.2016e-03	2.5010e-05	5.7027e-06

Table 4.19: $|\bar{e}|$, calculated with Taylor summation, $l_c = 2$, $N_x = 2^6$, and $N_z = 2^6$

ε	$N = 2$	$N = 4$	$N = 8$	$N = 16$
0.01	1.4233e-11	ϵ_{mach}	ϵ_{mach}	ϵ_{mach}
0.05	2.7307e-07	9.9492e-11	ϵ_{mach}	ϵ_{mach}
0.1	2.8737e-05	1.2525e-07	2.7330e-12	6.2088e-16
0.2	4.9507e-03	1.2104e-04	3.9225e-07	6.8661e-08

Table 4.20: σ_e^2, calculated with Taylor summation, $l_c = 2$, $N_x = 2^6$, and $N_z = 2^6$

ε	$N = 2$	$N = 4$	$N = 8$	$N = 16$
0.01	6.1819e-08	2.5283e-11	1.0194e-13	9.5634e-14
0.05	2.3038e-05	2.8777e-07	1.2082e-10	1.1854e-10
0.1	3.6471e-04	1.7822e-05	4.5307e-09	2.2776e-09
0.2	5.3370e-03	1.3013e-03	2.6168e-06	4.1579e-08

Table 4.21: $|\bar{e}|$, calculated with Padé summation, $l_c = 2$, $N_x = 2^6$, and $N_z = 2^6$

ε	$N = 2$	$N = 4$	$N = 8$	$N = 16$
0.01	1.9093e-11	ϵ_{mach}	ϵ_{mach}	ϵ_{mach}
0.05	2.5798e-07	2.5242e-11	ϵ_{mach}	ϵ_{mach}
0.1	1.1674e-05	1.6278e-08	3.9093e-15	6.1736e-16
0.2	3.7505e-04	1.7937e-05	3.7684e-10	8.8890e-14

Table 4.22: σ_e^2, calculated with Padé summation, $l_c = 2$, $N_x = 2^6$, and $N_z = 2^6$

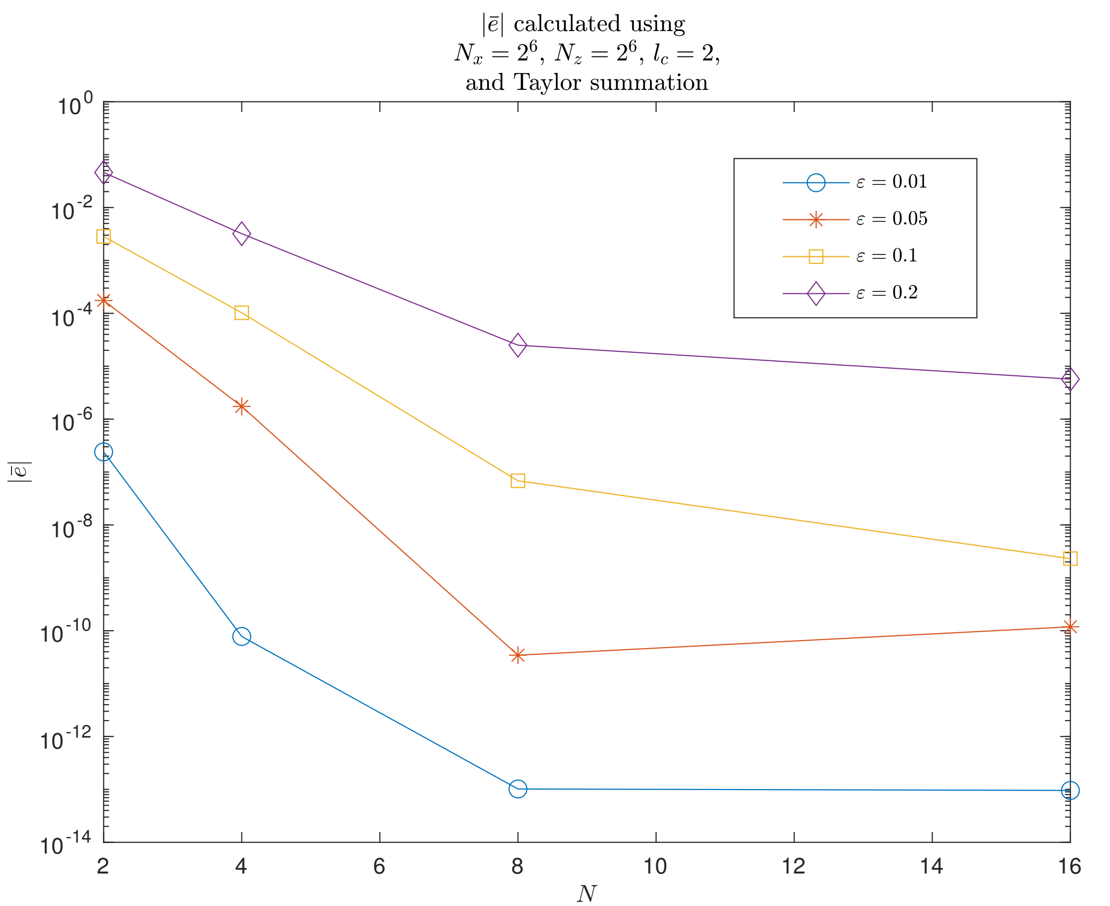

Figure 4.16: $|\bar{e}|$, calculated with $N_x = 2^6$, $N_z = 2^6$, $l_c = 2$, and Taylor summation

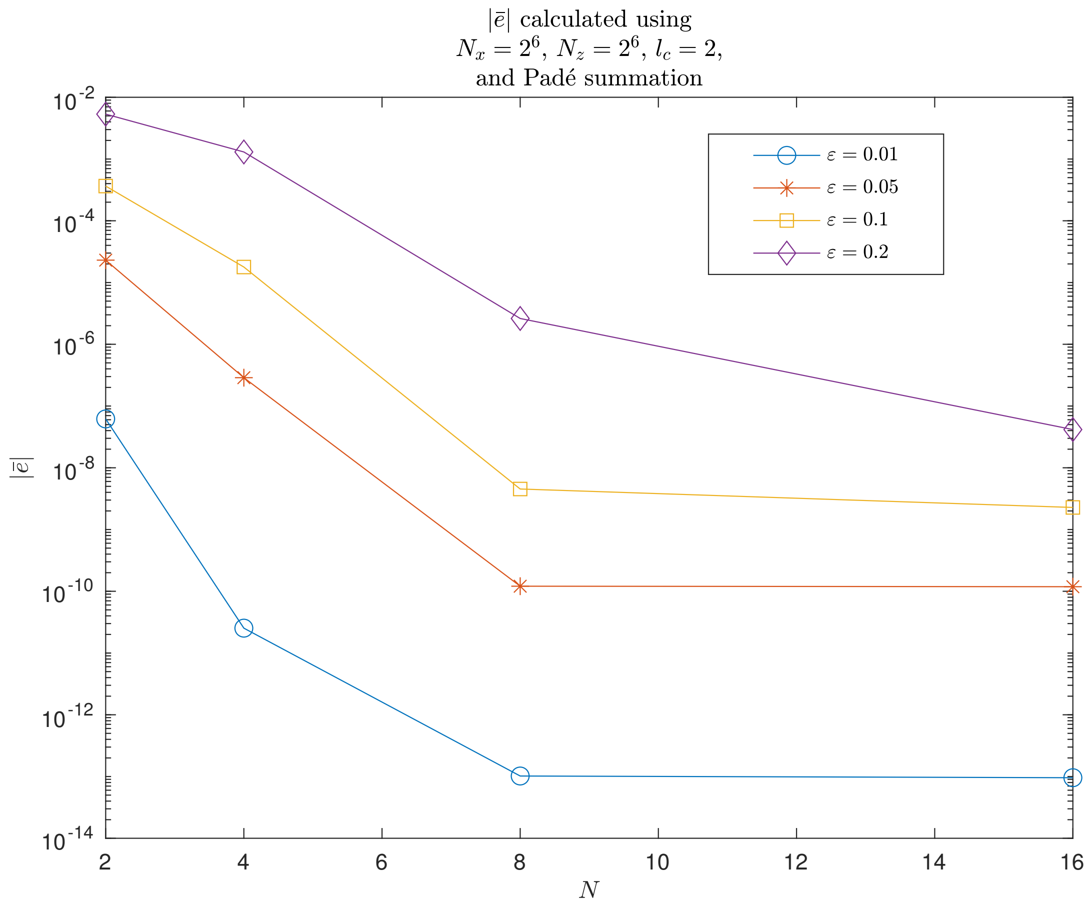

Figure 4.17: $|\bar{e}|$, calculated with $N_x = 2^6$, $N_z = 2^6$, $l_c = 2$, and Padé summation

In Example 7, we compare the absolute value of the mean energy defect and the variance of the energy defect for varying values of ε and N when using a Taylor summation versus the Padé summation. From the numerical results shown in Tables 4.19 - 4.22 and Figures 4.16 and 4.17, we see that for fixed values of $N_x = 2^6$, $N_z = 2^6$, and correlation length $l_c = 2$ (increased from $l_c = 1$ in Example 6 to $l_c = 2$), as ε is increased, higher Taylor orders are required to achieve high accuracy when using both the Taylor summation and the Padé summation. We also observe that the Padé summation outperforms the Taylor summation, particularly as the value of ε is increased, starting around $\varepsilon = 0.2$. The results are very similar to Example 6.

To summarize Examples 4 - 7, we can see that for smaller values of ε, the calculations done using Taylor summation and the calculations done using Padé summation are very comparable. On the other hand, for larger values of ε, we already observe the Padé summation outperforming the Taylor summation.

4.2.9 Taylor vs. Padé: Radius of Convergence

In the results to follow, larger values of ε are tested, showcasing the Padé summation's outstanding ability to approximate the solutions for points of analyticity that are outside the disk of convergence for the Taylor series. In the below results, The following parameters were fixed. The wavenumber in the upper layer was set to $k^{(0)} = 2\pi$; the wave number in the middle layer was set to $k^{(1)} = \pi$; the wavenumber in the lower layer was set to $k^{(2)} = 2\pi$; the upper artificial boundary was set to $z = a = 2.1$; the lower artificial boundary was set to $z = b = -2.1$; the period in the x-direction was set to $d = 9$; the thickness of the inner layer after the domain-flattening change of variables was set to 2.2; the incident angle was set to $\theta = 0$; and $R = 10^4$ Monte Carlo samples were used. These parameters are the same as used before with the exception of the upper and lower artificial boundaries. Additionally, for $\varepsilon > 1$, the thickness of the inner layer was set to 3.2, the upper artificial boundary was set to $a = 4.1$, and the lower artificial boundary was set to $b = 4.1$ due to overlapping of the layers as ε is increased for some samples ξ. For these results, only the absolute value of the mean of the energy defect was recorded because it is there that the comparisons between Taylor and Padé summations are the most visible.

ε	$N = 2^3$	$N = 2^4$	$N = 2^5$	$N = 2^6$	$N = 2^7$
0.1	7.8669e-08	9.5712e-09	9.6114e-09	9.6099e-09	9.6017e-09
0.2	2.4983e-05	5.4705e-06	1.3548e-08	1.4908e-07	1.3980e-07
0.4	4.0993e-01	1.6469e+03	2.3238e+11	1.5042e+28	1.6546e+62

Table 4.23: $|\bar{e}|$, calculated with Taylor summation $l_c = 2$, $N_x = 2^6$, and $N_z = 2^6$

ε	$N = 2^3$	$N = 2^4$	$N = 2^5$	$N = 2^6$	$N = 2^7$
0.1	6.9990e-09	9.5992e-09	9.6114e-09	9.6099e-09	9.6017e-09
0.2	2.5644e-06	1.3940e-07	1.3943e-07	1.3987e-07	1.3962e-07
0.4	1.2791e-03	2.3498e-06	1.7707e-06	1.7775e-06	1.7735e-06
0.6	2.5179e-02	1.8212e-04	6.7339e-06	6.5450e-06	6.5431e-06
0.8	1.2679e-01	8.4429e-03	1.6977e-05	2.0144e-05	5.9514e-06
1	3.6152e-01	1.1361e-01	2.6508e-03	1.5363e-03	1.1851e-03
1.1	9.3667e-01	9.3128e-01	1.0762e-02	6.0850e-03	8.1016e-03
1.2	1.6302	0.9515	0.0654	3.2271e-02	4.1812e-02

Table 4.24: $|\bar{e}|$, calculated with Padé summation, $l_c = 2$, $N_x = 2^6$, and $N_z = 2^6$

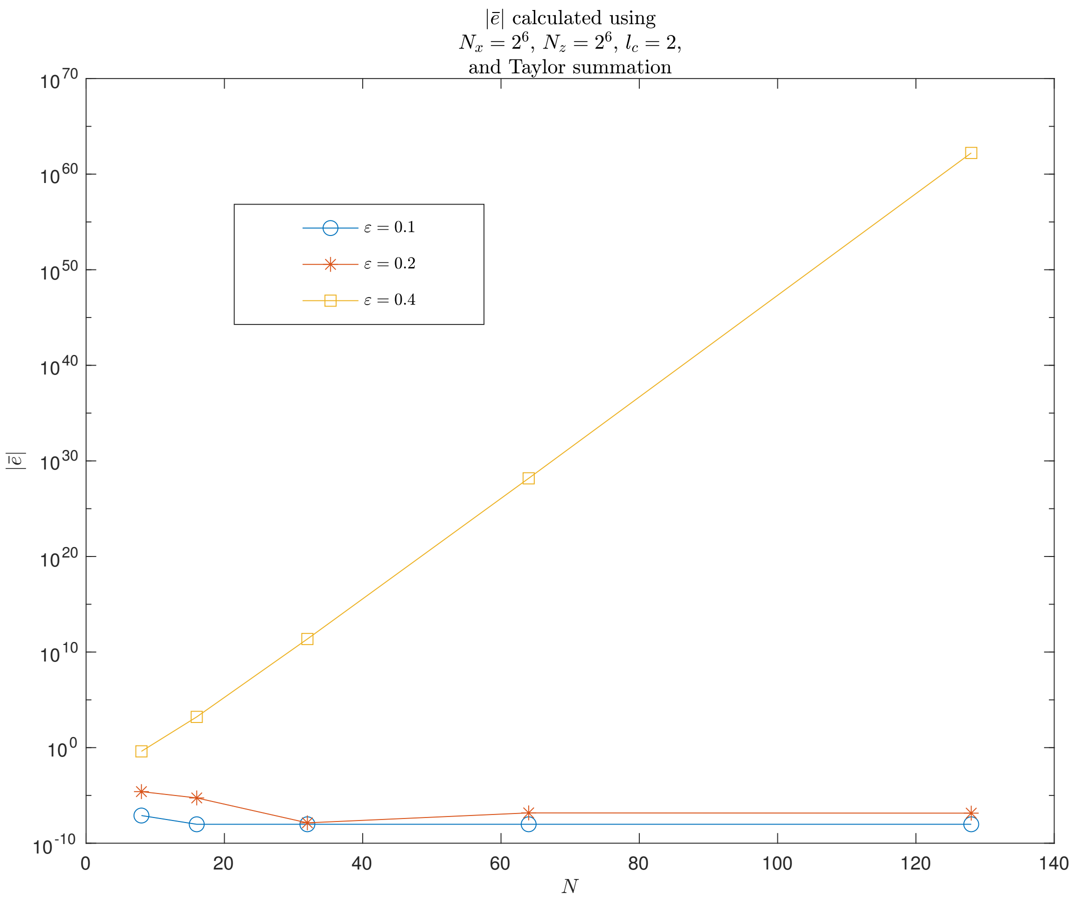

Figure 4.18: $|\bar{e}|$, calculated with $N_x = 2^6$, $N_z = 2^6$, $l_c = 2$, and Taylor summation

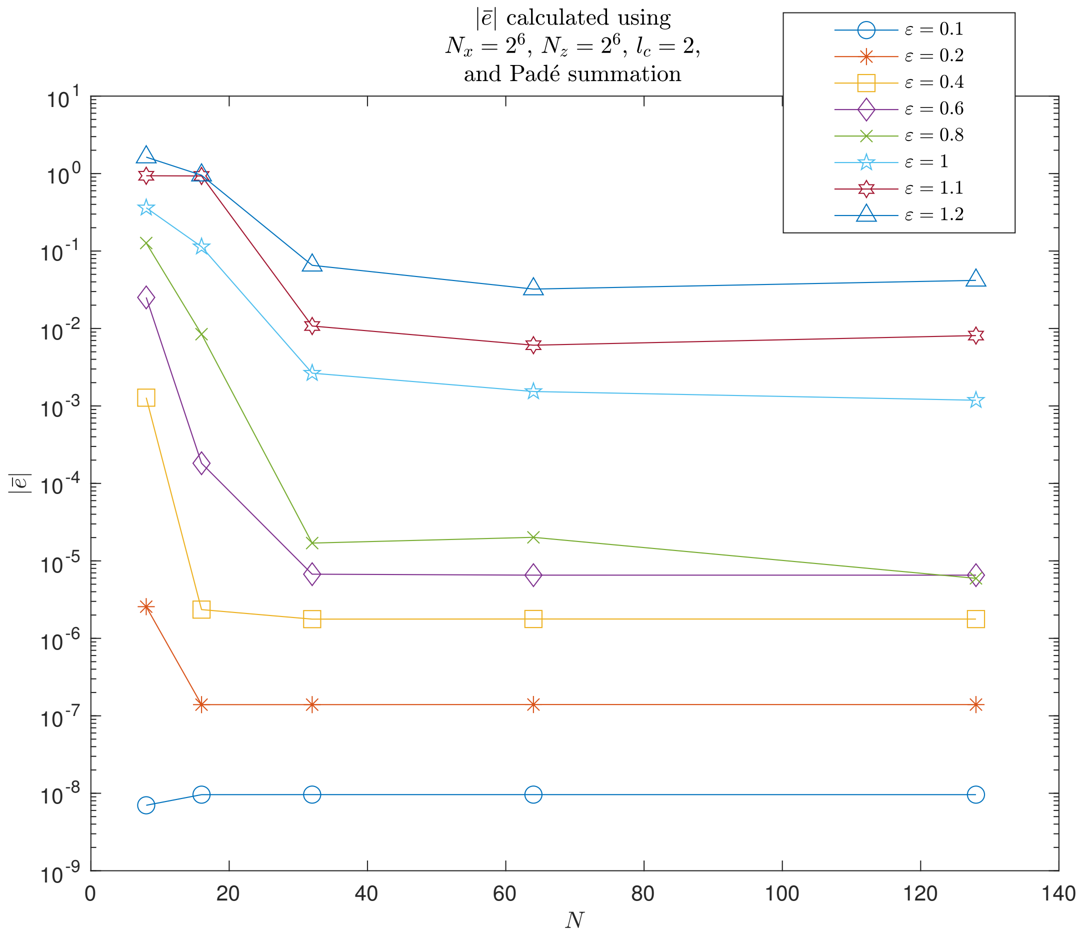

Figure 4.19: $|\bar{e}|$, calculated with $N_x = 2^6$, $N_z = 2^6$, $l_c = 2$, and Padè summation

From the numerical results shown in Tables 4.23 and 4.24 and Figures 4.18 and 4.19, we can see that the radius of convergence for the Taylor series is somewhere between 0.2 and 0.4. On the other hand, the radius of convergence for the Padé series extends well beyond that of the Taylor series.

Chapter 5

Conclusion

To summarize, we have presented a numerical method to efficiently and accurately model the scattering of electromagnetic fields by layered random surfaces. The primary components of the numerical algorithm are the combination of the Monte Carlo Transformed Field Expansion method and the use of impedance-impedance operators to formulate the boundary. Through the use of this method, we find that the discretized differential operator remains the same for each Monte Carlo sample and for each Taylor order. This major advantage leads to significant savings in computational cost. Through numerical examples, we have also shown that the Padé summation worked as a great tool for analytic continuation of the approximation with its ability to approximate the solutions at points of analyticity that are outside the radius of convergence of the Taylor summation. The presented numerical results demonstrate the accuracy and convergence of the algorithm.

Some ideas for future work on this problem are the following. Currently the method uses Monte Carlo sampling to sample the probability space. While the Monte Carlo method is simple and clear, it is quite slow. It would be nice to apply a sampling technique that is more efficient than Monte Carlo sampling, for example quasi-Monte Carlo. The Matlab code used to find the numerical results accommodates three layers right now. Some future work could be to modify the current code to accommodate more than three layers. Lastly, some future work could consist of extending the problem to two-dimensional interfaces.

Bibliography

[1] Ahlfors, Lars Valerian. *Complex Analysis.* McGraw-Hill, 1979.

[2] Ascher, U. M., and Chen Greif. *A First Course in Numerical Methods.* Society for Industrial and Applied Mathematics (SIAM, 3600 Market Street, Floor 6, Philadelphia, PA 19104), 2011.

[3] Baker, George A., and Peter Graves-Morris. *Padé Approximants.* Addison-Wesley, 1981.

[4] Bao, Gang, et al. "Computational Optimal Design of Random Rough Surfaces in Thin-Film Solar Cells." *Communications in Computational Physics*, vol. 25, no. 5, 2019, doi:10.4208/cicp.oa-2018-0013.

[5] Billingham, John, and Andy C. King. *Wave Motion.* Cambridge University Press, 2000.

[6] Bruno, Oscar P., and Fernando Reitich. "Numerical Solution of Diffraction Problems: a Method of Variation of Boundaries." *Journal of the Optical Society of America A*, vol. 10, no. 6, 1993, p. 1168., doi:10.1364/josaa.10.001168.

[7] Caflisch, Russel E. "Monte Carlo and Quasi-Monte Carlo Methods." *Acta Numerica*, edited by A. Iserles, vol. 7, Cambridge University Press, 1998, pp. 1-49.

[8] Chandezon, J, et al. "A New Theoretical Method for Diffraction Gratings and Its Numerical Application." *Journal of Optics*, vol. 11, no. 4, 1980, pp. 235-241., doi:10.1088/0150-536x/11/4/005.

[9] Coe, James V., et al. "Extraordinary Transmission of Metal Films with Arrays of Sub-wavelength Holes." *Annual Review of Physical Chemistry*, vol. 59, no. 1, 2008, pp. 179?202., doi:10.1146/annurev.physchem.59.032607.093703.

[10] Collino, Francis, et al. "Domain Decomposition Method for Harmonic Wave Propagation: a General Presentation." *Computer Methods in Applied Mechanics and Engineering*, vol. 184, no. 2-4, 2000, pp. 171-211., doi:10.1016/s0045-7825(99)00228-5.

[11] Evans, Lawrence C. *Partial Differential Equations.* 2nd ed., American Mathematical Society, 2010.

[12] Feller, W. *An Introduction to Probability Theory and Its Applications*, Vol.1. (3rd Edition). John Wiley and Sons, Inc, 1968.

[13] Feng, Xiaobing, et al. "An Efficient Monte Carlo-Transformed Field Expansion Method for Electromagnetic Wave Scattering by Random Rough Surfaces." *Communications in Computational Physics*, vol. 23, no. 3, 2018, doi:10.4208/cicp.oa-2017-0041.

[14] Fung, A.K., et al. "Backscattering from a Randomly Rough Dielectric Surface." *IEEE Transactions on Geoscience and Remote Sensing*, vol. 30, no. 2, 1992, pp. 356?369., doi:10.1109/36.134085.

[15] Garcia-Vidal, F. J., et al. "Light Passing through Subwavelength Apertures." *Reviews of Modern Physics*, vol. 82, no. 1, 2010, pp. 729-787., doi:10.1103/revmodphys.82.729.

[16] Gillman, Adrianna, et al. "A Spectrally Accurate Direct Solution Technique for Frequency-Domain Scattering Problems with Variable Media." *BIT Numerical Mathematics*, vol. 55, no. 1, 2014, pp. 141?170., doi:10.1007/s10543-014-0499-8.

[17] He, Ying, et al. "An Efficient and Stable Spectral Method for Electromagnetic Scattering from a Layered Periodic Structure." *Journal of Computational Physics*, vol. 231, no. 8, 2012, pp. 3007-3022., doi:10.1016/j.jcp.2011.10.033.

[18] Homola, Jiří. "Surface Plasmon Resonance Sensors for Detection of Chemical and Biological Species." *Chemical Reviews*, vol. 108, no. 2, 2008, pp. 462-493., doi:10.1021/cr068107d.

[19] Horn, Roger A., and Charles R. Johnson. *Matrix Analysis*. 2nd ed., Cambridge University Press, 2017.

[20] Ibe, Oliver C. *Fundamentals of Applied Probability and Random Processes*. Elsevier, Acad. Press, 2014.

[21] Ishimaru, Akira. *Wave Propagation and Scattering in Random Media*. IEEE Press, 1997.

[22] Jacobi, C. G. J. "Über Die Darstellung Einer Reihe Gegebner Werthe Durch Eine Gebrochne Rationale Function." *Journal Fr Die Reine Und Angewandte Mathematik* (Crelles Journal), vol. 1846, no. 30, 1846, pp. 127?156., doi:10.1515/crll.1846.30.127.

[23] Kirsch, A., P. Monk, "An analysis of the coupling of finite-element and Nystrm methods in acoustic scattering," *IMA Journal of Numerical Analysis*, Volume 14, Issue 4, October 1994, Pages 523-544, https://doi.org/10.1093/imanum/14.4.523

[24] Kowalczewski, Piotr, et al. "Engineering Gaussian Disorder at Rough Interfaces for Light Trapping in Thin-Film Solar Cells." *Optics Letters*, vol. 37, no. 23, 2012, p. 4868., doi:10.1364/ol.37.004868.

[25] Li, Jichun, and Yi-Tung Chen. *Computational Partial Differential Equations Using MATLAB*. CRC Press, 2009.

[26] Lin, Bing, et al. "Relationship between GPS Signals Reflected from Sea Surfaces and Surface Winds: Modeling Results and Comparisons with Aircraft Measurements." *Journal of Geophysical Research: Oceans*, vol. 104, no. C9, 1999, pp. 20713?20727., doi:10.1029/1999jc900176.

[27] Lord, Gabriel J., et al. *An Introduction to Computational Stochastic PDEs*. Cambridge University Press, 2014.

[28] Malcolm, Alison, and David P. Nicholls. "A Field Expansions Method for Scattering by Periodic Multilayered Media." *The Journal of the Acoustical Society of America*, vol. 129, no. 4, 2011, pp. 1783?1793., doi:10.1121/1.3531931.

[29] McLean, William. *Strongly Elliptic Systems and Boundary Integral Equations*. Cambridge University Press, 2000.

[30] Moskovits, Martin. "Surface-Enhanced Spectroscopy." *Reviews of Modern Physics*, vol. 57, 1985.

[31] Nicholls, David P., and Fernando Reitich. "A New Approach to Analyticity of Dirichlet-Neumann Operators." *Proceedings of the Royal Society of Edinburgh: Section A Mathematics*, vol. 131, no. 6, 2001, pp. 1411-1433., doi:10.1017/S0308210500001463.

[32] Nicholls, David P., and Jie Shen. "A Rigorous Numerical Analysis of the Transformed Field Expansion Method." *SIAM Journal on Numerical Analysis*, vol. 47, no. 4, 2009, pp. 2708-2734., doi:10.1137/080741914.

[33] Nicholls, David P., and Fernando Reitich. "Analytic Continuation of Dirichlet-Neumann Operators." *Numerische Mathematik*, vol. 94, no. 1, 2003, pp. 107?146., doi:10.1007/s002110200399.

[34] Nicholls, David P., et al. "Fast High-Order Perturbation of Surfaces Methods for Simulation of Multilayer Plasmonic Devices and Metamaterials." *Journal of the Optical Society of America A*, vol. 31, no. 8, 2014, p. 1820., doi:10.1364/josaa.31.001820.

[35] Nicholls, David P. "Method of Field Expansions for Vector Electromagnetic Scattering by Layered Periodic Crossed Gratings." *Journal of the Optical Society of America A*, vol. 32, no. 5, 2015, p. 701., doi:10.1364/josaa.32.000701.

[36] Nicholls, David P. "On Analyticity of Linear Waves Scattered by a Layered Medium." *Journal of Differential Equations*, vol. 263, no. 8, 2017, pp. 5042-5089., doi:10.1016/j.jde.2017.06.012.

[37] Nicholls, David P., and Fernando Reitich. "Shape Deformations in Rough-Surface Scattering: Cancellations, Conditioning, and Convergence." *Journal of the Optical Society of America A*, vol. 21, no. 4, 2004, pp. 590-605., doi:10.1364/josaa.21.000590.

[38] Nicholls, David P., and Fernando Reitich. "Shape Deformations in Rough-Surface Scattering: Improved Algorithms." *Journal of the Optical Society of America A*, vol. 21, no. 4, 2004, p. 606., doi:10.1364/josaa.21.000606.

[39] Nicholls, David P. "Stable, High-Order Computation of Impedance-Impedance Operators for Three-Dimensional Layered Medium Simulations." *Proceedings of the Royal Society A: Mathematical, Physical and Engineering Sciences*, vol. 474, no. 2212, 2018, p. 20170704., doi:10.1098/rspa.2017.0704.

[40] Nicholls, David P. "Three-Dimensional Acoustic Scattering by Layered Media: a Novel Surface Formulation with Operator Expansions Implementation." *Proceedings of the Royal Society A: Mathematical, Physical and Engineering Sciences*, vol. 468, no. 2139, 2011, pp. 731?758., doi:10.1098/rspa.2011.0555.

[41] Nuttall, J. "The Convergence of Padé Approximants of Meromorphic Functions." *Journal of Mathematical Analysis and Applications*, vol. 31, 1970, pp. 147-153.

[42] Ogilvy, J. A., and Harold M. Merklinger. "Theory of Wave Scattering from Random Rough Surfaces." *The Journal of the Acoustical Society of America*, vol. 90, no. 6, 1991, pp. 3382?3382., doi:10.1121/1.401410.

[43] Petit, Roger, editor. *Electromagnetic Theory of Gratings*. Springer, 1980.

[44] Phillips, N. A. "A Coordinate System Having Some Special Advantages For Numerical Forecasting." *Journal of Meteorology*, vol. 14, no. 2, 1957, pp. 184?185., doi:10.1175/1520-0469(1957)014¡0184:acshss¿2.0.co;2.

[45] Pólya, G., and G. Szegö. *Isoperimetric Inequalities in Mathematical Physics*. Princeton Univ. Press, 1951.

[46] Quarteroni, A., and A. Valli. "Theory and Application of Steklov-Poincare Operators for Boundary-Value Problems." *Applied and Industrial Mathematics*, 1991, pp. 179?203., doi:10.1007/978-94-009-1908-2-14.

[47] Raether, Heinz. *Surface Plasmons on Smooth and Rough Surfaces and on Gratings*. Springer Berlin, 2013.

[48] Rasooly, Avraham, and Keith E. Herold. *Biosensors and Biodetection*. Humana Press, 2009.

[49] Rodrigo, Sergio G., et al. "Extraordinary Optical Transmission: Fundamentals and Applications." *Proceedings of the IEEE*, vol. 104, no. 12, 2016, pp. 2288-2306., doi:10.1109/jproc.2016.2580664.

[50] Shen, Jie, and T. Tang. *Spectral and High-Order Methods with Applications*. Science Press, 2006.

[51] Strutt, John William. "On the Dynamical Theory of Gratings." *Proceedings of the Royal Society of London. Series A, Containing Papers of a Mathematical and Physical Character*, vol. 79, no. 532, 2 Aug. 1907, pp. 399-416., doi:10.1098/rspa.1907.0051.

[52] Thompson, Donald R., et al. "An Improved Geometrical Optics Model for Bistatic GPS Scattering from the Ocean Surface." *IEEE Transactions on Geoscience and Remote Sensing*, vol. 43, no. 12, 2005, pp. 2810-2821., doi:10.1109/tgrs.2005.857895.

[53] Trefethen, Lloyd N. *Spectral Methods in MATLAB*. SIAM, 2000.

[54] Tsang, Leung, et al. *Theory of Microwave Remote Sensing*. Wiley, 1985.

[55] Zayats, Anatoly V., et al. "Nano-Optics of Surface Plasmon Polaritons." *Physics Reports*, vol. 408, no. 3-4, 2005, pp. 131?314., doi:10.1016/j.physrep.2004.11.001.

[56] Zinn-Justin, J. "Convergence of Padé Approximants in the General Case." *Rocky Mountain Journal of Mathematics*, vol. 4, no. 2, 1974, pp. 325?330., doi:10.1216/rmj-1974-4-2-325.